SYNTHESIS AND PROPERTIES OF POLY(2,6-DIARYLPHENYLENE ETHER)S

A THESIS

By

Hu Yang

Submitted to the Faculty of Graduate Studies and Research in partial fulfillment of the requirements for the degree of Doctor of Philosophy

Department of Chemistry
McGill University
Montreal, Quebec, Canada
H3A 2K6

To My Parents

Synthesis and Properties of Poly(2,6-diarylphenylene ether)s

Abstract

Modifications of poly(2,6-diphenylphenylene ether) (P3O), to attain reduced melting temperatures and melt processible thermoplastics, are described.

In order to prepare a series of P3O polymers with systematically varied structures, a series of substituted 2,6-diphenylphenol monomers with corresponding structural variations are synthesized. Several possible procedures for monomer synthesis are examined depending on the substituents to be introduced. The corresponding homopolymers and copolymers are prepared from these monomers and their properties are examined. The desired reduction in melting points and retention of crystallinity in some of the resulting polymers have been realized. The structure-property relationships are discussed.

It is found that fluoro substitution on the polymers significantly depresses the crystallinity and melting temperatures in the P3O polymer derivatives. These effects have been further studied by synthesizing a series of systematically fluoro-substituted P3O polymers and determining their properties.

The fluoro substitution effects are even more pronounced in the poly(ether ether ketone)s with pendant phenyl rings attached to the backbone. The biphenol monomers are synthesized from the corresponding 2,6-diarylphenols by a carbon-carbon coupling reaction. Whereas the parent polymer is a highly rigid, highly crystalline and insoluble material, the introduction of fluorine onto the pendant phenyl rings completely eliminates crystallinity resulting in totally amorphous and soluble polymers.

Additional modification of P3O with acetylene functionality yields melt-processible polymers which can be subsequently cross-linked.

Synthèse et Propriétés des Poly(diaryl-2,6-phénylène éther)s

Sommaire

Des modifications sont apportées au poly(diphényl-2,6-phénylène éther) (P3O) afin d'atteindre des températures de fusion réduites et pour accéder des thermoplastiques moulables au point de fusion.

Pour la préparation des polymères dérivés du P3O avec les structures variées systématiquement, on a synthétisé une serie de monomères qui possedent divers fonctionalités apportées au diphényl-2,6-phénol. Plusieurs procédures de synthèse des monomères sont examinées et varient selon les groupes fonctionels desirés. De ces monomères on a préparé les homopolymères et co-polymères correspondant et on a fait l'étude de leur propriétés. La réduction du point de fusion et la retention de cristallinité ont été réalisées comme l'indiquent certaines propriétés de ces polymères. Les relations entre structure et propriétés sont décrites.

On a découvert que les groupements fluoro des polymères dérivés du P3O dépriment la cristallinité et la température de fusion. Cette investigation a été effectuée par la synthèse systématique des substituants fluoro sur le P3O et l'étude de leur propriétés. L'effet de la fonctionalité fluoro est plus prononcé dans le cas des poly(éther éther cétone)s qui possèdent des groupements phényles pendants à la chaine principale. Tandis que le polymère d'origine est très rigide, d'une haute cristallinité et insoluble, l'introduction du fluoro sur les phényles pendants élimine la cristallinité et produit des polymères amorphes et solubles.

Une modification additionnelle au polymère P3O avec les groupements acétylènes résulte à des polymères qui sont d'abord moulables à la température de fusion et suivant un chauffage produisent des structures croisées qui éliminent leur solubilité et augmentent la résistance aux solvants.

ACKNOWLEDGEMENTS

The author would like to express his most sincere gratitude to Professor Allan S. Hay, supervisor of this thesis, for his enthusiasm, excellent advice and financial support during the research and in the preparation of the thesis.

I would like to thank the Department of Chemistry providing me with the opportunity to benefit from their excellent teaching and research program.

I gratefully acknowledge Ed Elce, Martino Paventi, Gerry Barbiero and Kevin Yeomans who read preliminary versions of the manuscript and offered valuable suggestions. Special thanks to Dr. Paventi for the French translation of the abstract.

I would like to express thanks to my colleagues: Marko, Ed, Kim, Gerry and others in the laboratory for their valuable discussions and friendly help during the course of this research.

Special thanks to Professor Zhiyuan Wang for his valuable assistance and suggestions during this research.

Thanks also due to:

Dr. J. Finkenbine and Dr. Nadim Saade for mass spectrum analyses.

Dr. Rosi Hynes for X-ray analyses.

The General Electric Company for providing starting materials for this research.

CONTENTS

List of Tables

List of Figures

List of Abbrivation

DSC	differential scanning calorimetry
TGA	thermogravimetric analysis
GPC	gel permeation chromatography
Tm	melting transition temperature
Tg	glass transition temperature
Tc	crystallization temperature
ΔHm	heats of fusion
ΔHc	heats of crystallization
ΔCp	heat capacity change at Tg
DPP	2,6-diphenylphenol
$DPPF_2$	2,6-Bis(4-fluorophenyl)phenol
$DPPmF_2$	2,6-Bis(3-fluorophenyl)phenol
$DPPCl_2$	2,6-Bis(4-chlorophenyl)phenol
$DPPBr_2$	2,6-Bis(4-bromophenyl)phenol
$DPPI_2$	2,6-Bis(4-iodophenyl)phenol
$DPP(CN)_2$	2,6-Bis(4-cyanophenyl)phenol
$DPP(CF_3)_2$	2,6-Bis(4-trifluoromethylphenyl)phenol
$DPPBu_2$	2,6-Bis(4-t-butylphenyl)phenol
$DPP(OPh)_2$	2,6-Bis(4-phenoxyphenyl)phenol
DPPpF	2-phenyl-6-(4-fluorophenyl)phenol
DPPmF	2-phenyl-6-(3-fluorophenyl)phenol
DPP(phthalimidyl)	2-phenyl-6-(4-phthalimidylphenyl)phenol
DPP(CN)	2-phenyl-6-(4-cyanophenyl)phenol
DPP(OMe)	2-phenyl-6-(4-methoxyphenyl)phenol

PPO	poly(2,6-dimethylphenylene ether)
P_3O	poly(2,6-diphenylphenylene ether)
P_3OF_2	poly[2,6-Bis(4-fluorophenyl)phenylene ether]
P_3OCl_2	poly[2,6-Bis(4-chlorophenyl)phenylene ether]
P_3OBr_2	poly[2,6-Bis(4-bromophenyl)phenylene ether]
P_3OI_2	poly[2,6-Bis(4-iodophenyl)phenylene ether]
$P_3O(CN)_2$	poly[2,6-Bis(4-cyanophenyl)phenylene ether]
$P_3O(CF_3)_2$	poly[2,6-Bis(4-trifluoromethylphenyl)phenylene ether]
P_3OBu_2	poly[2,6-Bis(4-t-butylphenyl)phenylene ether]
$P_3O(OPh)_2$	poly[2,6-Bis(4-phenoxyphenyl)phenylene ether]
P_3OpF	poly[2-phenyl-6-(4-fluorophenyl)phenylene ether]
P_3OmF	poly[2-phenyl-6-(3-fluorophenyl)phenylene ether]
P_3O(phthalimidyl)	poly[2-phenyl-6-(4-phthalimidylphenyl)phenylene ether]
$P_3O(CN)$	poly[2-phenyl-6-(4-cyanophenyl)phenylene ether]
$P_3O(OMe)$	poly[2-phenyl-6-(4-methoxyphenyl)phenylene ether]
PE5	P_3O containing 5% mol of ethynyl-substituted co-monomer
PE10	P_3O containing 10% mol of ethynyl-substituted co-monomer
PEϕ5	P_3O containing 5% mol of phenylethynyl-substituted co-monomer
PEϕ10	P_3O containing 10% mol of phenylethynyl-substituted co-monomer

CHAPTER 1. INTRODUCTION

1.1. THE SCOPE OF THE RESEARCH

Since Wallace Carothers at Du Pont invented nylon in the 1930's, plastics have extensively penetrated people's daily life. We have witnessed trends where one material has evolved to replace another for efficiency, performance and economic reasons. Thermally stable polymers or high temperature polymers have been recognized as a separate area within polymer chemistry for nearly thirty years. Research in this area which was at its peak in the late fifties and early sixties was driven by aerospace and military industries. The research in this time period provided valuable knowledge about the relationship between polymer structure and thermal stability[1-7]. The characteristic structures of thermally stable polymers are those having a rigid aromatic backbone, such as a heterocyclic ladder polymer or polyphenylene. However, the inherent intractability and insolubility of these polymers severely restricted processing and consequently limited the commercial significance of these very high temperature polymers.

The engineering plastics have been developed over the past thirty years which are thermally stable materials useful from a fabrication standpoint and serviceable at elevated temperature under a variety of extreme conditions. Polymeric materials with higher temperature stability which can be processed in the melt or in solution are being developed. One example is poly(ether imide)s[8] which possesses high stability at elevated temperature and can be fabricated like a conventional thermoplastics on conventional equipment. Many of these polymers are relatively recent introductions and manufactured in small quantities and they often are high priced, in some cases approaching $100 per lb[9]. However, they generally fill a critical need in applications that require light weight, low flammability and high temperature performance and easy processing.[9-11].

The major objective of the research is the synthesis of polyphenylene ether polymers which contain aryl substituents in the 2- and 6- positions. The parent polymer poly-(2,6-diphenylphenylene ether) **P3O**[12], is a thermally stable polymer with a very high melting temperature which makes it unprocessable in the melt. One objective is to lower the melting point of **P3O** to a melt processable temperature range, which would allow the polymer to be processed as a thermoplastic using conventional processing equipment. We set up to synthesize a series of modified P3O polymers with systematically varied structures and to study their property changes. A second objective is the synthesis of biphenols from the 2,6-diarylphenols which can be converted to poly(aryl ether)s with highly rigid structures.

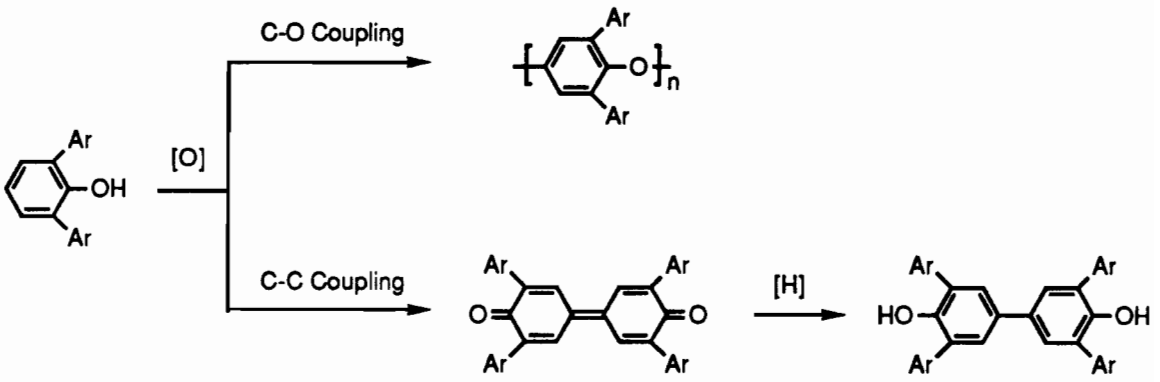

1.2. OVERVIEW OF THERMALLY STABLE POLYMERS[2-4]

High temperature polymers are defined as polymers which will maintain useful properties for a stated period of time at elevated temperature under defined conditions. The general terminology "elevated temperature" varies depending on the specific application and is clearly interrelated with the surrounding atmosphere. The practical requirements for a thermally stable polymer can be generalized as follows:

1. High softening temperature, dictated by either Tg for amorphous polymers and semicrystalline polymers or Tm for highly crystalline polymers.

2. Polymer structure is stable to thermolysis.
3. The structure is stable to chemical species in the application environment.
4. Retention of specific properties of interest in the application temperature range. Such properties depend on the application, but could include: tensile strength, modulus, wear-rate, dielectric properties, bulk, film or surface integrity.

Thermal stability in polymeric materials covers two basically different mechanisms of property loss, both of which are temperature dependent. The first mechanism is a reversable process involving thermal transitions (Tg, Tm) which determine "the softening" of a material at those temperatures. The softening temperature (i.e. the temperature at which the polymer loses properties) is directly related to the intrinsic structural features of the polymers, such as chain rigidity, chain symmetry, and intermolecular cohesion from secondary forces including van der Waals forces, hydrogen bonding or ionic interactions. For amorphous polymers, the Tg is the most important parameter in determining the softening point. However, when a polymer possesses high crystallinity, the softening point can approach the Tm. For a semicrystalline polymer, the crystalline regions in effect act as crosslinks in the polymer matrix and, therefore, the loss of mechanical properties at Tg is prevented. Cross-linking from chemical bonding between polymer chains has a similar effect in strengthening the polymer matrix above the Tg and the magnitude of the effect depends on the intensity of the cross-linking. This can be illustrated by comparing the elastic modulus of polystyrene for semicrystalline (isotactic), amorphous (atactic) and cross-linked polystyrene (atactic) samples. Figure 1.1 illustrates that amorphous polystyrene suffers a rapid drop in modulus at the Tg, while the modulus of the crystalline sample is not reduced as significantly and undergoes a rapid drop at the Tm. In cross-linked polystyrene, the viscous flow is prevented by the cross-links in the sample[13].

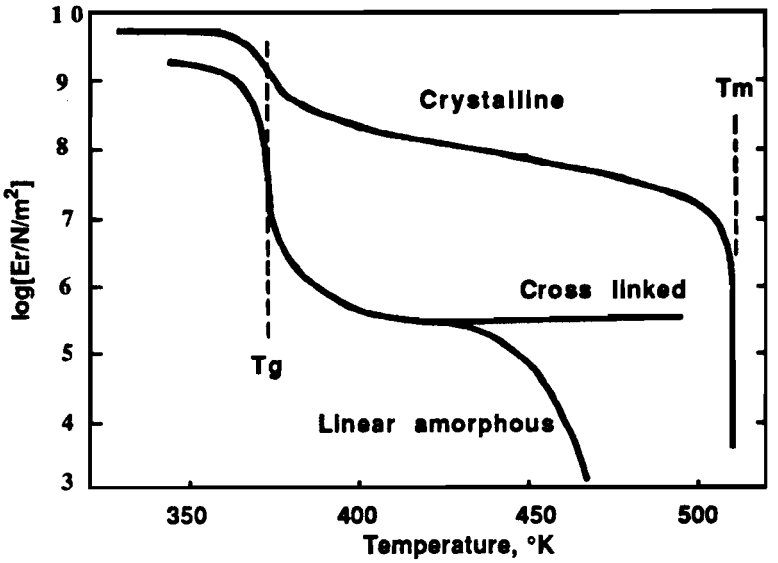

Fig. 1.1. Illustration of the variation in the modulus with increasing temperature for three types of polystyrene

The second mechanism for the loss of properties in polymers involves irreversible decomposition of the polymeric material caused by heat. The strength of the chemical bonds imposes an upper limit on the stability of the polymers. The bond dissociation energy of a carbon-carbon single bond is 83.6 kcal/mole, while a carbon-carbon double bond is 145.8 kcal/mole. In an aromatic system, an extra resonance stabilization of 40-70 kcal/mole is added. Hence, the polymer systems with the highest temperature stability will be those containing a minimum of hydrogen and a maximum of highly stable structural units such as aromatic and /or aromatic heterocyclic rings. Therefore, polyphenylene and aromatic heterocyclic ladder polymers are amoung the most stable polymer systems studied. Additional stability can be derived from secondary valence forces which increase thermal stability by slowing down the degradation process.

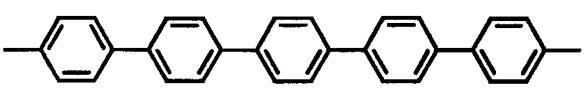

Polyphenylene

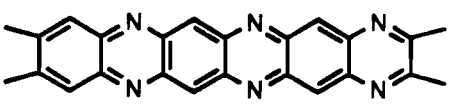

Polyquinoxaline

1.3. PROCESSING REQUIREMENTS FOR THERMALLY STABLE POLYMERS[5,9]

In the initial phase of thermally stable polymer research, the inherent stability of organic compound based systems was realized. However these highly stable polymers which were characterized by highly rigid aromatic backbones were often infusible and insoluble. Subsequently, efforts were focused on structural modifications which would provide processing feasibility. The general strategy was to introduce flexibility into such rigid systems to decrease the softening point and increase solubility. Almost without exception these changes led to lower stability, but were nonetheless necessary if applications were to be developed. The most common method was to incorporate flexible linkages into the backbone of rigid polymer systems. In order to maintain high stability toward thermolysis, linkages with weak bonds must be excluded. In addition, oxidative and hydrolytic stability in the application environments is critical. This narrows the number of candidate systems significantly, eliminating those groups with alkyl hydrogens which are susceptible to oxidation; and esters or amide groups which are susceptible to hydrolysis. To meet these requirements, desirable functional groups are ether, sulfide, sulfone and ketone groups instead of alkyl, alicyclic, or amino functions. These characteristic structural features can be seen in most of the successfully developed high performance engineering thermoplastics manufactured today, i.e. a rigid aromatic moiety which gives high stability and a flexible linkage which allows facile fabrication.

Commercial High Temperature Polymers

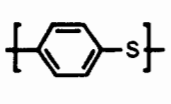

PPS

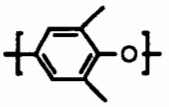

PPO

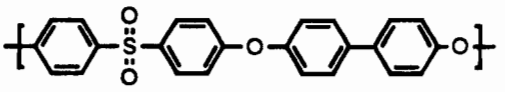

Polyethersulfone

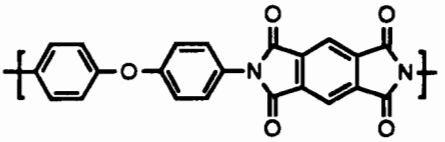

Polyetherimide

1.4. HISTORY AND PROPERTIES OF P3O[10]

In 1956, Allan S. Hay of General Electric discovered a novel synthesis of a high molecular weight linear polyphenylene ether by the oxidative polymerization of 2,6-dimethylphenol[14]. The polymerization takes place in solution at room temperature by the oxidation of the phenol with molecular oxygen in the presence of an amine complex of a copper salt. The polymer was called PPO® resin. Among the various substituted phenols, 2,6-dimethylphenol gave the polymer with the most attractive properties.

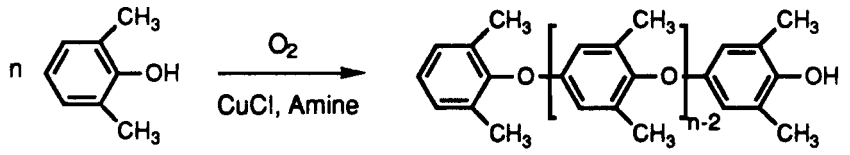

2,6-Dimethylphenol **PPO**

Subsequently, because of the property profile of this polymer, an effort to explore a commercial process for making the monomer, 2,6-dimethylphenol, was undertaken and resulted in a simple reaction discovered by Stephen Hamilton at GE[15]. However, PPO was found to be difficult to process due to the high Tg which required high processing temperatures and resulted in a pronounced tendency to oxidize at the process temperatures. Fortunately, a rather rare compatibility was found between PPO and polystyrene throughout the composition range. The reduced melt viscosity and lower processing temperature required for this blend resulted in a processable material. The blends appeared to combine the favorable features of both polymers and it was named Noryl® Resin. Noryl resin is one of the five major engineering thermoplastics manufactured today[16,17].

A few years after discovery of PPO, Hay extended this reaction to the synthesis of the totally aromatic polymer from 2,6-diphenylphenol[12]. The monomer can be readily prepared from cyclohexanone by a two-step reaction. The high molecular weight polymer can be obtained by oxidation with molecular oxygen using copper-tetramethylethylene diamine complex as catalyst at ambient temperature. The totally aromatic composition

and the highly rigid backbone of P3O make this material an ideal candidate for potential application as a high temperature material. Attempts at commercial development were made in early 70's and a detailed property evaluation has not been published. The available property data for this material is listed in the following table[18-20].

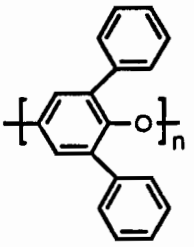

P3O TENAX^{R}

Table 1.1. Properties of P3O

Tg	235 °C
Tm	480 °C (onset), 501 °C(peak)
Density, g/cm^3	1.213 (crystalline); 1.140 (amorphous)
Coefficient of thermal expansion below Tg	45.5 x 10^{-6} (α_o, °C^{-1})
Coefficient of thermal expansion above Tg	102 x 10^{-6} (α_ω, °C^{-1})
Tensile Modulus (psi)	4.6 x 10^5
Moisture absorption in air at 65%RH	<0.2%
Dissipation factor (tan δ in air at 20 °C, 50 Hz)	2.5 x 10^{-4}
Dielectric constant (20°C; 50Hz)	2.76

P3O has a highly regular arrangement of pendant phenyl rings along the backbone which results in the crystallizability of this polymer. It is crystallized readily by a thermal treatment or by the interaction with solvents. The thermal crystallization occurs above the Tg with a maximum rate in the temperature range of 370 °C to 400 °C. The higher transition temperatures of P3O apparently results from the bulky phenyl substitution which yields a very rigid backbone. In polyphenylene ether structures, this trend can be seen in

the series in the following table. Phenyl substitution appeares to raise the melting temperatures more significantly than the Tg[21].

Polyarylether	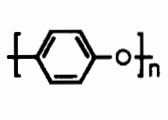	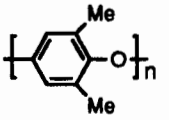	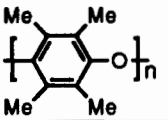	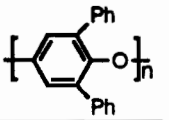
Tg, °C	90	207	-	235
Tm, °C	262	262	290	480

However, the rigid backbone of P3O which results in the high transition temperatures does not completely inhibit molecular motion at temperatures below the Tg and a well defined subglass transition was observed in a DMTA study[22,23] in which it was suggested that this material should have good impact strength which is characteristic for polyarylether polymers. The totally aromatic rings linked with thermally stable ether linkages impart to this polymer a very high thermal stability and chemical inertness toward bases and acids. The nonpolar nature of the P3O backbone also contributes to its very low dielectric constant and very low moisture absorption.

The presence of a crystalline phase in P3O has a profound influence on its properties, especially in the high temperature region where the most interest lies. This is illustrated in figure 1.2 in which the presence of crystalline region not only largely reduces the magnitude of the mechanical loss, but also produces a significant shift toward higher temperatures[18].

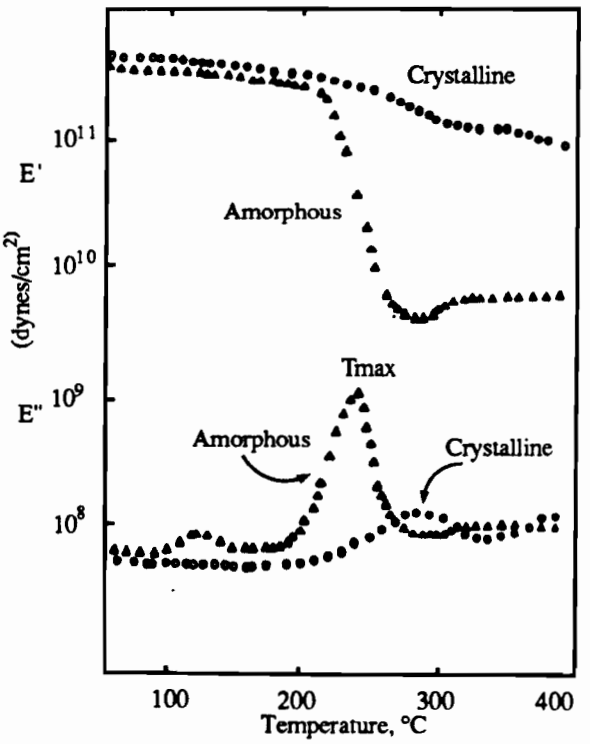

Fig. 1.2. Dynamic-mechanical relaxation spectrum of amorphous and crystalline P3O. (heating rate: 5°C/min., at 110 Hz).

The dielectric properties of P3O are also significantly affected by the presence of crystalline regions. Figure 1.3 shows that nearly a 100 °C increase in dielectric relaxation results when the crystallinity of P3O changes from 0% to 52% by repeated thermal cycle treatments[18].

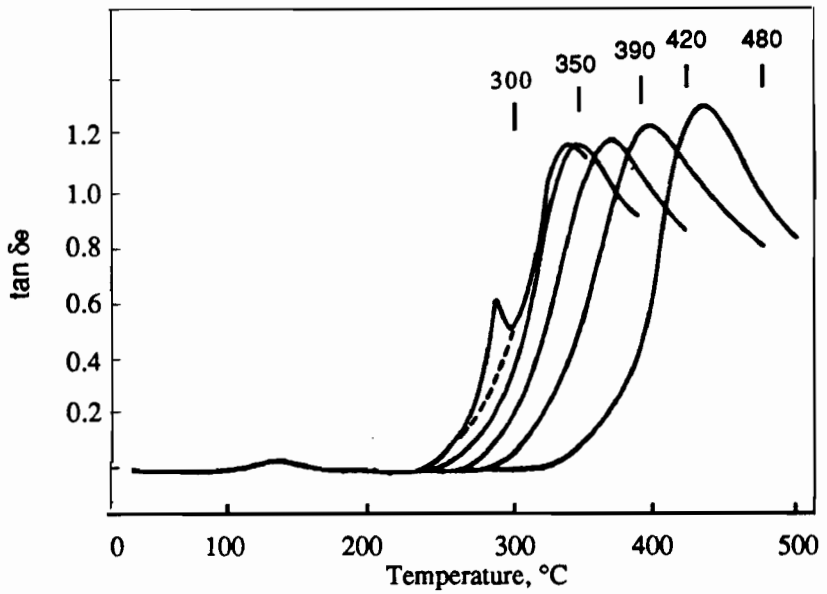

Fig. 1.3. Effect of crystallinity on dielectric relaxation (heating rate 5 °C/min. at 110 Hz)

P3O possesses a very attractive property profile for applications as a high temperature material. However, it cannot be melt-processed because of the very high melting point of P3O which is close to the decomposition temperature. Therefore, all the attempted development was limited to the solution processable materials, such as commercial development for packing material on high temperature GC[19] and fibers for electrical insulation materials[20]. In order to attain the desired melt processability of P3O, a series of efforts were made to modify this material to reduce the melting point, therefore making melt processing feasible. In addition, the maintenance of crystallinity is also a critical requirement for maintaining the most favorable properties.

The initial attempts made by Hay and Clark[24] introduced a series of substituents into the P3O backbone as follows.

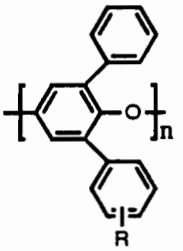

R = p-CH_3, m-CH_3, p-t-Bu, o-Ph, m-Ph, etc.

The results indicated that this unsymmetrical substitution in the polymer structure does not change the Tg significantly but results in complete loss of crystallinity for all the polymers prepared. This suggested that chain symmetry is critical for the resulting polymer to maintain any crystallizability. Hence, attempts[25] were subsequently confined to the preparation of some symmetrically substituted derivatives as follows.

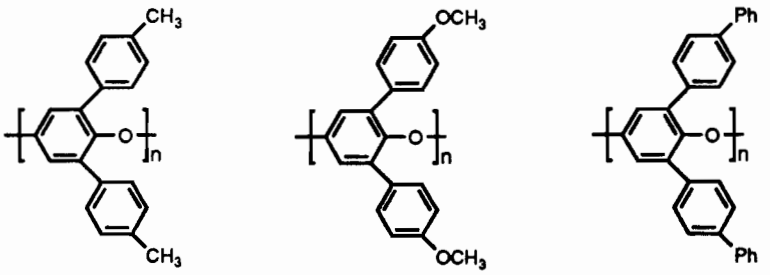

It was found that when the substituents are methyl groups, the polymerization proceeds to high molecular weight and the polymer obtained crystallizes only with difficulty. With methoxy substituents high molecular weight polymer could not be obtained by direct oxidation of the phenol. The polymer was highly crystalline and it precipitated from the reaction mixture. The polymer has a melting point of 365 °C. When the substituents are phenyl even very low molecular weight oligomers are insoluble.

1.4. PROPOSAL

In the past decades, the growing demand from the electrical and electronic industries for polymeric materials with high temperature performance and excellent dielectric prop-

erties resulted in extensive research in the design and development of high temperature polymeric materials[9,26]. This resulted in high temperature thermoplastics such as poly (ether sulfone)[27,28] and poly(ether imides)[8,27] which are widely used in electric/electronic components, such as connectors, printed circuit boards, coil formers, etc. The unique property combination of P3O, i.e. high temperature stability and very low dielectric constant, appears to position P3O as an ideal candidate for applications in this area where high temperature performance and low dielectric constant are mostly desired. A comparison of the basic properties of P3O with commercial poly(ether sufone) Udel and poly (ether imide) Ultem is listed in the following table.

Table 1.2. Property Comparison of P3O with Udel and Ultem

Polymer	Tg, °C	Tm, °C	HDT*, °C	Tensile Modulus(psi)	dielectric constant
P3O	235	501	**	4.6×10^5	2.76 (50Hz, 20°C)
Udel	184	-	174	3.6×10^5	3.51 (60Hz, 20°C)
Ultem	215	-	200	4.3×10^5	3.15 (1kHz, 20°C)

* Heat distortion temperature. ** Data unavailable.

The unique structural features of P3O make it attractive in comparison with other commercial high temperature polymers, such as poly(ether sulfone), poly(ether ether ketone) and poly(ether imide) whose high softening temperatures originate from both rigid backbones and strong chain cohesion due to dipole interaction. However, a low dielectric constant which is desired in many specific applications is not possible due to the presence of the polar groups in these polymers which results in dielectric constants in the typical range of 3.10 to 3.50. While the high transition temperatures in P3O mainly originate from its rigid chain structure, the absence of polar groups in the polymer results in this material having a very low dielectric constant and very low moisture absorption.

Considering this attractive property combination, i.e. high temperature performance and

very low dielectric constant, it would be of particular interest if this material could be processed on conventional equipment for potential applications. However, as we described early, sufficient crystallinity is critical for the resultant polymer to maintain most favorable properties. Therefore, we set out to meet two major requirements: 1, reduce the Tm of P3O below the decomposition temperature; 2, maintain a high degree of crystallinity in the polymers.

The previous studies indicated the importance of chain symmetry in maintaining crystallizability in the resultant polymers, so we designed a series of P3O polymers with symmetrical arrangements of the substituents on the pendant rings. Since ortho substitution would be expected to inhibit the polymerization, the substitution positions on the pendant rings are confined to either the para or meta positions.

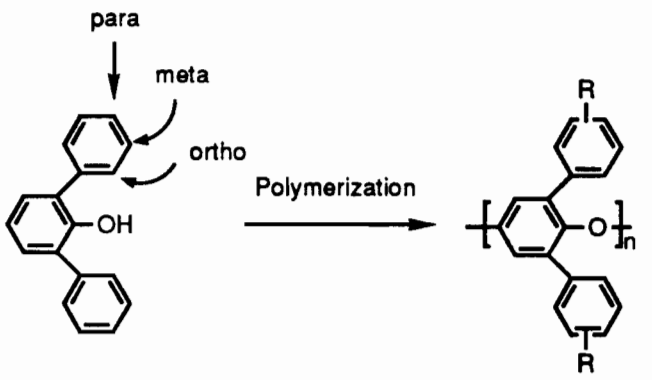

Other information from the previous study indicated that the crystallizability of the substituted polymers is dependent on the nature of the substituents. For example, symmetrically substituted P3O with methyl groups has a low degree of crystallinity while the substitution with methoxy is highly crystalline and insoluble. Since there was no obvious trend to follow, we selected a relatively wide spectrum of monomers with substituents ranging from polar to nonpolar, and small to bulky groups. Also, the substituents chosen have to be thermooxidatively stable, so that high thermal stability can be achieved. Since the previous investigation did not cover unsymmetrically substituted P3O polymers with polar groups, we also planned to prepare some unsymmetrically substituted P3O mono-

mers with polar substituents. The polymers we set out to synthesize are shown below:

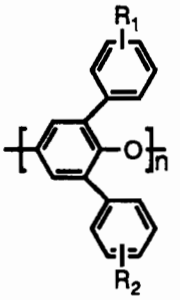

R_1 = p-t-Bu p-OPh p-CF_3 p-F m-F p-Cl p-Br p-I p-CN p-F m-F p-CN p-OMe p-phthalimidyl

R_2 = p-t-Bu p-OPh p-CF_3 p-F m-F p-Cl p-Br p-I p-CN H H H H H

In addition, the property variations resulting from the systematically structural variations of the resulting polymers should provide an ideal system for studying the structure-property relationship in this rigid polymer system.

References:

1. Frazer, A. H., High Temperature Resistant Polymers, *Polymer Reviews*, Vol. 17., John Wiley & Sons, Inc., **1968**.
2. Conley, R. T., *Thermal Stability of Polymers*, Marcel Dekker, Inc., New York, **1970**.
3. Wright, W. W., The Development of Heat-Resistant Organic Polymers in *Degradation and Stabilisation of Polymers*. Edited by Geqskens, G., John Wiley & Sons., Inc., **1975**, p43.
4. Arnold, Jr. C., Stability in High-Temperature Polymers in *Macromolecular Rev.*, Vol. 14, **1979**, p265.
5. Cassidy, P. E., *Thermally Stable Polymers*, Marcel Dekker, Inc., New York & Basel, **1980**.
6. Critchley, J. P., Knight, G. J., and Wright, W. W., *Heat Resistant Polymers*. Plenum Press., **1983**.
7. Hergenrother, P. M., Heat-Resistant Polymers in *Polymers: An Encyclopedic Sourcebook of Engineer ing Properties*, Edited by Kroschwitz, J. I., Wiley & Sons., Inc., **1987**. p427.
8. Wilson, D., Stenzenberger, H. D., and Hergenrother, P. M., Polyimides, Chapman and Hall, New York, **1990**.
9. Reisch, M. S., *Chemical and Engineering News*, **1989**, Sept. 4, p21.
10. Seymour, R. B., and Kirshenbaum, G. S. "High Performance Polymers: Their Origin and Development" *Proceedings of the Symposium of the History of High Performance Polymers at the American Chemical Society Meeting held in New York*, **1986**, April 15-18.
11. Fox, D. W., and Peters, E. N., Engineering Thermoplastics: Chemistry and Technology in *Applied Polymer Science*, Edited by Tess, R. W., and Poehlein, G. P., ACS Washington, D.C., **1985**, p495.
12. Hay, A. S., Macromolecules, 1969, 2, 107.
13. Cowie, J. M. G., *Polymers: Chemistry & Physics of Modern Materials*, , Chapman and Hall, New York, **1973**. Chapter 10, p275.
14. Hay, A. S., Blanchard, H. S., Endres, G. F., and Eustance, J. W., *J. Am. Chem. Soc.*, **1959**, 81, 6335. Hay, A. S., **U.S.** 3,306,874; 3,306,874 (GE).
15. Hamilton, S. B., US Pat., 3,446,856.
16. Aycock, D., Abolins, V., and White, D. M., *Encyclopedia of Polymer Science and Technology*, Wiley, New York, **1985**, 13, 1.

17. Warren, R. I., *Polymer Engineering and Science*, **1985**, Vol: 25, 477.

18. Wrasidlo, W., *Macromolecules*, **1971**, 4, 642.

19. *Technical Bulletin* No. 24., of Applied Science Laboratories, Inc., State College, Pennsylvania, 16801.

20. Vermeer, J., Boone, W., Bussink, J., and Breakel, H., ***1970 Annual Report, Conference on Electrical Insulation and Dielectric Phenomena***, NAS Publ. p52. **CA**. 153114p, **1971**, 75.

21. Cassidy, P. E., *Thermally Stable Polymers*, Marcel Dekker, Inc., New York & Basel, **1980**. p48.

22. Tonelli, A. E., *Macromolecules*, **1973**, 6, 503.

23. Petris, S., *Makromol. Chem.*, **1972**. 1621.

24. Hay, A. S. and Clark, R. F., *Macromolecules*, **1970**, 3, 533.

25. Hay, A. S., and Dana, D. E., *J. Polym. Sci. Polym. Chem. Ed.*, **1989**, 27, 873.

26. Lupinski, J. H., and Moore, R. S., *Polymeric Materials for Electronics Packaging and Interconnection*, ACS, Washington, D. C., **1989**.

27. Margolis, J. M., *Engineering Thermoplastics: Properties and Applications*, Marcel Dekker, Inc., **1985**.

28. Harris, J. E. and Johnson, R. N., *Encyclopedia of Polymer Science and technology*, Vol. 13, **1985**. 196.

CHAPTER 2. MONOMER SYNTHESIS

2.1. INTRODUCTION

The principal objective of this section is to describe the synthesis of a series of substituted 2,6-diphenylphenol (**DPP**) monomers with a wide spectrum of substituents on the pendant phenyl rings of **DPP**. A general approach to the synthesis of these monomers with a variety of substituents is not feasible. Therefore we have to examine specific approaches to the synthesis of the monomers with different substituents.

A literature search revealed that the synthesis of the parent monomer, 2,6-diphenylphenol (**DPP**), represents the simplest procedure for constructing this type of diarylphenol. It is a two-step synthesis in which cyclohexanone is self-condensed in the presence of sodium hydroxide to produce a mixture of trimers followed by dehydrogenation with palladium on carbon as catalyst[1].

Scheme 2.1

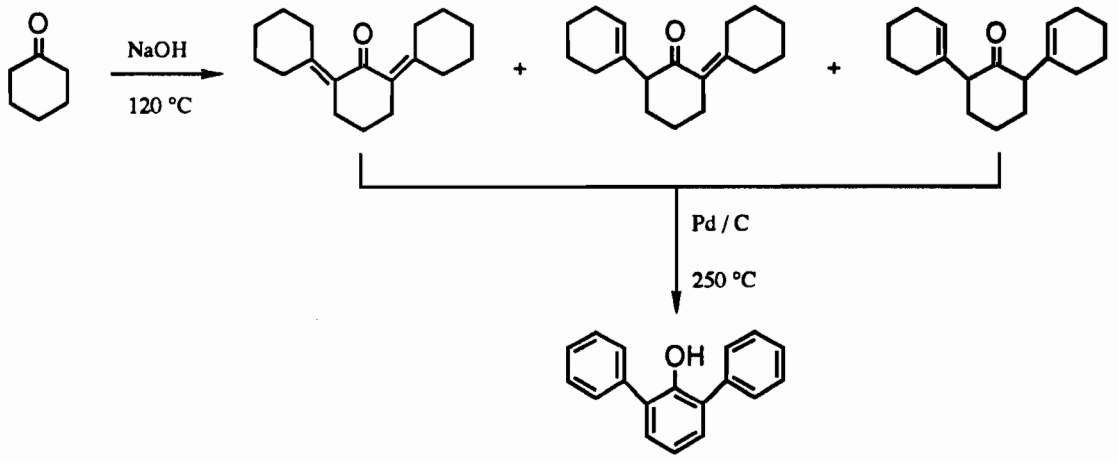

1 (DPP)

However, this approach can not be used for introduction of the substituents symmetrically onto pendant phenyl rings of **DPP. DPP** has also been synthesized by Friedel-Craft alkylation of phenol with cyclohexene and the resulting 2,6-dicyclohexylphenol can

then be converted into DPP by dehydrogenation. However, under $AlCl_3$ catalysis, the low regiospecific preference in alkylation of phenol with substituted cyclohexenes would make this procedure impractical[2] (scheme 2.2).

Scheme 2.2

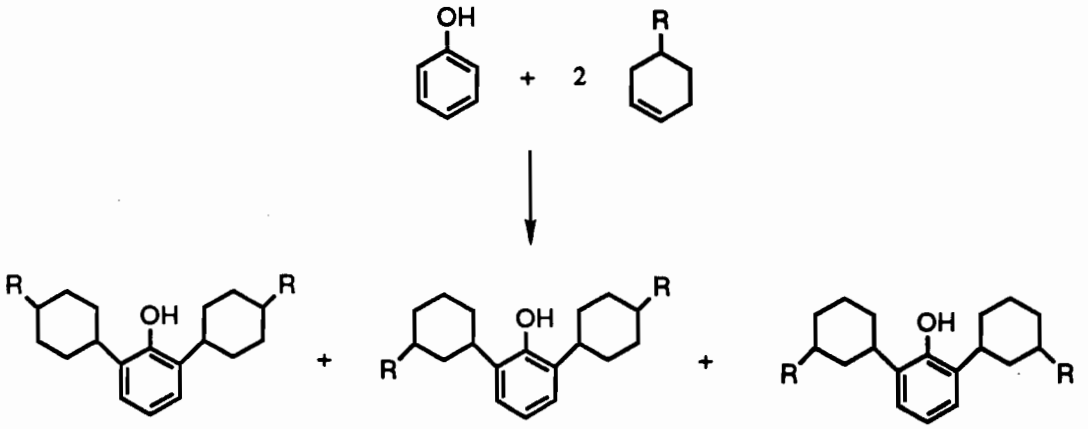

Another potential route to 2,6-diarylphenol was reported by Hay and Clark[3] in which the condensation of acrolein with dibenzyl ketone yielded the cyclohexenone and subsquent dehydrogenation gave the phenol **2** (scheme 2.3). However the extensive polymerization of acrolein under such reaction condition precludes this route from being used as a practical method.

Scheme 2.3

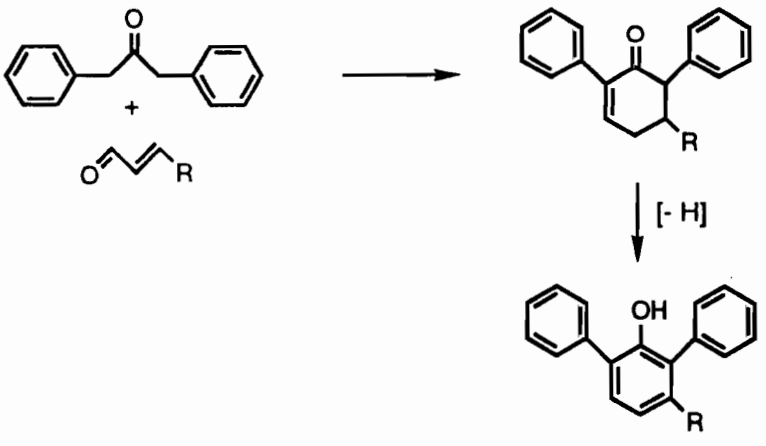

2 a R = H
b R = Ph

Hay and Dana[4] used 1,3-dibromopropane to condense with dibenzyl ketones under basic conditions in the presence of a phase transfer catalyst to give cyclohexanone intermediates in moderate yields. The intermediates were readily converted into 2,6-diarylphenols in good yields with Pd/C as catalyst at elevated temperature. The precursor substituted dibenzyl ketones are prepared from the corresponding phenylacetic acid esters by a Claisen condensation[4]. This method provides one option for the synthesis of some of our monomers.

Scheme 2.4

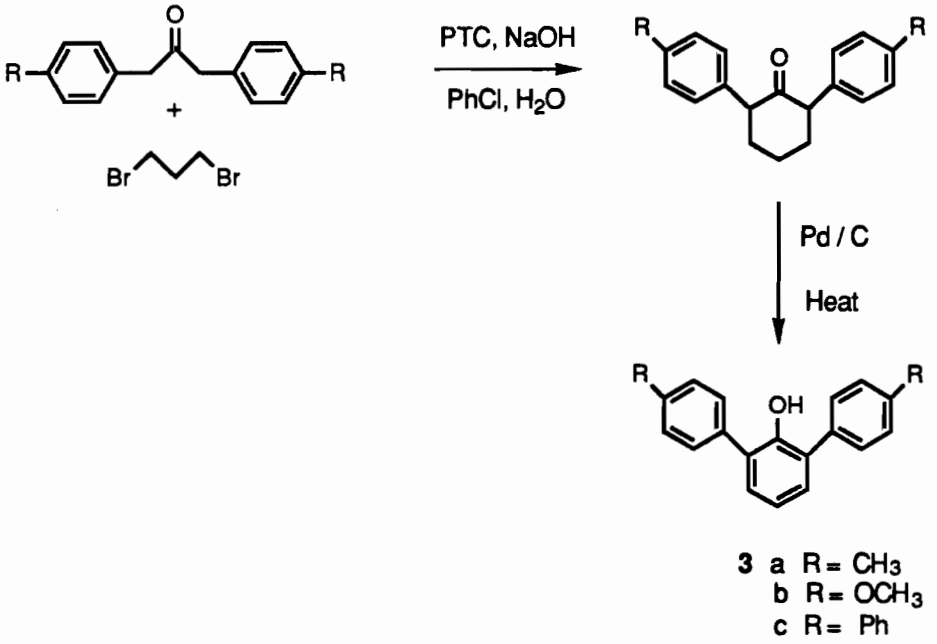

3 a R= CH_3
b R= OCH_3
c R= Ph

Hypothetically, a more convergent approach to substituted diarylphenols would be through direct regiospecific ortho arylation of phenol. Barton and coworkers developed a procedure[5,6] in which phenol reacts with an arylated Bi^V reagent to give an O-Bi bonded intermediate which decomposes under heating to give exclusive ortho phenylation products. They demonstrated that even the very crowded phenol **4** in scheme 2.5 can be prepared from a highly hindered phenol in good yield by this technique. Although this reaction proceeds under very mild conditions, the bismuth(V) reagents are not readily available and the preferred base used, N-tert-butyl-N',N''-tetramethylguanidine (**BTMG**) is not commercially available[6, 7].

Scheme 2.5

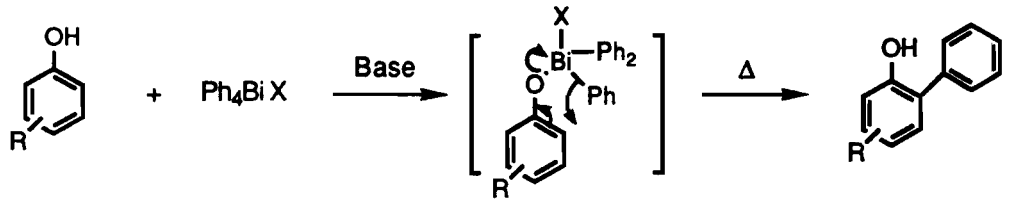

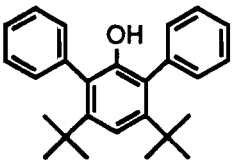

4

In the past decade, the palladium(0)-catalyzed cross coupling reaction has become a powerful tool in constructing aromatic systems by aryl-aryl bond formation[8]. Since palladium is coordinated relatively weakly by oxygen, the reaction has proved to be tolerant to such functionality either adjacent or remote from the reacting center[9,10]. The synthons for the aryl carbanion in the sequence could be arylzinc[11], arylmagnesium[12] or nickel reagents[13] but with some limitations because of their lability toward some functionalities. The scope of the reaction was later extended by Suzuki with the application of aryl boric acid as the synthon of the carbanion for the cross coupling reaction[14].

Scheme 2.6

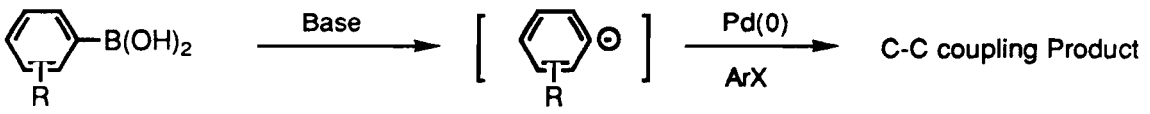

The first application of the Suzuki reaction to the regiospecific construction of diarylphenols was reported by Snieckus[15,16]. The regioselectivity was achieved by a directed metalation chemistry and the resulting carbanion yielded arylboric acid by quenching with trialkoxy borate. The subsequent cross-coupling reaction of the boronic acid with arylbromide gives the arylation product. The bisarylation of the protected phenol can be accomplished by repeating the same reaction sequence.

Scheme 2.7

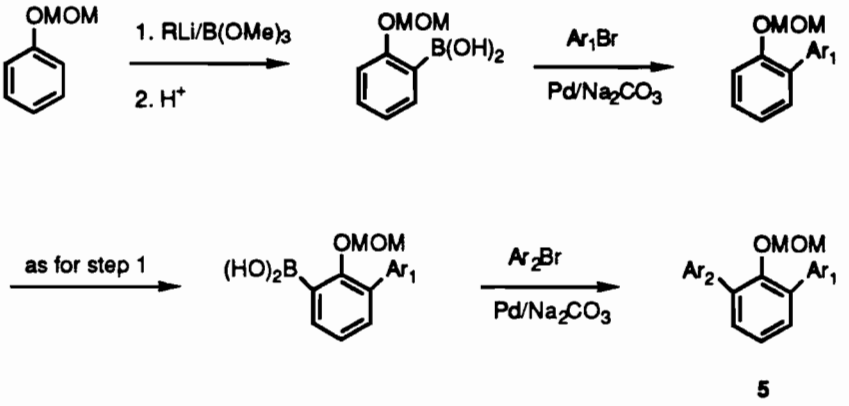

5

Despite the recognized tolerance toward oxygen functionality in palladium catalyzed bond formation, the cross coupling reaction had never been extended to the arylation of free phenols until recently Heiner Jendralla and Li-Jian Chen[17] reported a direct arylation of phenol by a palladium(0)-catalyzed coupling reaction with excess Grignard reagent. This method works extremely well for monoarylation, but bis-arylation in the ortho positions of phenols gave only a very low yield of a mixture (**6** & **7**, scheme 2.8). However this procedure demonstrated the tolerance of palladium catalysis to free phenol systems. This approach implied a possible procedure for constructing disubstituted arylphenols in a very few steps.

Scheme 2.8

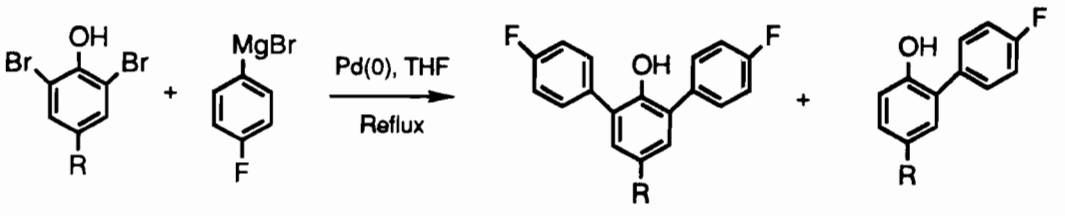

R = CH_3, F

6 a R = F trace
b R = CH_3 22%

7 a R = F 14%
b R = CH_3 20%

2.2. RESULTS AND DISCUSSIONS

Considering the substituents we wish to be introduced and the available synthetic tactics, three possible entries into these target molecules are illustrated in scheme 2.9.

(1) *The formation of the central phenolic moiety by condensation reactions of substituted dibenzylketones with a 1,3-dihalopropane and subsequent dehydrogenation to furnish the final product.*

(2) *Direct introduction of substituents onto the pendant phenyl rings of DPP by electro - philic substitution reactions.*

(3) *Aryl-aryl bond formation by palladium (0) catalyzed cross coupling reaction at both ortho positions of phenols.*

The specific approach utilized will depend on the nature of the substituents to be introduced. In the following sections we will examine these approaches for synthesizing various substituted monomers.

Scheme 2.9

Synthetic Approaches to 2,6-Diarylphenols

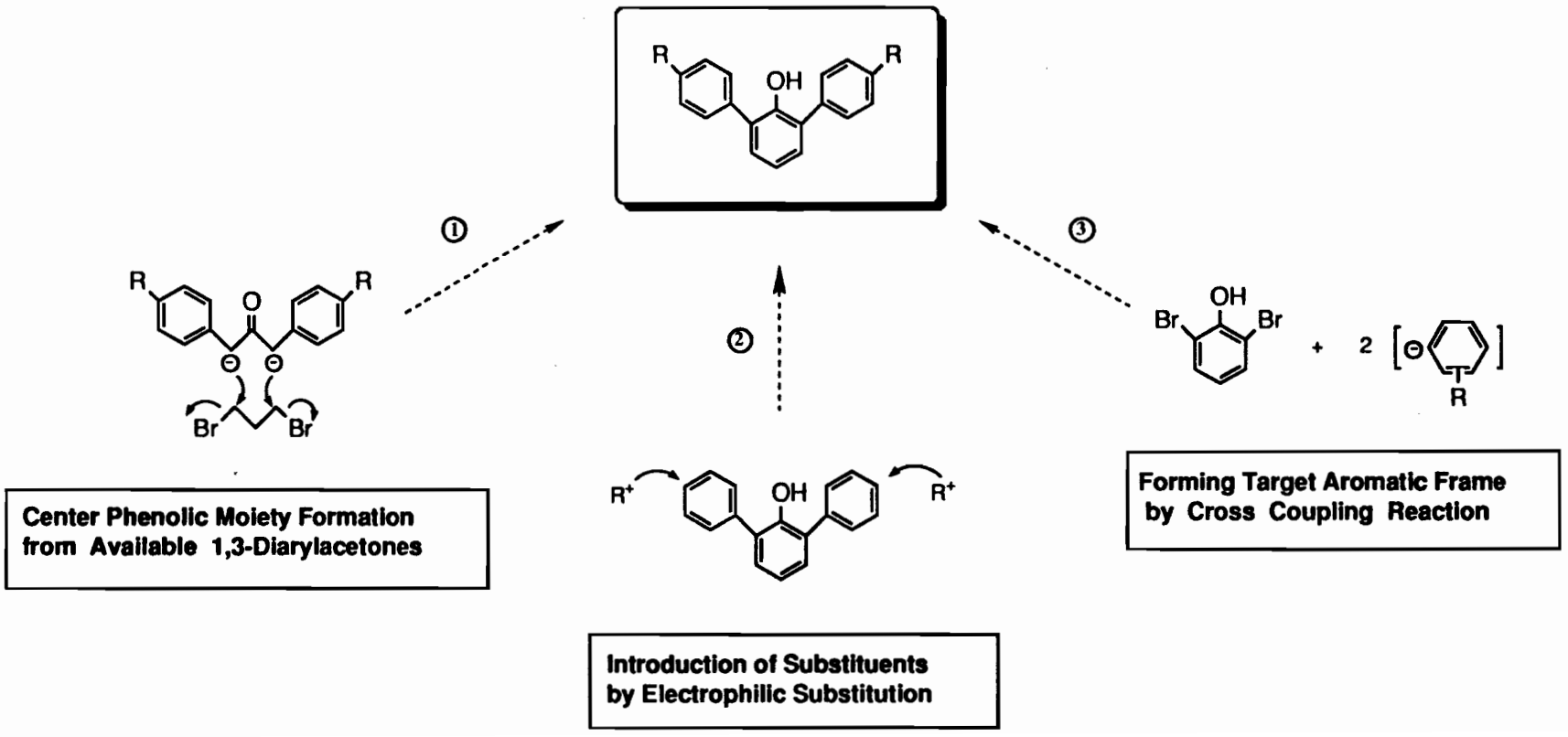

2.2.1. Condensation Approach

In the condensation procedure, the key step is the preparation of the precursor substituted dibenzyl ketones. In Dana and Hay's approach, the substituted dibenzyl ketones are prepared by a two step sequence from the corresponding phenylacetonitriles. Recently Wolfe[18] reported the preparation of bis(4-bromobenzyl)ketone in 74% yield by reacting readily available 4-bromophenylacetic acid with magnesium oxide at high temperature under vacuum. We have found that the fluoro and chloro substituted dibenzyl ketones, **9a** and **9b**, can be prepared by this method in good yield. In this reaction it is critical that the temperature be maintained as low as possible in order to avoid decomposition of the salt formed and this requires that the pressure be maintained as low as possible. 4-Methoxyphenylacetic acid gives only very low yield in this reaction because of extensive decomposition during the reaction.

The 4-fluoro and 4-chloro substituted dibenzyl ketones **9a** and **9b** were then converted to the corresponding cyclohexanones **10a** and **10b** in moderate yield. During the subsequent aromatization step with Pd/C as catalyst in diphenylether, 2,6-bis(4-fluorophenyl)phenol **11a** was obtained in good yield. But the aromatization of **10b** only gave a very low yield of desired product under the conditions that were successful with **10a** because of extensive reductive cleavage of the Ar-Cl bond as shown in scheme 2.11 (C).

Scheme 2.10

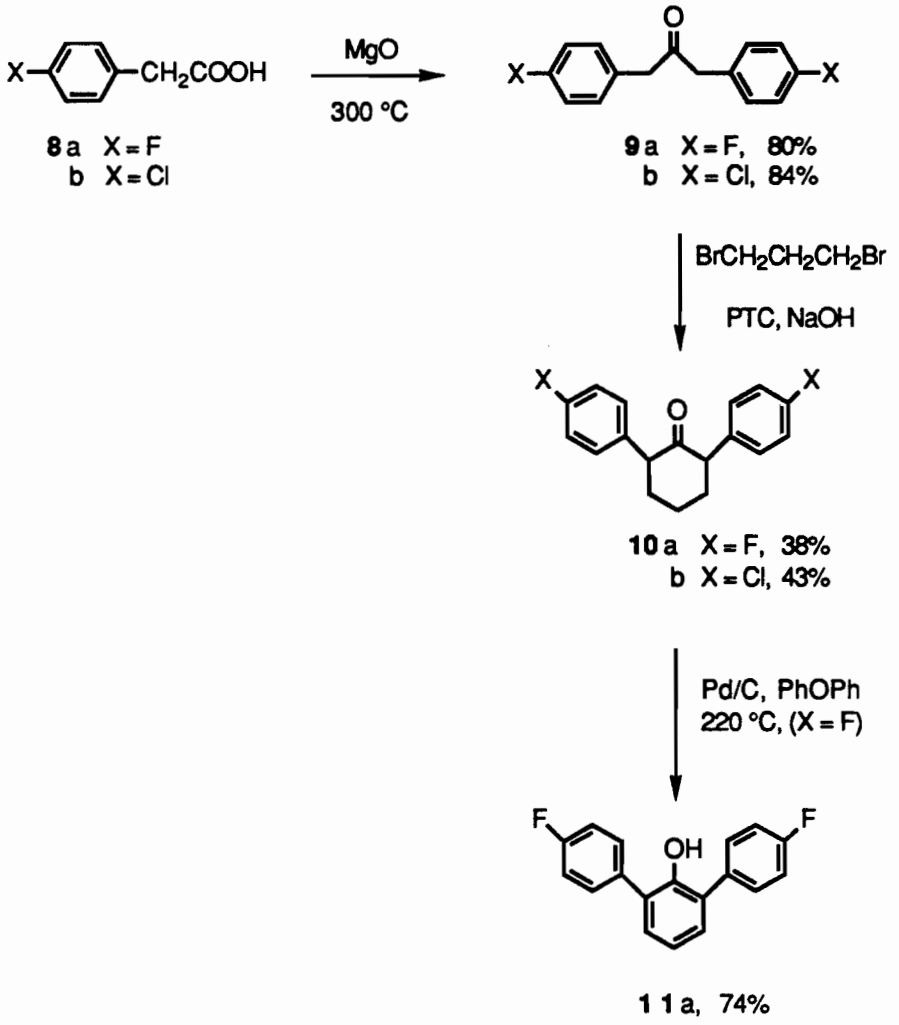

The attempted aromatization of **10b** under milder condition with sulfur as dehydrogenating agent[19] also failed to give an acceptable yield because the reductive side reaction still can not be efficiently eliminated (C, scheme 2.11). A further attempt was made by applying a two-step sequence[20] including first the bromination of the two α-hydrogens of **10b** followed by an elimination reaction under basic condition. Subsquent isomerization afforded the final product **11b** in 41% yield (B, scheme 2.11). Further improvement in this conversion was achieved by using the sulfuric acid-acetic anhydride system[21] which yields the acetate of the aromatized intermediate. Subsquent hydrolysis yielded **11b** in 62% overall yield (A, scheme 2.11).

Scheme 2.11

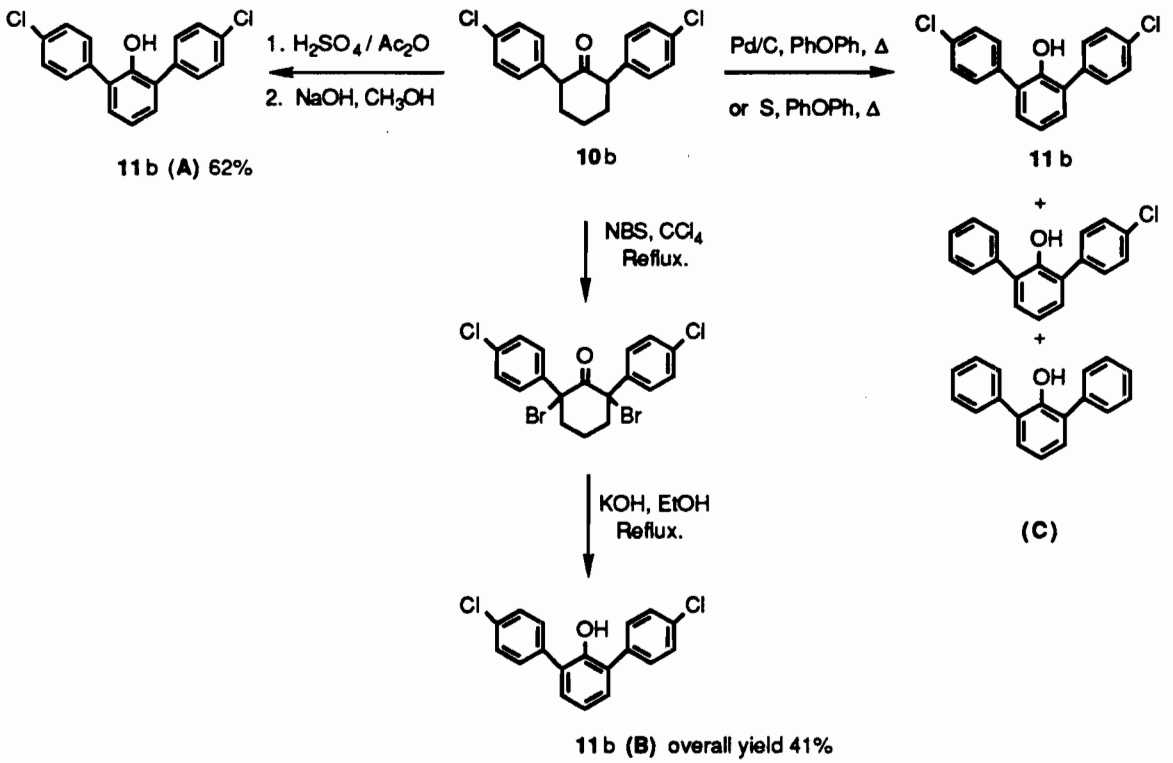

2.2.2. Electrophilic Substitution Approach

The above approach is not adaptable to the preparation of monomers bearing substituents such as bromo or iodo groups since such functional groups will not survive the dibenzyl ketone forming reaction at high temperature, and also dehalogenation by hydrogenolysis would be expected to dominate the reaction in the aromatization step. The most straightforward method appears to be introduction of substituents such as bromine, iodine and t-butyl groups onto the pendant rings of readily available **DPP** by electrophilic substitution reactions after properly blocking the center phenolic ring of **DPP**.

The t-butyl group appeared ideal for the protection of the para position since its stability towards halogenation reactions and the conditions used for deprotection of phenol are well defined. However, the desirable selective t-butylation of **DPP** at the para position of the central phenol moiety turned out to be much more difficult than expected. The typical Friedel-Crafts conditions[22] listed below all failed to give satisfactory selectivity.

Table 2.1. Selective t-butylation of **DPP 1**

Reagent	Catalyst	Solvent	Result
t-BuBr	$AlCl_3$		No selectivity
"	F_3CSO_3H		"
Isobutene	Oleum		"
"	F_3CSO_3H		"
t-BuBr	Amberlite		No reaction
Isobutene	Amberlite		"
t-BuOH	H_3PO_4		"
"	$ZnCl_2$		"
Isobutene	CH_3SO_3H		60% + (Oligomers of Isobutene)

We then attempted to introduce the t-butyl group via a transalkylation reaction in which 2,6-di-t-butyl-4-methylphenol was used as t-butyl donor with aluminum chloride as catalyst. By using the deactivated catalyst $AlCl_3$-$CH_3CH_2NO_2$ complex, t-butylated product **12** was obtained in 63% yield. Methylation of **12** with dimethyl sulfate in the presence of a phase transfer catalyst afforded the fully protected intermediate **13**.

Scheme 2.12

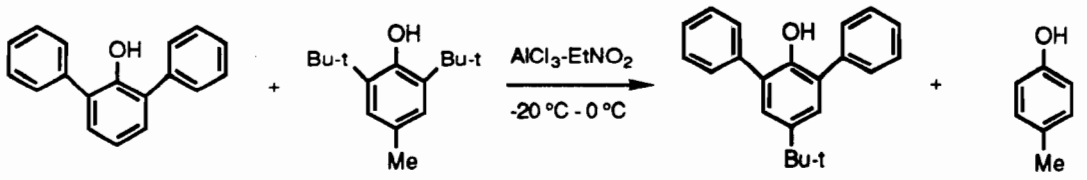

1 **12** 63%

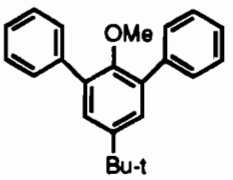

13

The attempts to introduce the bromo function onto the pendant rings of **DPP 1** are outlined in scheme 2.13. For bromination of **12**, stronger bromination conditions are required due to the less nucleophilic nature of the pendant phenyl ring compared to the phenol moiety. A literature search revealed that the bromination conditions[23] for relatively deactivated aromatic nuclei usually employ some oxidative co-reagents and therefore are not adaptable to the free phenol system. With a large excess of bromine in relatively concentrated acetic acid solution, we obtained the acetate derivative **14a** in moderate yield. Since the only side product in the reaction is mono bromination product, the potential yield could be further improved with a recycle sequence. Saponification of **14a** yields the phenol **14b**. The t-butyl group was successfully removed by a trans-t-butylation reaction with benzene as the t-butyl aceptor to afford **15** without detectable debromination product being formed. Compound **15** then was treated with cuprous cyanide in NMP to afford **16** in good yield. Intermediate **13** was subjected to a large excess of bromine in acetic acid to yield **17**. Compound **17** was then allowed to react with phenoxide catalyzed by copper chloride to yield **18**. The final product **20** was obtained efficiently by demethylation of **18** with boron tribromide followed by a transalkylation reaction catalyzed by aluminum chloride in benzene.

Scheme 2.13

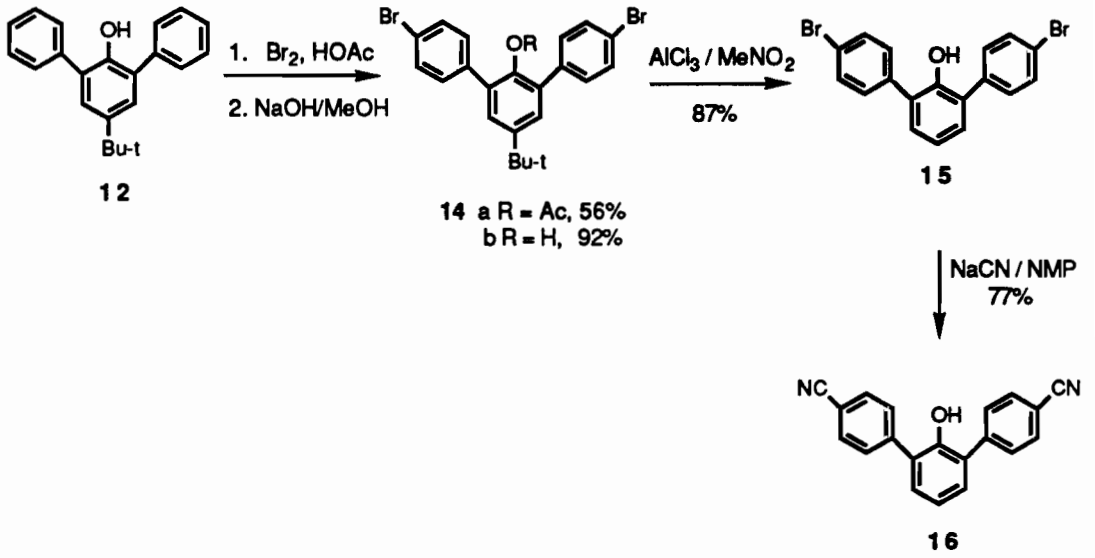
OH
Bu-t
12
1. Br2, HOAc
2. NaOH/MeOH
Br
OR
Br
Bu-t
14 a R = Ac, 56%
b R = H, 92%
AlCl3 / MeNO2
87%
Br
OH
Br
15
NaCN / NMP
77%
NC
OH
CN
16

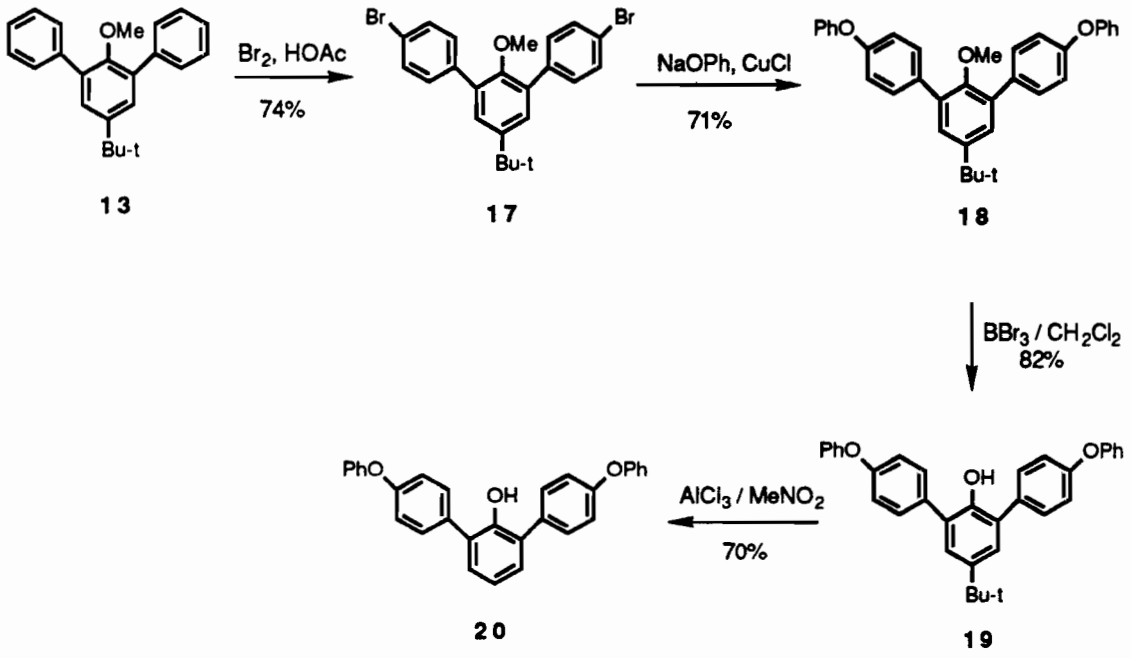
OMe
Bu-t
13
Br2, HOAc
74%
Br
OMe
Br
Bu-t
17
NaOPh, CuCl
71%
PhO
OMe
OPh
Bu-t
18
BBr3 / CH2Cl2
82%
PhO
OH
OPh
Bu-t
19
AlCl3 / MeNO2
70%
PhO
OH
OPh
20

Scheme 2.14 outlines the attempts to prepare the iodo substituted intermediate from which other monomers can be prepared. Since molecular iodine is the least reactive halogen in electrophilic aromatic substitutions, direct iodination of unactivated aromatic compounds usually requires drastic reaction conditions such as nitric acid/sulfuric acid, sulfuric acid or strong oxidizing agent which oxidizes iodine to a better electrophile[24]. Recently Wing-Wah[25] reported simple and mild reaction conditions for the iodination of aromatics by iodine-silver sulfate in methylene dichloride at room temperature. The conversion of **13** to **21** was accomplished according to this method but reflux temperature was required to complete the iodination. Compound **21** was subjected to a sequence of demethylation and transalkylation reactions under conditions similar to those described previously which furnishes **23** in good yield

Under conditions reported recently by Heiner and Chen[17], the cross coupling between **23** with excess p-fluorophenyl Grignard gave **24** in moderate yield. The coupling reaction between **23** and trimethylsiloethyne under standard conditions [$Pd(II)(PhCN)_2Cl_2$, $Cu(OAc)_2$, CuI, isopropylamine, under reflux] gave **25a** in good yield. The subsequent deprotection with tetrabutylammonium fluoride in THF afforded **25b**. Under similar conditions, the conversion of **23** to **26** proceeded in moderate yield.

Intermediate **21** was treated with sodium trifluoroacetate and CuI as catalyst to afford **27**. Subsequent removal of methyl and t-butyl groups as described above furnishes **28b**.

Scheme 2.14

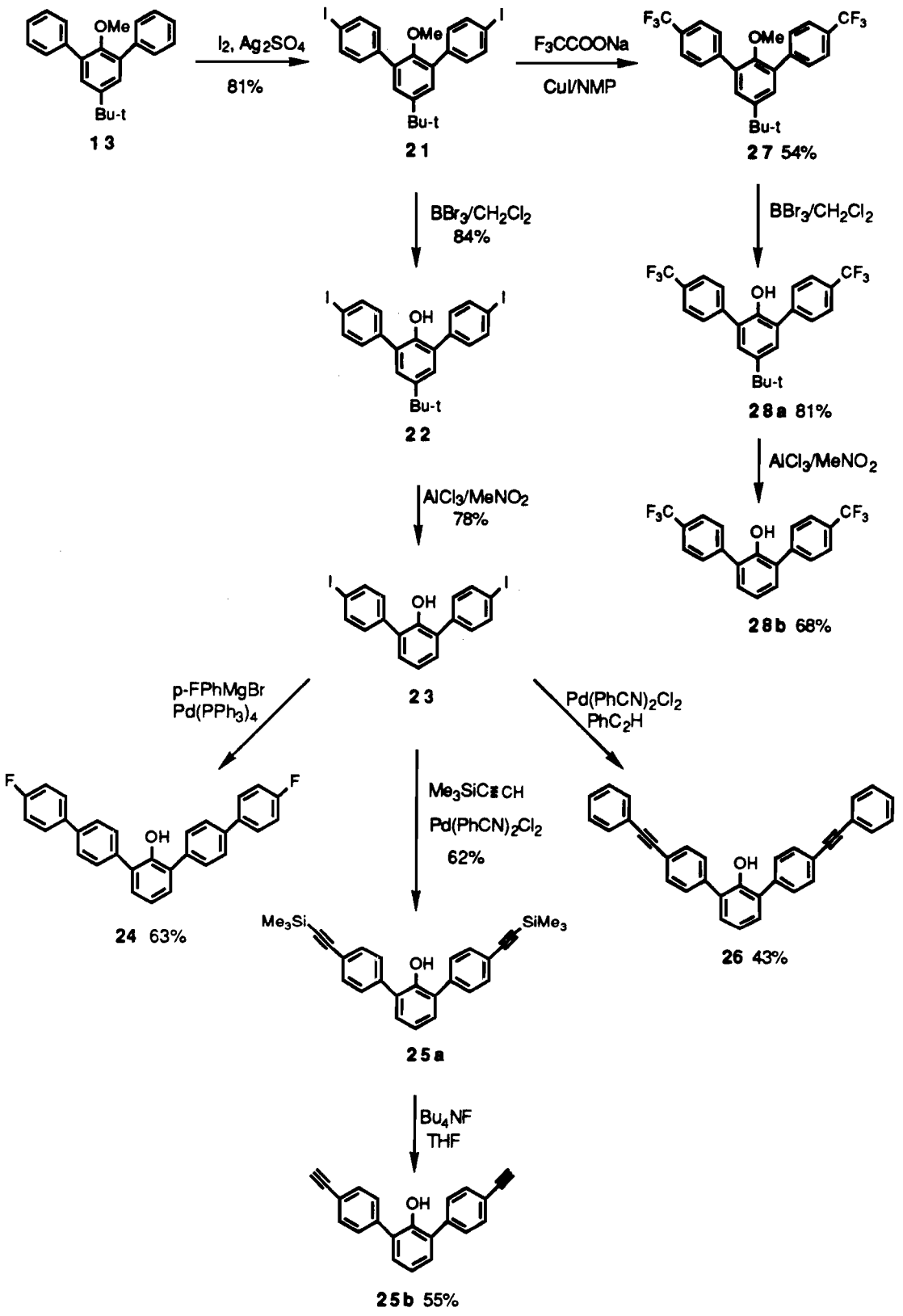
OMe
Bu-t
13
I2, Ag2SO4
81%
I
OMe
Bu-t
21
F3CCOONa
CuI/NMP
F3C
CF3
OMe
Bu-t
27 54%
BBr3/CH2Cl2
84%
OH
22
BBr3/CH2Cl2
28a 81%
AlCl3/MeNO2
78%
28b 68%
23
p-FPhMgBr
Pd(PPh3)4
Pd(PhCN)2Cl2
PhC2H
Me3SiC≡CH
Pd(PhCN)2Cl2
62%
F
24 63%
Me3Si
SiMe3
25a
26 43%
Bu4NF
THF
25b 55%

Our initial attempt to introduce the t-butyl group onto the pendant rings of **DPP** is illustrated in scheme 2.15. Hypothetically, the condensation product **29** could yield **30** by dehydrogenation and subsequent selective removal of t-butyl group could yield the target molecule **34** (scheme 2.16). However, the dehydrogenation reaction gave a mixture of products with the unexpected terphenyl **31** as the major component from the reaction.

Scheme 2.15

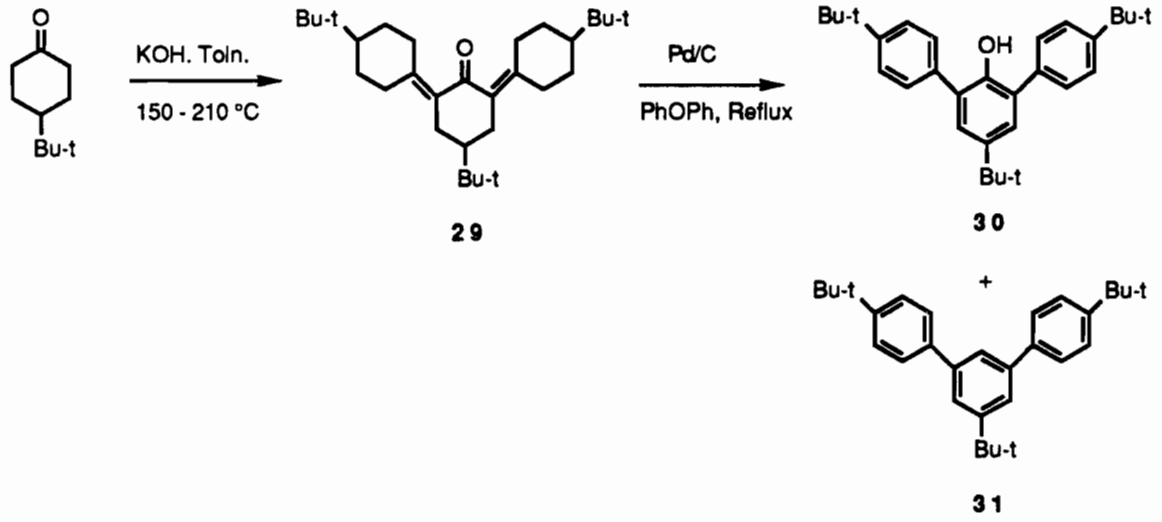

So we turned to the approach illustrated in scheme 2.16 by subjecting bromo-blocked intermediate **32** to Friedel-Craft reaction conditions. We found an efficient reaction can be achieved by employing aluminum metal as catalyst which in this case is greatly superior to the traditional Friedel-Craft alkylation reaction conditions we have used previously. The bromo group of **33** was efficiently removed by hydrogenolysis with hydrazine in the presence of palladium on carbon to give the final product **34** in good yield.

Scheme 2.16

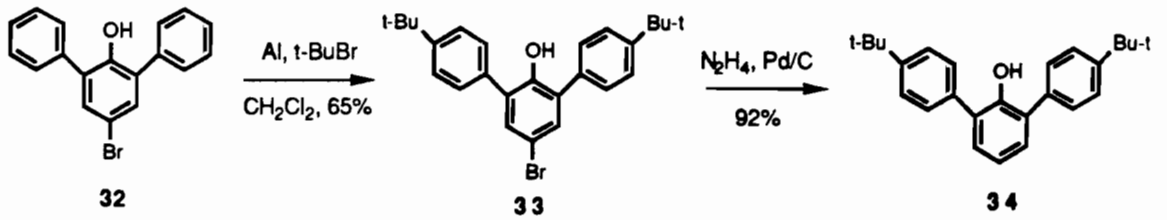

2.2.3. Aryl-aryl coupling approach

The most convergent approach to 2,6-diarylphenols is the coupling of the organometallic synthetic equivalent of a substituted phenyl carbanion with regiospecific halophenols.

Scheme 2.17

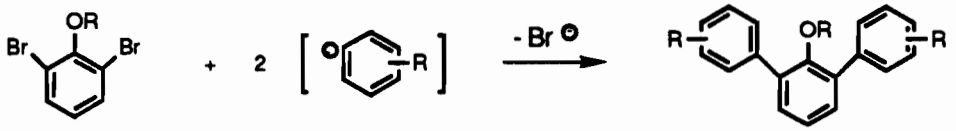

The ortho bromophenols **35, 36** (scheme 2.18) can be readily obtained either from tetrabromo-bisphenol A by transalkylation[26] or from phenol by amine-mediated ortho bromination[27]. A one-pot approach to diarylphenol using Heiner's method by coupling of excess aromatic Grignards with dibromophenols gave a low yield. The major side-product resulted from the exchange of the second bromo atom for hydrogen. We attempted to further modify this method for preparing diarylphenols by a one-step reaction.

Scheme 2.18

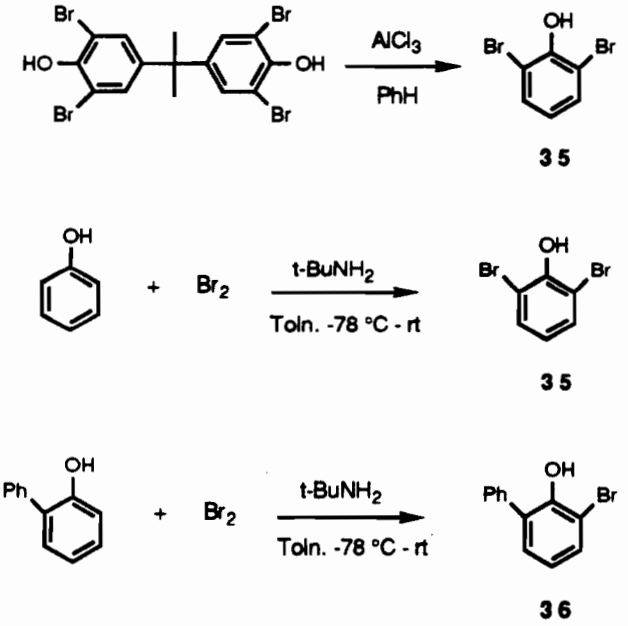

Initially we assumed that the low yield was caused by the adjacent hydroxyl group which facilates the debromination. However, when capped dibromophenol **37** was al-

lowed to react with phenylmagnesium bromide at reflux temperature for 10 hours, only a small amount of the desired double phenylation product **38** was obtained (Scheme2.19).

Scheme 2.19

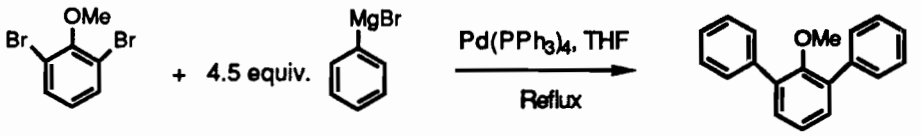

38 Low yield

We then explored Suzuki conditions in which arylboric acid is the organometallic equivalent and studied the feasibility of double arylation in the free phenol system. The substituted arylboric acids were conveniently obtained by simply quenching the corresponding Grignards with isopropyl borate to give good yields of **39.** The initial results for the double phenylation reactions gave average yields of 20 to 30% (**40a, 40b** and **40c**, scheme 2.20). We observed an average 10% increase in the yield over the standard Suzuki conditions in the presence of tetrabutylammonium bromide (TBAB).

Scheme 2.20

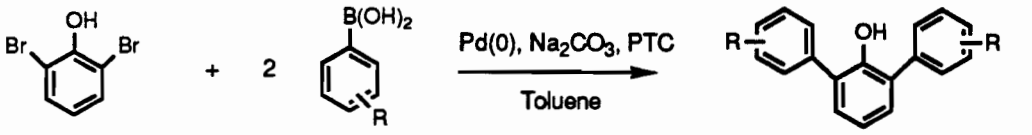

35

39 a R = p-F
b R = m-F
c R = p-OMe

40 a R = p-F (43%)
b R = m-F (36%)
c R = p-OMe (59%)

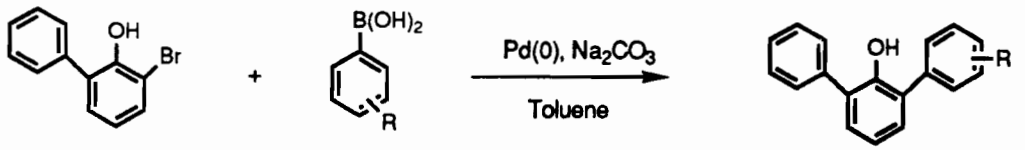

36

39 a R = p-F
b R = m-F
c R = p-OMe

41 a R = p-F (77%)
b R = m-F (59%)
c R = p-OMe (62%)

Under the same conditions, some unsymmetrically-substituted phenols were also prepared in good yields from readily available 2-bromo-6-phenylphenol **36**. Thus, the mono and double regiospecific ortho arylations of phenol were achieved by a one-step synthesis from readily available starting materials in acceptable yields.

2,6-Bis(4-methoxyphenyl)phenol was used as intermediate to prepare hydroxyl substituted derivative **42**. Compound **42** was allowed to react with tert-butyldimethylsilyl chloride in DMF to afford **43.** This protecting group was demonstrated to be stable to the oxidative polymerization condition and therefore this monomer can be incorporated into P3O polymer. The hydroxyl function can be readily released on the polymer in the presence of fluoride ion.

Scheme 2.21

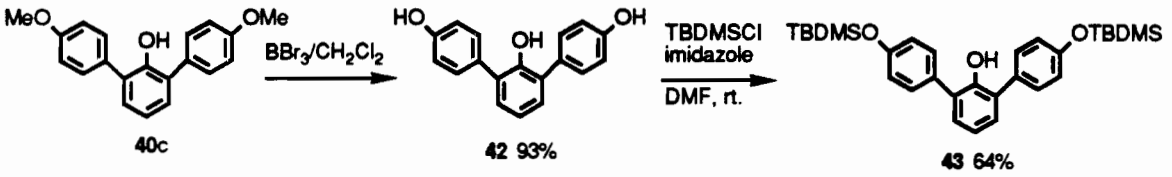

40c 42 93% 43 64%

Our next attempt was to prepare cyano and phthalimidyl mono-substituted monomers. The above procedure however is not adaptable to these types of substituents because the preparation of their arylboric acids requires the intermediacy of organomagnesium or lithium reagents and they are incompatible with the functionality to be introduced. Instead, the intermediate **45** was prepared from **36** by a two-step sequence : methylation of the phenol **36** which afforded **44**; the Grignard prepared from **44** was then quenched with triisopropylborate at low temperature to give arylboric acid **45.** The boric acid **45** was then subjected to the coupling reaction with either 4-cyano or 4-phthalimidyl substituted phenylbromide to give **46a** and **46b** respectively. The removal of methyl group was carried out as described previously to give **47a** and **47b** in good yield.

Scheme 2.22

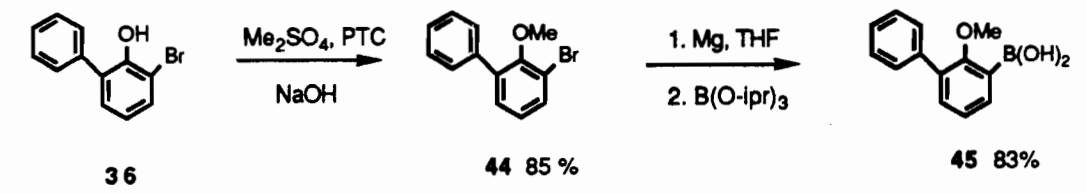

36 **44** 85 % **45** 83%

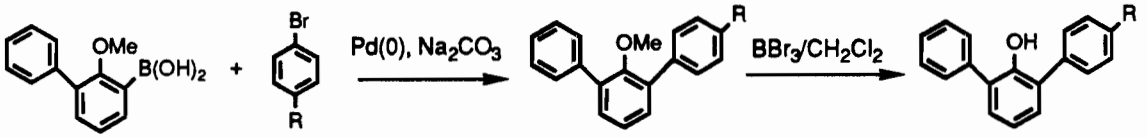

45 R = CN, Phthalimidyl **46** a R = CN, 72%; b R = Phthalimidyl, 57% **47** a R = CN, 59%; b R = Phthalimidyl,

We next attempted to expand the scope of this reaction to a synthesis which involves a higher number of arylation reactions in order to construct more complicated aromatic phenol systems in a one step reaction. Commercially available tetrabromo-bisphenol A was subjected to the described conditions. When tetrabromo-bisphenol A was subjected to the coupling reaction in the absence of TBAB, incomplete arylation was observed with a yield of less than 20%. In the presence of TBAB, a 53% yield of tetraphenylation product **48** was obtained.

Scheme 2.23

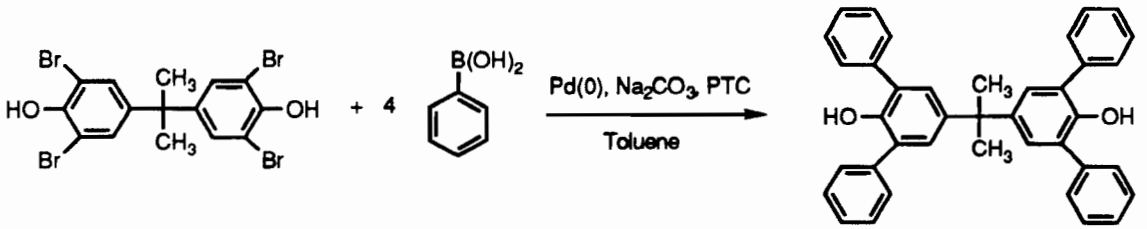

48 53%

Finally we investigated the possibility of expanding the scope of the reaction to the aniline system. Initial attempts to prepare compound **52** by the sequence shown in scheme 2.24 are based on the known Semmler-Wolff conversion[28] of **50** to **51**. The high tempera-

ture catalytic aromatization of **50** to yield **52** proceeded in low yield. When 2,6-dibromoaniline was allowed to react with phenylboric acid under Suzuki conditions for 10 hours at reflux, none of the desired product was detected and the starting material was recovered. When the reaction was instead carried out in the presence of TBAB, the double phenylation product **52** was isolated in 86 percent yield.

Scheme 2.24

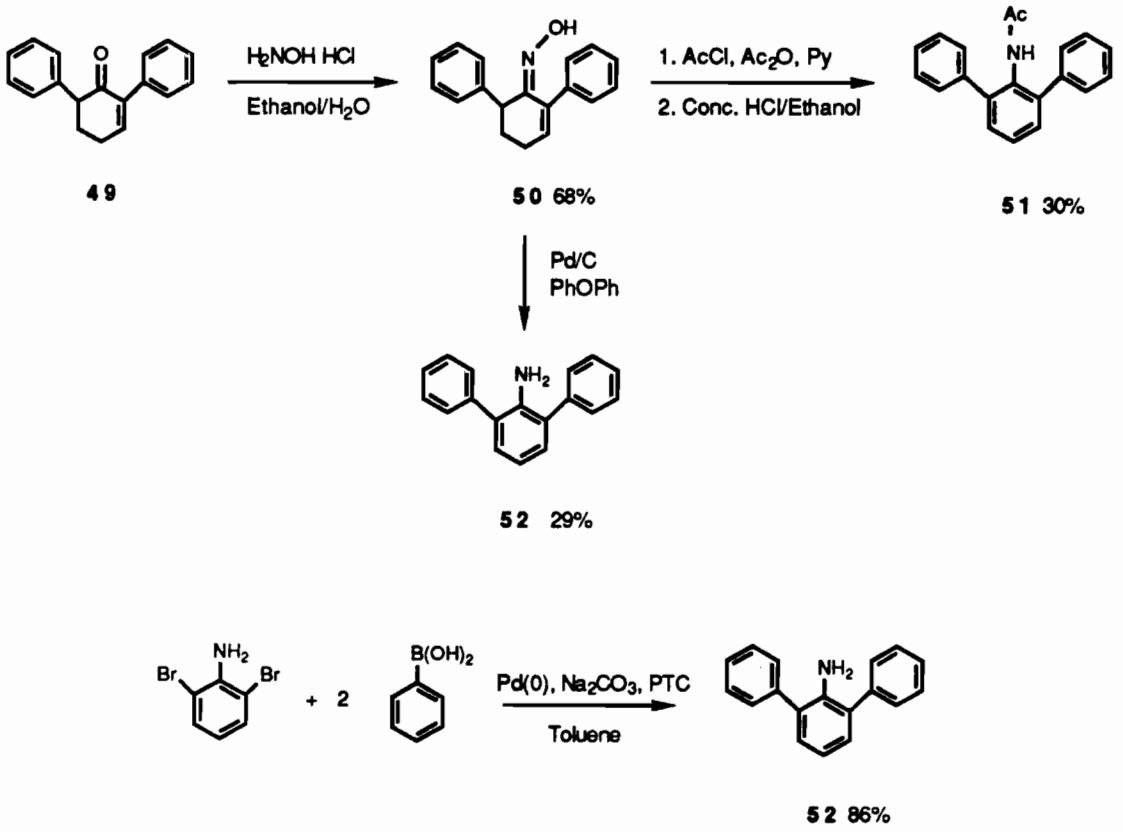

49

50 68%

51 30%

52 29%

52 86%

2.3. EXPERIMENTAL

Melting points were measured on a Fisher-Johns melting point apparatus and are uncorrected. Flash chromatography was done on silica gel 60 (32-63 mm) from **BDH**. ^1H NMR spectra were recorded in chloroform-d solution at 200 MHz on a Varian XL-200 NMR spectrometer and reported in ppm from tetramethylsilane on the δ scale. Mass spectra were recorded at 70 eV with a direct insertion probe on a DuPont 21-492B Mass spectrometer. Microanalyses were obtained from the **Galbraith Laboratory Inc.**, Knoxville, TN. All chemicals and solvents were reagent grade and used without further purification. The reactions were routinely monitored on a **Milton Roy HPLC** instrument, using a Spherisorb ODS2 reverse-phase column (250 X 4.6 mm, 5 mm) and methanol as an eluent at a flow rate of 1.0 mL per minute with a UV detector set at 254 nm wavelength.

1,3-Bis(4-fluorophenyl)-2-propanone 9a A mixture of p-fluorophenylacetic acid (4.62 g, 30 mmol) and MgO (1.33 g, 33 mmol) is finely ground and added into a 25 mL three neck flask with a short-neck distillation tube. The flask is put in a sand bath and the temperature is slowly raised while the reaction mixture is held under vacuum (2 mm Hg). When the temperature reaches about 300 °C, the product begins to distill out as colorless oil and the temperature is maintained until no further product distills out. The solidified product is recrystallized from ethanol to give **9a** as white needle crystals; yield: 2.96 g (80%); mp 64 °C.

$C_{15}H_{12}F_2O$ calc. C 73.16 H 4.91

(246.3) found 73.63 4.97

MS (70 eV): m/z = 246 (M^+, 12), 137 (M^+ - $FPhCH_2$, 23), 109 ($FPhCH_2^+$, 100).

^1H-NMR ($CDCl_3$): δ = 3.70 (s, 4 H, CH_2), 7.05 (m, 8 Harom).

1,3-Bis(4-chlorophenyl)-2-propanone 9b. A mixture of p-chlorophenylacetic acid (5.12 g, 30 mmol) and MgO (1.33 g, 33 mmol) is finely ground and added into a 25 mL flask with a short-neck distillation tube. The flask is put in a sand bath and the temperature is slowly raised while the reaction mixture is main-

tained under vacuum (2 mm Hg). The temperature is maintained at 300 °C until no further product distills out. The solidified product is recrystallized from ethanol giving **9b** as light yellow crystals; yield: 3.52 g (84%); mp 96-97 °C.

$C_{15}H_{12}Cl_2O$ calc. C 64.54 H 4.33

(279.2) found 64.52 4.53

MS (70 eV): m/z = 278 (M^+ - H, 8), 153 (M^+ - $ClPhCH_2$ - H, 16), 125 ($ClPhCH_2^+$, 100).

^{1}H-NMR ($CDCl_3$): δ = 3.69 (s, 4 H, CH_2), 7.06 (d, 4 Harom, *J* = 8.5 Hz), 7.29 (d, 4 Harom, *J* = 8.5 Hz).

2,6-Bis(4-fluorophenyl)cyclohexanone 10a. To a stirred suspension of **9a** (23.2 g, 94 mmol), tetrabutylammonium bromide (12.9 g, 40 mmol), sodium hydroxide (50 mL, 50%) and chlorobenzene (30 mL), is added 1,3-dibromopropane (18.9 g, 94 mmol) very slowly under nitrogen atmosphere at room temperature. Following the addition, the reaction is allowed to stir overnight at room temperature and the color of the organic phase changes from dark brown to yellow. The mixture is then poured into water (400 mL) and the organic phase is diluted with chloroform (100 mL), washed with water until neutral and dried (MgSO4). The solvent is evaporated and the yellow oil is recrystallized from hexane-ethanol giving **10a** as white crystals; yield: 10.2 g (38%); mp 139-140 °C.

$C_{18}H_{16}F_2O$ calc. C 75.51 H 5.63

(286.3) found: 75.87 5.62

MS (70 eV): m/z = 286 (M^+, 85), 258 (M^+ - CO, 14), 135 (100).

^{1}H-NMR ($CDCl_3$): δ = 2.12 (m, 4 H, 2 CH_2), 2.38 (m, 2 H, CH_2), 3.80 (m, 2 H, 2 CH), 6.95-7.16 (m, 8 Harom).

2,6-Bis(4-chlorophenyl)cyclohexanone 10b. To a stirred suspension of **9b** (27.9 g, 100 mmol), tetrabutylammonium bromide (12.9 g, 40 mmol), sodium hydroxide (50 mL, 50%), and chlorobenzene (30 mL), is added 1,3-dibromopropane (20.2 g, 100 mmol) very slowly under nitrogen at room temperature. Following the addition, the reaction is allowed to stir overnight. The mixture is then poured into water (400 mL) and the organic phase is diluted with chloroform (100 mL). The chloroform solution is washed with water until neutral and dried (MgSO4). The solvent is distilled in vacuo and to the crude yellow oil is added hexane

(30 mL) and the mixture is agitated. The oil quickly solidifies into crystals and further recrystallization from ethanol gives **10b** as white crystals; yield: 13.7 g (43%); mp 159-160 °C.

$C_{18}H_{16}Cl_2O$ calc. C 67.72 H 5.05

(319.2) found 67.76 5.06

MS (70 eV): m/z = 318 (M^+ - H, 62), 290 (M^+ - CO - H, 16), 138 (100).

^{1}H-NMR ($CDCl_3$): δ = 2.07 (m, 4 H, 2 CH_2), 2.40 (m, 2 H, CH_2), 3.77 (m, 2 H, 2 CH), 7.08 (d, 4 Harom, *J* = 8.5 Hz), 7.28 (d, 4 Harom, *J* = 8.5 Hz).

2,6-Bis(4-fluorophenyl)phenol 11a. A mixture of compound **10a** (7.99 g, 27.9 mmol), Pd/C (2 g, 5%) and diphenyl ether (25 mL) is heated under reflux for 20 h. After cooling to room temperature, the mixture is diluted with acetone (50 mL) and the catalyst is removed by filtration. The solvent is evaporated on a rotovap under reduced pressure to give a light yellow oil. The oil is dissolved in warm hexane and set in the refrigerator overnight to give **11a** as white crystals; yield: 5.8 g (74%); mp 62-65 °C.

$C_{18}H_{12}F_2O$ calc. C 76.59 H 4.28

(282.3) found 76.81 4.36

MS (70 eV): m/z = 282 (M^+, 100).

^{1}H-NMR ($CDCl_3$): δ = 5.22 (s, 1 H, OH), 7.10-7.30 (m, 8 Harom), 7.48-7.58 (m, 3 Harom).

2,6-Bis-(4-chlorophenyl)phenol 11b. (Method A) To a mixture of **10b** (6.38 g, 20 mmol), acetic acid (60 mL) and acetic anhydride (60 mL), concentrated sulfuric acid (8 mL) is added slowly at room temperature. The reaction mixture is then heated at 90 °C for 3 h. The reaction mixture is then poured into ice-water (200 mL), followed by extraction with ether (2 x 100 ml). The combined ether extracts are washed with water (2 x 200 mL) and dried ($MgSO_4$). The solvent is evaporated and the residue is dissolved in ethanol (100 mL). A solution of potassium hydroxide (15 g) in water (50 mL) is added to above solution. The mixture is heated at reflux for 3 h under nitrogen atomsphere. The reaction mixture is then poured into cold water (200 mL) with agitation. The solid is collected by filtration and purified by recrystallization from ethanol to give **11b** as white crystals; yield: 3.9 g (62%); mp 135-137 °C.

$C_{18}H_{12}Cl_2O$ calc. C 68.59 H 3.84

(315.2) found 68.18 3.98

MS (70 eV): m/z = 316 (M^+ + H, 21), 178 (100).

^{1}H-NMR ($CDCl_3$): δ = 5.22 (s, 1 H, OH), 7.05 (t, 1 Harom, *J* =7.4 Hz), 7.24 (d, 2 Harom, *J* =7.4 Hz), 7.46 (m, 8 Harom).

2,6-Bis-(4-chlorophenyl)phenol 11b.(Method B) To a 250 mL flask, was combined **10b** (6.3 g, 20 mmole), NBS (8.9 g, 50 mmole) and carbon tetrachloride (50 mL). The mixture was heated in an oil bath to reflux and continued for 15 h. The mixture was then filtered hot and washed with carbon tetrachloride. The solution was diluted with methylene dichloride (50 mL) and subsquently washed with sodium bisulfite solution (1%, 150 mL) and water (2 X 100 mL). After removal of solvents, the crude product was subjected to the next step without further purification. The crude product was added into potassium hydroxide in methanol (10%, 50 mL) and refluxed for 5 h. The mixture was diluted with water (50 mL) and acidified with HCl (10%). The mixture was extracted with methylene dichloride (2 x 100 mL) and dried with anhydrous magnesium sulfate overnight. Removal of solvent gave a yellow colored crude product and crystallization from ethanol yields **11b** as light yellow crystals 2.6 g (41%).

2,6-Diphenyl-4-(t-butyl)phenol 12 A suspension of 2,6-diphenylphenol (24.6 g, 100 mmol) and 4-methyl-2,6-di-t-butylphenol (12.0 g, 55 mmol) in nitroethane (100 mL) is cooled to -20 °C in a cooling bath. To the mixture a solution of aluminum chloride (13.3 g, 100 mmol) in nitroethane (30 mL) is added with stirring and the solution instantly becomes dark colored. The reaction is continued for 15 min and the reaction is quenched by pouring the reaction mixture into ice water (500 mL). The organic phase is separated and the solvent is distilled in vacuo. The residue is dissolved in methylene dichloride (200 mL) and washed with hydrochloric acid (18%, 200 mL), water (150 mL), sodium hydroxide solution (10%, 150 mL) and water (150 mL). The organic phase is dried ($MgSO_4$) and the solvent is removed under reduced pressure. The residue is dissolved in warm hexane and set in the refrigerator for 24 h to give **12** as white crystals; yield: 18.9 g (63%); mp 91-92.5 °C.

$C_{22}H_{22}O$ calc. C 87.38 H 7.33

(302.4) found 87.59 7.51

MS (70 eV) m/z = 302 (M^+, 41), 287 (M^+ - CH_3, 100).

^{1}H-NMR ($CDCl_3$): δ = 1.36 (s, 9 H, t - C_4H_9), 5.26 (s, 1 H, OH), 7.29 (s, 2 Harom), 7.40-7.60 (m, 10 Harom).

2,6-Diphenyl-4-(t-butyl)anisole 13. To a solution of **12** (30.2 g, 100 mmol), dimethyl sulfate (18.9 g, 150 mmol) and tetrabutylammonium bromide (2 g) in methylene dichloride (250 mL), is added a solution of sodium hydroxide (6 g) in water (250 mL). The mixture is stirred at room temperature overnight. The organic layer is washed thoroughly with water until neutral and dried (MgSO4). The solvent is evaporated and the light yellow oil is dissolved in warm hexane and set in the refrigrator overnight to give **13** as white crystals; yield: 24.7 g (78%); mp 86-87 °C.

$C_{23}H_{24}O$ calc. C 87.30 H 7.64

(316.5) found 87.04 7.81

MS (70 eV): m/z = 316 (M^+, 48), 301 (M^+ - CH_3, 100).

^{1}H-NMR ($CDCl_3$): δ = 1.36 (s, 9 H, t - C_4H_9), 3.14 (s, 3 H, OCH_3), 7.34 - 7.63 (m, 12 Harom).

Acetate of 4-t-Butyl-2,6-bis(p-bromophenyl)phenol 14a. To a suspension of **12** (16.3 g, 54 mmol) in acetic acid (100 mL), bromine (43.5 g, 270 mmol) is added at room temperature. The mixture is heated to 85 °C when a clear solution is obtained. The reaction is continued for 16 h. and during the reaction the product separates out from the solution. The mixture is cooled to room temperature and the product is collected by filtration. The solid is washed with acetic acid and recrystallization from ethanol gives **14a** as white crystals; yield: 15.3 g (56%); mp 212-213 °C.

$C_{24}H_{22}Br_2O_2$ calc. C 57.40 H 4.42

(502.3) found 57.24 4.45

MS (70 eV): m/z = 502 (M^+, 6), 460 (M^+ - CH_3CO + H, 100).

^{1}H-NMR ($CDCl_3$): δ = 1.36 (s, 9 H, t - C_4H_9), 1.83 (s, 3 H, $COCH_3$), 7.33 (s, 2 Harom), 7.31 (d, 4 Harom, J = 8.0 Hz), 7.54 (d, 4 Harom, J = 8.0 Hz).

4-t-Butyl-2,6-bis(p-bromophenyl)phenol 14b To a mixture of compound **14a** (41.2 g, 82 mmol) and methanol (400 mL), a solution of potassium hydroxide (30 g) in water (100 mL) is added. The temperature is raised to reflux and a clear solution is formed. The reaction is continued for 3 h . The solution is poured into cold water (500 mL) with vigorous agitation. The white solid is filtered and washed with water. Recrystallization from ethanol-chloroform gives a first portion of white crystals (30.0 g). Further concentration gives another portion of white crystals (4.8 g) of **14b** ; yield: 34.8 g (92%); mp 161-162 °C.

$C_{22}H_{20}Br_2O$ calc. C 57.42 H 4.38

(460.2) found 58.05 4.58

MS (70 eV) m/z = 460 (M^+, 52), 445 ($M^+ - CH_3$, 100).

^{1}H-NMR ($CDCl_3$): δ = 1.34 (s, 9 H, t - C_4H_9), 5.07 (s, 1 H, OH), 7.24 (s, 2 Harom), 7.42 (d, 4 Harom, J = 8.5 Hz), 7.60 (d, 4 Harom, J = 8.5 Hz).

2,6-Bis(p-bromophenyl)phenol 15. To a stirred solution of compound **14b** (34.5 g, 75 mmol) in benzene (250 mL) at 50 °C, a solution of aluminum chloride (11.33 g, 85 mmol) in nitromethane (50 mL) is added. The reaction is continued at 50 °C for 3.5 h. The mixture is poured into ice water (500 mL). The organic layer is seperated and the solvent is distilled in vacuo. Recrystallization from ethanol-chloroform gives **15** as white crystals; yield: 26.5 g (87%); mp 147-148.5 °C.

$C_{18}H_{12}OBr_2$ calc. C 53.64 H 2.75

(403.1) found 53.46 2.99

MS (70 eV) m/z = 404 (M^+ + H, 79), 244 (M^+ - 2 Br - H, 100).

^{1}H-NMR ($CDCl_3$): δ = 5.21 (s, 1 H, OH), 7.06 (t, 1 Harom, J = 7.6 Hz), 7.25 (d, 2 Harom, J = 7.6 Hz), 7.41 (d, 4 Harom, J = 8.7 Hz), 7.65 (d, 4 Harom, J = 8.7 Hz).

2,6-Bis-(p-cyanophenyl)phenol 16. In a 250 mL flask equipped with magnetic stirring, nitrogen inlet and condenser, a mixture of compound **15** (8.06 g, 20 mmol), cuprous cyanide (5.37 g, 60 mmol) and N-methylpyrrolidinone (100 mL) is added. The mixture is heated at reflux under a nitrogen atmosphere for 22 h. The brown colored solution is cooled to 100 °C and poured into warm aqueous sodium cyanide solution (10%, 250 mL). The grey colored solid is collected by filtration and washed with warm sodium cyanide so-

lution (10 %, 200 mL) and water (2 x 200 mL). Recrystallization from ethanol affords 2.0 g of light yellow crystals. The filtrate is concentrated and purified by flash chromatography (methylene dichloride-hexane 1:1) giving another 2.6 g of **16** as light yellow crystals ; yield: 4.6 g (77%); mp 261-262.5 °C.

$C_{20}H_{12}N_2O$ calc. C 81.07 H 4.08

(296.3) found 80.55 4.13

MS (70 eV): m/z = 296 (M^+, 100).

^{1}H-NMR ($CDCl_3$): δ = 5.19 (s, 1 H, OH), 7.13 (t, 1 Harom, J = 7.6 Hz), 7.29 (d, 2 Harom, J = 7.6 Hz), 7.66 (d, 4 Harom, J = 8.3 Hz), 7.77 (d, 4 Harom, J = 8.3 Hz).

2,6-Bis-(4-bromophenyl)-4-(t-butyl)-anisole 17 To a stirred suspension of **13** (15.8 g, 50 mmol) in acetic acid (100 mL), bromine (12.9 mL, 250 mmol) is added. The solution is heated to 80 °C and a clear solution is formed. The reaction is continued for 2.5 h. The product continuously separates out of the solution during the reaction. The mixture is cooled to room temperature and the solid is collected by filtration and washed with cool acetic acid. Recrystallization from ethanol-chloroform gives **17** as white crystals; yield: 17.6 g (74%); mp 145-146 °C.

$C_{23}H_{22}OBr_2$ calc. C 58.25 H 4.68

(474.2) found 58.32 4.72

MS (70 eV) m/z = 474 (M^+, 68), 459 (M^+ - CH_3, 100).

^{1}H-NMR ($CDCl_3$): δ = 1.35 (s, 9 H, t - C_4H_9), 3.13 (s, 3 H, OCH_3), 7.30 (s, 2 Harom), 7.47 (d, 4 Harom J = 8.7 Hz), 7.56 (d, 4 Harom, J = 8.7 Hz).

2,6-Bis-(4-phenoxyphenyl)-4-(t-butyl)anisole 18. To a 250 mL three neck flask equipped with a condenser, Dean-Stark trap, nitrogen inlet and magnetic stirring bar, phenol (10.74 g, 114 mmol), sodium hydroxide (4.44 g, 111 mmol), DMSO (45 mL) and benzene (30 mL) are added. The mixture is heated at 110 °C for 4 h until no further water comes out of the reaction mixture. Compound 17 (8.54 g, 18 mmol) and cuprous chloride (2.94 g, 30 mmol) are added under nitrogen atomsphere. The temperature is raised to 130 °C and continued for 3 h. The mixture is poured into water and the solid is collected by filtration. The solid is taken up in dichloromethane (2 x 100 mL) and the solution is washed with sodium hydroxide solution

(10%, 100 mL) and water (2 x 100 mL). The organic layer is dried over anhydrous magnesium sulfate and the solvent is removed under reduced pressure. Recrystallization from ethanol-dichloromethane gives **18** as light yellow crystals; yield: 6.4 g (71%); mp 169-171 °C.

$C_{35}H_{32}O_3$ calc. C 83.97 H 6.44

(500.6) found 84.16 6.37

MS (70 eV): m/z = 500 (M^+, 1), 393 ($M^+ - C_6H_5 - 2\ CH_3$, 100),.

^{1}H-NMR ($CDCl_3$): δ = 1.37 (s, 9 H, t = C_4H_9), 3.21 (s, 3 H, OCH_3) , 7.02 - 7.60 (m, 20 Harom).

2,6-Bis(4-phenoxyphenyl)-4(t-butyl)phenol 19. To a stirred solution of **18** (5.0 g, 10 mmol) in methylene dichloride (20 mL) which is cooled to - 70 °C with an acetone-dry ice bath, is added a solution of boron tribromide (1.0 M in methylene dichloride, 30 mL, 30 mmol) by syringe in 10 min under a nitrogen atomsphere. The reaction temperature is allowed to rise to room temperature over 1.5 h. The orange colored solution is poured into ice water (200 mL). The organic layer is washed with water (2 x 100 mL) and dried ($MgSO_4$). The solvent is distilled in vacuo and the light yellow oil is recrystallized from ethanol-chloroform giving 3.5 g of white crystals. Further concentration gives another 0.5 g of crystals of **19** ; yield: 4.0 g (82%); mp 167-168.5 °C.

$C_{34}H_{30}O_3$ calc. C 83.92 H 6.21

(486.6) found 84.07 6.33

MS (70 eV): m/z = 394 ($M^+ - C_6H_5 - CH_3$, 16), 83 (100).

^{1}H-NMR ($CDCl_3$): δ = 1.35 (S, 1 H, t -C_4H_9), 5.24 (s, 1 H, OH), 7.27 (s, 2 Harom), 7.08-7.54 (m, 18 Harom).

2,6-Bis-(p-phenoxyphenyl)phenol 20 To a stirred solution of **19** (3.65 g, 7.5 mmol) in benzene (30 mL) at 70 °C, is added a solution of aluminum chloride (1.13 g, 8.5 mmol) in nitromethane (5 mL). A dark color rapidly developed. The reaction is continued for 1.5 h . The reaction mixture is then poured into cold water (100 mL). The organic layer is washed with hydrochloric acid solution (10%, 50 mL), then with water (2 x 50 mL). The organic layer is dried ($MgSO_4$) and the solvent is distilled in vacuo and the solid is purified by crystallization twice from ethanol to give **20** as light yellow crystals; yield: 2.3 g (70%); mp 118-120 °C.

$C_{30}H_{22}O_3$ calc. C 83.70 H 5.15

(430.5) found 83.61 5.26

MS (70 eV): m/z = 430 (M^+, 63), 244 (M^+ - 2 C_6H_5O, 12), 78 (100).

^{1}H-NMR ($CDCl_3$): δ = 1.37 (s, 9 H, t -C_4H_9), 3.21 (s, 3 H, OCH_3) , 7.02 - 7.60 (m, 20 Harom).

2,6-Bis(p-iodophenyl)-4-(t-butyl)anisole 21: A stirred mixture of compound **13** (8.86 g, 28 mmol), silver sulfate (21.7 g, 70 mmol), iodine crystals (17.8 g, 35 mmol) and dichloromethane (250 mL) is heated at gentle reflux under nitrogen atmosphere for 24 h . The solid is removed by filtration and the solution is washed with dilute sodium thiosulfate (5%, 300 mL) water, (2 x 200 mL) and dried ($MgSO_4$). The solvent is distilled in vacuo and recrystallization from ethanol-chloroform gives **21** as light yellow crystals; yield: 12.9 g (81%); mp 174-175 °C.

$C_{23}H_{22}I_2O$ calc. C 48.62 H 3.90

(568.2) found 48.63 3.91

MS (70 eV) m/z = 568 (M^+, 100), 553 (M^+ - CH_3, 99), 426 (M^+ - I - CH_3 - H, 17).

^{1}H-NMR ($CDCl_3$): δ = 1.35 (s, 9 H, t -C_4H_9), 3.13 (s, 3 H, OCH_3), 7.29(s, 2 Harom), 7.35(d, 4 Harom, J = 8.5 Hz), 7.76(d, 4 Harom, J = 8.5 Hz).

2,6-Bis(p-iodophenyl)-4-(t-butyl)phenol 22: To a stirred solution of **21** (4.43 g, 7.8 mmol) in dichloromethane (10 mL) which is cooled to - 70 °C with an acetone-dry ice bath, is added a solution of boron tribromide-dichloromethane (1.0 M in methylene dichloride, 23.4 mL, 23.4 mmol) by syringe in 10 min. The temperature rises to 0°C in 1 h and the reaction is quenched by pouring the solution into ice-water (100 mL). The organic layer is washed with water (2 x 50 mL) and dried ($MgSO_4$). The solvent is evaporated and the residue is purified by recrystallization from ethanol to give **22** as light yellow crystals; yield: 3.6 g (84%); mp 160-161 °C.

$C_{22}H_{20}I_2O$ calc. C 47.68 H 3.64

(554.2) found 47.80 3.61

MS (70 eV): m/z = 554 (M^+, 88), 539 (M^+ - CH_3, 100), 412 (M^+ - I - CH_3 - H, 17).

^{1}H-NMR ($CDCl_3$): δ = 1.33 (s, 9 H, t -C_4H_9), 5.09 (s, 1 H, OH), 7.24 (s, 2 Harom), 7.29 (d, 4 Harom, J =

8.4 Hz), 7.80 (d, 4 Harom, J = 8.4 Hz).

2,6-Bis(4-iodophenyl)phenol 23 To a stirred solution of **22** (2.99 g, 5.4 mmol) in benzene (30 mL) at 70 °C, a solution of aluminum chloride (0.93 g 7.0 mmol) in nitromethane (5 mL) is added. The reaction is continued at 70 °C for 3 h. The mixture is poured into ice water (100 mL). The organic layer is separated, dried (MgSO4) and the solvent is evaporated. The crude solid is purified by recrystallization from ethanol-chloroform giving **23** as light yellow crystals; yield: 2.1 g (78%); mp 151-153 °C.

$C_{18}H_{12}I_2O$ calc. C 43.40 H 2.43

(498.1) found 43.83 2.43

MS (70 eV) m/z = 498 (M^+, 100), 372 (M^+ - I, 5).

^{1}H-NMR ($CDCl_3$): δ = 5.23 (s, 1H, OH), 7.04 (q, 1 Harom), 7.23 (d, 2 Harom), 7.28 (d, 4 Harom, J = 8.5 Hz), 7.80 (d, 4 Harom, J = 8.5 Hz).

2,6-Bis[p-(4-fluorophenyl)phenyl]phenol 24 A stirred solution of **23** (4.0 g, 8 mmole) in THF (20 mL) is purged with argon for 15 min. $(PPh_3)_4Pd$ (0.2 g) is added under argon atomsphere. To the yellow solution, 4-fluorophenylmagnesium bromide (40 mL, 40 mmole, 1.0 M in THF) is added through syringe in 10 min. Initially a strong exothermic reaction raise the temperature to reflux and the solid precipated out rapidly. The reaction was continued for 1 h at refluxing temperature. The mixture was poured into conc. HCl (40 mL/ice 80 g) and extracted with ether (2 x 80 mL). The organic phase was washed with water (2 x 150 mL) and dried ($MgSO_4$). The solvent was evaporated and the residue was purified by flash chromtography (Hexane : Ethyl acetate 100:2). Further recrystallization from ethanol-chloroform gave **24** as light yellow crystals; yield: 2.2 g(63%); mp. 235-237 °C.

$C_{30}H_{20}OF_2$ calc. C 82.92 H 4.64

(434.5) found 82.37 4.60

MS (70 eV) m/z = 434 (M^+, 100).

^{1}H-NMR ($CDCl_3$): δ = 5.47 (s, 1 H, OH), 7.11-7.7.36 (m, 7 Harom), 7.57-7.7.66 (m, 12 Harom).

2,6-Bis[4-(trimethylsilyl)ethynylphenyl]phenol 25a To a solution of **23** (6.25g, 12.5 mmol) in diisopropylamine (100 mL), were added dichlorobis(benzonitrile)palladium (0.24 g, 0.625 mmol), triphenylphosphine (0.33 g,1.25 mmol), and copper(II) acetate hydrate (0.125 g, 0.625 mmol). The solution was degassed by passing a rapid stream of argon through it. TMSA (2.95 g, 4.25 mL, 30 mmol) was added in 10 min at room temperature. The color changed rapidily to grey with the formation of a heavy precipitate. The mixture was heated to reflux for 2 h. The dark brown mixture was cooled to room temperature and was diluted with diisopropylamine (75 mL) and the precipitate was removed by filtration. The solvent was removed at reduced pressure and the residue was taken up in methylene chloride (100 mL). The solution was washed with dilute HCl (5%,150 mL) and water (2 × 100 mL). The solution was dried ($MgSO_4$) and the dark oil was purified by flash chromotography (hexane-ethyl acetate 10 : 1). The product was further purified by crystallization from ethanol to afford **25a** as white crystals; yield: 3.4 g (62%); mp. 120-122 °C.

$C_{28}H_{30}OSi_2$	calc.	C	76.66	H	6.89
(438.7)	found		76.08		6.31

MS (70 eV) m/z = 438 (M^+, 100), 423 (99.6), 204 (11.0).

^{1}H-NMR ($CDCl_3$): δ = 0.26 (s, 18 H, $SiMe_3$), 5.29 (s, 1 H, OH), 7.05 (q, 1 Harom), 7.25 (t, 2 Harom), 7.48 (d, 4 Harom. J = 8.5 Hz), 7.56 (d, 4 Harom. J = 8.5 Hz).

2,6-Bis(4-ethynylphenyl)phenol 25b To a solution of **25a** (0.22g, 0.5 mmole) in THF (10 mL), was added tetrabutylamonium fluoride monohydrate (0.52g, 2 mmole). The solution was allowed to stir at room temperature for 8 h. The solution was poured into water (20 mL) and extracted with ether (2 × 30 mL). The ether solution was washed with water (2 × 50 mL) and dried ($MgSO_4$). Removal of solvent at reduced pressure gave a residue that was purified by crystallization from hexane-chloroform to afford **25b** as white crystals; yield: 81 mg (55%); m.p. 154 °C.

$C_{22}H_{14}O$	calc.	C	89.77	H	4.79
(294.4)	found		89.27		4.43

MS (70 eV) m/z = 294 (M^+, 100), 263 (14.7), 147 (5.4).

^{1}H-NMR ($CDCl_3$): δ = 3.12 (s, 2 H, Hacetylene), 5.29 (s, 1 H, OH), 7.06 (t, 1 Harom, J = 7.61 Hz), 7.27 (d, 2 Harom, J = 6.88 Hz), 7.55 (q, 8 Harom, J = 8.20 Hz).

2,6-Bis[4-(phenylethynyl)phenyl]phenol 26 To a solution of **23** (3.11g, 6.25 mmol) in diisopropylamine (50 mL), were added dichlorobis(benzonitrile)palladium (0.12 g, 0.31 mmol), triphenylphosphine (0.165 g,0.625 mmol), and copper(II) acetate hydrate (62.5 mg, 0.31 mmol). The solution was degassed by passing a rapid stream of argon through it. Phenylacetylene (1.65 mL, 15 mmol) was added in 10 min at room temperature. The color changed rapidily to grey with the formation of a heavy precipitate. The mixture was heated to reflux for 1 h. The dark brown mixture was diluted with diisopropylamine (50 mL) and filtered hot to remove solids. The solvent was removed at reduced pressure and the residue was taken up in methylene chloride (100 mL). The solution was washed with dilute HCl (5%,150 mL) and water (2 x 100 mL) and dried ($MgSO_4$). Removal of solvent at reduced pressure gave a residue that was purified by flash chromatography (hexane-ethyl acetate 10 : 1). The light color product was further purified by crystallization from ethanol to afford **26** as white crystals; yield: 1.2 g (43%); m.p. 179 °C.

$C_{34}H_{22}O$	calc.	C	91.45	H	4.97
(446.6)	found		91.20		4.85

MS (70 eV) m/z = 446 (M^+, 100), 223 (13.9).

^{1}H-NMR ($CDCl_3$): δ = 5.40 (s, 1 H, OH), 7.03-7.11 (m, 3 Harom), 7.26-7.53 (m, 18 Harom).

2,6-Bis-(4-trifluoromethylphenyl)-4-(t-butyl)-anisole 27 To a 250 mL of three-neck flask equipped with magnetic stirring, nitrogen inlet and condenser, was added **21** (7.96 g, 14 mmole), sodium trifluoroacetate (15.26 g, 112 mmole), cuprous iodide (10.64 g, 56 mmole) and NMP (100 mL). The mixture was heated to 160 °C under nitrogen with stirring for 6.5 hours. The heavy brown mixture was poured into water (200 mL) and extracted with chloroform (2 x 100 mL). The organic phase was washed with water (2 x 200 mL) to remove NMP. The organic layer was dried ($MgSO_4$) and the solvent was removed by distillation on a rotovap. The residue was recrystallized from ethanol-chloroform giving **27** as light colored crystals; yield: 3.6 g (54%); m.p. 173-175 °C.

$C_{25}H_{22}OF_6$	calc.	C	66.37	H	4.90
(452.4)	found		66.57		4.60

MS (70 eV) m/z = 452 (M^+, 38%), 437 (100%).

^{1}H-NMR ($CDCl_3$): δ = 1.37 (s, 9 H, t-Bu), 3.13 (s, 3 H, CH_3O), 7.36 (s, 2 Harom), 7.71 (m, 8 Harom).

2,6-Bis-(4-trifluoromethylphenyl)-4-(t-butyl)-phenol 28a In a 200 mL flask with magnetic stirring and nitrogen inlet in a dry ice-acetone bath, **27** (3.6 g, 8 mmole) was dissolved in dichloromethane (80 mL). When the substrate was dissolved at -30 °C in the dry ice-acetone bath, boron tribromide-dichloromethane solution (20 mL, 1.0 M) was added by syringe. The reaction was kept at a temperature from -30 °C to -10 °C over 1.5 hours with stirring. The reaction was quenched by pouring the solution into ice-water. The organic layer was washed with water (2 × 80 mL) and dried ($MgSO_4$). The solvent was evaporated off and the residue was purified by recrystallization from ethanol-chloroform to give **28a** as white crystals; yield: 2.8 g (81%); m.p. 130-131 °C.

$C_{24}H_{20}OF_6$ calc. C 65.75 H 4.60

(438.4) found: 65.37 4.21

MS (70 eV) m/z = 438 (M^+, 31%), 423 (100%).

^{1}H-NMR ($CDCl_3$): δ = 1.36 (s, 9 H, t-Bu), 5.13 (s, 1 H, OH), 7.31 (s, 2 Harom), 7.72 (q, 8 Harom J = 8.50 Hz,).

2,6-Bis-(4-trifluoromethylphenyl)-phenol 28b To a stirred solution of the above compound **28a** (2.63 g, 6 mmol) in benzene (35 mL) at 50 °C, a solution of aluminum chloride (1.07 g, 8 mmol) in nitromethane (5 mL) was added. The reaction was continued at 50 °C for 3.5 h. The mixture was poured into ice water (100 mL). The organic layer was diluted with benzene (50 mL) and was separated. The solvent was distilled in vacuo. The residue was purified by recrystallization from ethanol-chloroform to give **28b** as white crystals; yield: (1.56 g, 68%); m.p. 125-125 °C.

$C_{20}H_{12}OF_6$ calc. C 62.83 H 3.16

(382.3) found 62.88 3.26

MS (70 eV) m/z = 382 (M^+, 100%).

^{1}H-NMR ($CDCl_3$): δ = 5.22 (s, 1 H, OH), 7.12 (t, 1 Harom. J = 7.55 Hz), 7.31 (d, 2 Harom, J =7.30 Hz), 7.71 (q, 8 Harom, J = 8.35 Hz).

4-Bromo-2,6-diphenylphenol 32. To a stirred solution of **1** (123 g, 500 mmol) in acetic acid (500 mL), bromine (80 g, 500 mmol) is added dropwise over 1 h at room temperature. The reaction is continued for 16 h. The light yellow solution is poured into sodium bisulfite solution (1%, 1L) with agitation. The white oil at the bottom of the flask solidifies in the refrigerator overnight. The solid is collected by filtration and washed thoroughly with water, then recrystallized from ethanol to give **32** (152 g, HPLC purity 96%) as white crystals. Further purification by recrystallization from petroleum ether gives **32** as white crystals; yield: 120 g (74%); mp 66 °C.

$C_{18}H_{13}BrO$ calc. C 66.48 H 4.03

(325.2) found 66.41 4.08

MS (70 eV): m/z = 326 (M^+ + H, 97), 325 (M^+, 25), 324 (M^+ - H, 100).

^{1}H-NMR ($CDCl_3$): δ = 5.39 (s, 1 H, OH), 7.50 (m, 13 Harom).

4-Bromo-2,6-bis(4-t-butylphenyl)phenol 33. A solution of **32** (65 g, 200 mmol) and t-butyl bromide (100 mL) in methylene dichloride (100 mL) is heated to 60 °C. Aluminum foil (cut in small pieces, 0.4 g) is added. In 1.5 h, a dark color develops and HBr evolution begins. The reaction is stopped at 2 h and the reaction is quenched by pouring the mixture into ice water (500 mL). The organic layer is washed with hydrochloric acid (10%, 2 x 200 mL), then with brine (2 x 200 mL). The organic phase is dried ($MgSO_4$) and the solvent is distilled in vacuo. The light yellow oil is purified by recrystallization from petroleum ether giving **33** as white crystals; yield: 57 g (65%); mp 176-177 °C.

$C_{26}H_{29}BrO$ calc. C 71.39 H 6.68

(437.4) found 71.73 6.72

MS (70 eV): m/z = 438 (M^+ + H, 64), 423 (M^+ - CH_3 + H, 78).

^{1}H-NMR ($CDCl_3$): δ = 1.36 (s, 18 H, 2 t -C_4H_9), 5.45 (s, 1 H, OH), 7.37 (s, 2 Harom), 7.48 (d, 8 Harom).

2,6-Bis(4-t-butylphenyl)phenol 34. To a suspension of **33** (43.7 g, 100 mmol) and Pd/C (10 g, 10%) in absolute ethanol (400 mL), is added anhydrous hydrazine (30 mL) by syringe under a nitrogen atomsphere. The mixture is heated to 70 °C and the reaction is continued overnight. The catalyst is removed by filtration and the product crystallizes rapidly from the filtrate by cooling. The solid is dissolved in methylene dichlo-

ride (300 mL), and washed with hydrochloric acid (10%, 2 x 300 mL), then by water (2 x 300 mL). The organic phase is dried ($MgSO_4$) and the solvent is distilled in vacuo. Recrystallization from petroleum ether gives **34** as white crystals; yield: 33 g (92%); mp 137-138 °C.

$C_{26}H_{30}O$ calc. C 87.09 H 8.44

(358.5) found 87.51 8.55

MS (70 eV): m/z = 358 (M^+, 65), 343 (M^+ - CH_3, 100).

^{1}H-NMR ($CDCl_3$): δ = 1.36 (s, 18 H, 2 t -C_4H_9), 5.47 (s, 1 H, OH), 7.05 (t, 1 Harom), 7.24 (d, 2 Harom), 7.49 (s, 8 Harom).

2-Bromo-6-phenylphenol 36 A stirred solution of tert-butylamine (29.26 g, 42 mL, 0.4 M) in toluene (500 mL) equipped with an addition funnel protected with a drying tube was cooled down to -20 to -30 °C in an isopropyl alcohol-dry ice bath. To the solution, bromine (31.96 g,10.25 mL, 0.2 mole) was added dropwise over 15 min. Then the mixture was cooled to -75 °C by the addition of more dry ice to the cooling bath at which time a solution of 2-phenylphenol (30.04 g, 0.2 mole) in methylene dichloride (50 mL) was added dropwise over 10 min. The mixture was stirred for 6 h at this temperature and warmed to room temperature over 3 h. The ammonium salts were removed by filtration and the solution was concentrated to half volume. Sodium hydroxide solution (20%, 300 mL) was added to the above solution and the sodium salt of the product precipitated out as white solid and was collected by filtration and transferred to water (300 mL) and the mixture was carefully acidified with concentrated hydrochloric acid. The product was taken up in ether (300 mL) and dried over magnesium sulfate. The solvent was removed by distillation at reduced pressure and the light orange residue was dissolved in warm hexane and kept in the refrigerator overnight to give **36** as white crystals; yield: 34 g (68%); m.p. 52 °C. (Lit. 38-39 °C).

$C_{12}H_9OBr$ calc. C 57.86 H 3.64

(249.1) found 58.05 3.72

MS (70 eV): m/z = 249 (M^+, 35.0), 248 (M - H, 100), 168 (M - Br, 37.8).

^{1}H-NMR ($CDCl_3$): δ = 5.69 (s, 1 H, OH), 6.89 (t, 1 Harom, J = 7.9 Hz), 7.25-7.58 (m, 7 Harom).

2,6-Bis(4-hydroxyphenyl)phenol 42 Compound **40c** (7.45 g, 24 mmole) was dissolved in dry methylene

dichloride (50 mL) in a 250 mL three neck flask with nitrogen inlet and magnetic stirring in a dry ice-acetone bath. When the temperature reached - 30 °C, boron tribromide (7.5 mL, 80 mmole) was added with a syringe over 20 min. Then the cooling bath was removed and the reaction was continued at room temperature for 3 hours. The reaction mixture was then poured into water (150 mL) and the organic phase was isolated and washed with water (3 x 100 mL). The organic phase was dried ($MgSO_4$) overnight. The solvent was evaporated off and the residue was crystallized from ethanol giving **42** as white crystals; yield: 6.20 g (93%); m.p . 243 - 243.5 °C.

$C_{18}H_{14}O_3$ calc. C 77.68 H 5.07

(278.3) found 77.32 5.21

MS (70 eV): m/z = 278 (M^+, 100), 249 (24.5), 231 (19.5), 202 (18.9), 184 (16.9), 139((15.5).

^{1}H-NMR (Acetone-d_6): δ = 2.90(s, 1 H, OH), 6.92(d, 4 Harom), 7.00(m, 1 Harom), 7.20(d, 2 Harom), 7.42 (d, 4 Harom), 8.45(s, 2 H, OH).

2,6-Bis[4-(dimethyl-t-butylsiloxyl)phenyl]phenol 43 Compound **42** (2.78g, 10 mmol) , imidazole (6.8 g, 0.1 mole) and t-butyldimethylsilyl chloride (6.2 g, 40 mmole) were added into dry DMF (40 mL) in a 100 mL flask equipped with nitrogen inlet and magnetic stirring. A clear solution was formed. A few minutes later, a white solid came out of solution. The reaction was stopped at 5 hours and the mixture was diluted with ether (40mL) which gave a clear solution.. The solution was washed with $NaHCO_3$ (5%, 100 mL) and water (2 x 100 mL). The organic phase was dried ($MgSO_4$) overnight and the solvent was removed by evaporation. The residue was crystallized from hexane-benzene giving **43** as white crystals; yield: 3.2 g (64%); m.p. 140 - 144 °C.

MS (70 eV): m/z = 506 (M^+, 100), 449 (55.6), 399 (10.1). 196 (85.8).

^{1}H-NMR ($CDCl_3$): δ 0.26 (s, 12 H, 4 Si-CH_3), 1.03 (s, 18 H, 2 t-Bu),5.40(s, 1 H, OH), 6.90-7.50(m, 11 H_{arom}).

2-Bromo-6-phenylanisole 44 A mixture of **36** (12.46 g, 50 mmole), dimethyl sulfate (9.45 g, 75 mmole) and tetrabutylammonium bromide (1.0 g) in methylene dichloride (125 mL) and sodium hydroxide (3.0 g) in water (125 mL) was stirred at room temperature for 6 h. The organic layer was washed with wa-

ter (2 x 200 mL) and dried ($MgSO_4$). The solvent was removed by distillation under vacuo. The residue was distilled on a Kugelrohr apparatus to give a colorless oil which slowly solidified into white crystals; yield: 11.2 g (85%); mp. 39-40 °C.

$C_{13}H_{11}OBr$ calc. C 59.34 H 4.21

(263.1) found 59.59 4.27

MS (70 eV): m/z = 263 (M^+, 11.2), 262 (57.1, M - 1), 168 (100), 139 (19.5).

^{1}H-NMR ($CDCl_3$): δ = 3.45 (s, 3 H, OCH_3), 7.04 (app t, 1 Harom, J = 7.9 Hz), 7.29 (app d, 1 Harom, J = 7.7 Hz), 7.35-7.58 (m, 6 Harom).

(2-Methoxy-3-phenylphenyl)boronic Acid 45 (a) Grignard Reagent: A suspension of magnesium turnings (3.83 g, 158 mmole) in dry THF (30 mL) is activated with iodine crystals. A solution of **44** (39.48 g, 150 mmole) in dry THF (120 mL) was added in portions. The first portion was added and the reaction was initiated and the addition was continued to maintain refluxing. The stirred solution was heated to reflux for 6 h to make sure the reaction was completed. (b) To a rapidly stirred solution of triisopropylborate (98%, 69.2 mL, 300 mmole) in dry THF (40 mL) cooled to -75 °C under a nitrogen atmosphere was added a solution of above prepared Grignard reagent dropwise over 10 min. and a white precipitate rapidly developed. The solution was allowed to warm to room temperature and stirred at room temperature for 30 min. The mixture was then partitioned between 400 mL of ether and 400 mL of 10% aqueous HCl. The ether extract was washed with water (400 mL) and dried over anhydrous magnesium sulfate. The solvents were removed under reduced pressure and the product was dried in vaccuo at room temperature for two days to afford a white solid 28.5 g (83%) which was used for the next reaction step without further purification. An analytical sample was obtained by crystallization from ether-hexane as white crystals. mp. 169-172 °C.

$C_{13}H_{13}O_3B$ calc C 68.47 H 5.75

(228.1) found 68.65 5.83

MS (70 eV): m/z = 228 (M^+, 100), 184 (21.9), 169 (63.6).

^{1}H-NMR ($CDCl_3$): δ = 3.41 (s, 3 H, OCH_3), 6.28 (app d, 2 H, $B(OH)_2$), 7.25 (t, 1 Harom), 7.35-7.59 (m, 6 Harom), 7.84 (q, 1 Harom).

2-Phenyl-6-(4-cyanophenyl)anisole 46a To a stirred solution of 4-bromobenzonitrile (20.02 g, 0.11 mole) and $Pd(PPh_3)_4$ (3.47 g, 3% equiv.) in toluene (400 mL) under a nitrogen atomsphere, was added aqueous sodium carbonate solution (100 mL, 2 M). To this vigorously stirred mixture was added **45** prepared above (22.8 g, 0.1 mole) dissolved in a minimum amount of ethanol. The reaction mixture was heated to reflux for 20 h. After the mixture cooled to room temperature, the mixture was extracted with ether (2 x 400 mL) and the ether layer was washed with water (400 mL) and dried ($MgSO_4$) . The solvent was removed under reduced pressure and the residue was purified by crystallization from ethanol-chloroform to afford **46a** as light yellow crystals; yield: 20.5 g (72%). mp. 140-141 °C.

$C_{20}H_{15}ON$	calc.	C	84.19	H 5.30
(285.4)	found		84.18	5.19

MS (70 eV): m/z = 285 (M^+, 100), 270 (40, M - CH3), 129 (11.1).

^{1}H-NMR ($CDCl_3$): δ = 3.14 (s, 3 H, OCH_3), 7.30 - 7.62 (m, 8 Harom), 7.23 (s, 4 Harom).

2-Phenyl-6-(4-phthalimidylphenyl)anisol 46b To a stirred suspension of 4-bromophenylphthalimide[29] **34** (12.09 g, 40 mmole) in toluene (120 mL) under a nitrogen atomsphere, was added aqueous sodium carbonate solution (40 mL, 2 M). The solution was degassed for 30 min with nitrogen bubbling through the solution and followed by the addition of $Pd(PPh_3)_4$ (1.38 g, 3% equiv.) under nitrogen atmosphere. To this vigorously stirred mixture was added **45** (9.12 g, 40 mmole) which was dissolved in a minium amount of ethanol. The reaction mixture was heated to reflux and the components in the organic phase gradually dissolved. The reaction was continued for 20 h and the organic phase became yellow in color. The mixture was first diluted with 100 mL of toluene and then extracted with ether (2 x 100 mL) and the ether layer was washed with water (200 mL) and dried over anhydrous magnesium sulfate overnight. The solvent was removed under reduced pressure and the residue was purified by crystallization from ethanol-chloroform to afford **46b** as light yellow crystals; yield: 9.2 g (57%). m.p. 187-188 °C.

MS (70 eV): m/z = 405 (M^+, 100), 390 (M - CH_3, 22.7), 215 (14.2).

^{1}H-NMR ($CDCl_3$): δ = 3.20 (s, 3 H, OCH_3), 7.28 - 7.74 (m, 12 Harom), 7.74 - 7.82 (q, 2 Harom), 7.96 (q, 2 Harom).

2-Phenyl-6-(4-cyanophenyl)phenol 47a A stirred suspension of **46a** (19 g, 66.6 mmole) in methylene dichloride (40 mL) was put in a cooling bath (isopropyl alcohol-dry ice) . Then a solution of BBr3 (166.5 mL, 166.5 mmole, 1.0 M in methylene dichloride) was added by syringe at -70 °C. The temperature was allowed to warm to room temperature in 3 h with constant HPLC monitoring. The solution was poured into ice water (500 mL) and the mixture was extracted with methylene dichloride (2 × 200 mL). The organic phase was washed with water (2 × 200 mL) and dried ($MgSO_4$). Removal of solvent at reduced pressure afforded a yellow solid which was purified by crystallization from hexane-chloroform to afford **47a** as light yellow crystals; yield: 10.7 g (59%); m.p. 185-186 °C.

MS (70 eV): m/z = 271 (M^+, 100), 240 (7.0), 129 (7.2).

^{1}H-NMR ($CDCl_3$): δ = 5.42 (s, 1 H, OH), 7.09 (t, 1 Harom), 7.28 (d, 1 Harom), 7.31 (d, 1 Harom), 7.46-7.54 (m, 5 Harom), 7.72 (br, 4 Harom).

2-Phenyl-6-(4-phthalimidylphenyl)phenol 47b A stirred suspension of **46b** (6.08 g, 15 mmole) in methylene dichloride (20 mL) was put in a cooling bath (isopropyl alcohol-dry ice). A solution of BBr_3 (45 mL, 45 mmole, 1.0 M in methylene dichloride) was added by syringe at -70 °C. The temperature was allowed to warm to room temperature in 3.5 h with constant HPLC monitoring. The solution was poured into ice water (300 mL) and the mixture was extracted with methylene dichloride (2 × 100 mL). The organic phase was washed with water (2 × 100 mL) and dried ($MgSO_4$). Removal of solvent at reduced pressure afforded a yellow solid which was purified by crystallization from ethanol-chloroform to afforded **49b** as light yellow crystals; yield: 3.8 g (65%); m.p. 210-212 °C.

MS (70 eV): m/z = 391 (M^+, 100),244 (17.0), 215 (9.2), 195 (9.5).

^{1}H-NMR ($CDCl_3$): δ = 5.45 (s, 1 H, OH), 7.08 (t, 1 Harom, J = 7.5). 7.27 - 7.75 (m, 11 Harom), 7.78 - 7.82 (q, 2 Harom), 7.96 - 8.00 (q, 2 Harom).

Oxime 50 A mixture of 2,6-diphenylcyclohexanone **49** (10.0 g), hydroxylamine hydrochloride (10 g), hydrated sodium acetate (20 g), water (100 mL) and ethanol (200 mL) was heated under reflux overnight. The mixture was cooled and filtered and washed with ethanol. Crystallization from ethanol afforded **50** as white crystals; yield: (7.2 g, 68%); m.p. 204 -206 °C.

Amide Dreivative 51 The resultant oxime **50** (2.5 g, 7.6 mmole) was added into a solution of acetic anhydride (12 mL) and pyridine (2.7 mL). The stirred mixture was cooled to 0 °C in an ice bath and acetyl chloride (2.1 mL) was added dropwise while a white solid precipitated. The mixture was warmed slowley to 90 °C, at which time the mixture became homogenous, and then heated at reflux under nitrogen for 2 h. After being cooled to room temperature, the resulting brown solution was poured onto ice and thrice extracted with ether. The combined ether extracts were washed with water, dried ($MgSO_4$), and concentrated in vacuo to give a yellow solid. The product was purified by crystallization from ethanol to give **51** as white crystals; yield: 0.65 g (30%), m.p. 244 °C

MS (70 eV): m/z = 287 (M^+, 36.3), 245 (100), 167 (5.2).

^{1}H-NMR ($CDCl_3$): δ = 1.68 (s, 3 H, $COCH_3$), 6.58 (s, 1 H, NH), 7.36-7.38 (m, 13 Harom).

2.6-Diphenylaniline 52 A mixture of compound **50** (0.5 g, 1.7 mmol), Pd/C (50 mg, 5%) and diphenyl ether (10 mL) is heated under reflux for 20 h. The mixture is diluted with acetone (20 mL) and the catalyst is removed by filtration. The solvent is evaporated on a rotovap under reduced pressure to give a light yellow oil. The crude product was subjected to flash chromatography with hexane as eluent to afford **52** as white crystals; yield: 0.12 g (29 %), m.p. 74 -75 °C.

$C_{18}H_{15}N$	calc.	C 88.13	H	6.16
(245.3)	Found	88.27		6.48

MS (70 eV): m/z = 245 (M^+, 100).

^{1}H-NMR ($CDCl_3$): δ = 3.85 (s, 2 H, NH_2), 6.90 (t, 1 Harom), 7.15 (d, 2 Harom), 7.51 (m, 10 Harom).

2,6-Diarylphenol Prepared from Cross-coupling Reaction:

General Procedure: **2-(4-Fluorophenyl)-6-phenylphenol 41a** 2-Bromo-6-phenylphenol (9.97 g, 40 mmol) is dissolved in toluene (200 mL) and sodium carbonate solution (2.0 M, 40 mL) is added. The solu-

tion is degassed by bubbling argon through the solution for 20 min. Then $Pd(PPh_3)_4$ (1.39 g, 3% equiv.) is added under an argon atmosphere. 4-Fluorophenylboric acid (6.72 g, 1.2 equiv) is dissolved in minimum amount of ethanol and added into the above solution through a syringe. The mixture was heated to gentle reflux with stirring for 10 h. During the reaction, the bottom layer changed from a suspension into a clear solution. The mixture is cooled to room temperature and the aqueous phase is removed and the organic phase is washed with water (2 x 300 mL) and dried ($MgSO_4$). The solvent was removed under reduced pressure. The residue was purified by flash chromotography (hexane-ethyl acetate). Further purification by crystallization from ethanol gave **41a** as white crystals; yield: 8.1 g (77%).

For the coupling reactions of phenols and aniline to prepare **40a-c**, **41a-c**, **48** and **52**, the following equivalents of arylboric acids, Pd(0) catalysts, n-tetrabutylammonium bromide TBAB (or NiL), and the following conditions, refluxing time and purification were applied:

40a: 2.5 equiv 4-fluorophenylboric acid, 3% equiv catalyst, TBAB 10% W, column and recrystallization in hexane. **40b**: 2.5 equiv m-fluorophenylboric acid, 3% equiv catalyst, TBAB 10%W, distillation with Kugelnohr in vac. at 120 °C. **40c**: 2.5 equiv p-methoxyphenylboric acid, 3% equiv catalyst, TBAB 10%W, column and recrystallization in ethanol-chloroform. **41b**: 1.2 equiv m-fluorophenylboric acid, 3% equiv catalyst, column and recrystallization in hexane-chloroform. **41c**: 1.2 equiv p-methoxyphenylboric acid, 3% equiv catalyst, column and recrystallization in ethanol-chloroform. **48**: 5.0 equiv phenylboric acid, 5% equiv catalyst, TBAB 10%W, column and recrystallization in hexane-chloroform. **52**: 2.5 equiv phenylboric acid, 3% equiv catalyst, TBAB 10%W, column and recrystallization in ethanol. The yields and the analysis data for the prepared compounds are listed in table 2.2 and 2.3.

Table 2.2. Phenylation of Phenols and Aniline by Cross-coupling Reaction

Aryl Halide	Boronic acid	Reaction Time	Product	Yield, %
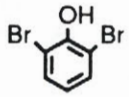	4-FPhB(OH)$_2$ (2.5 equv.)	10 h	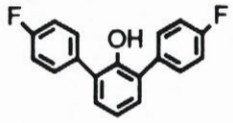 **40a**	43
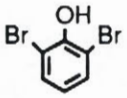	3-FPhB(OH)$_2$ (2.5 equv.)	10 h	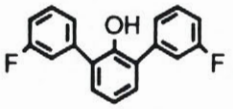 **40b**	36
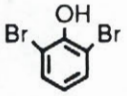	4-MeOPhB(OH)$_2$ (2.5 equv.)	10 h	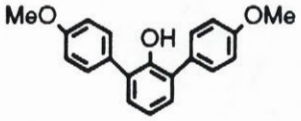 **40c**	59
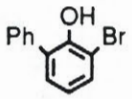	4-FPhB(OH)$_2$ (1.2 equv.)	10 h	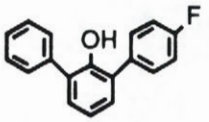 **41a**	77
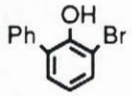	3-FPhB(OH)$_2$ (1.2 equv.)	10 h	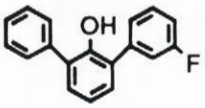 **41b**	59
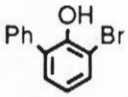	4-MeOPhB(OH)$_2$ (1.2 equv.)	10 h	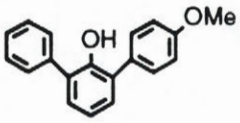 **41c**	62
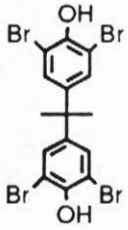	PhB(OH)$_2$ (4.5 equv.)	20 h	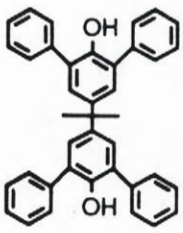 **48**	53
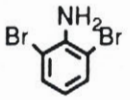	PhB(OH)$_2$ (2.5 equv.)	20 h	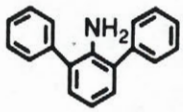 **52**	86

Table 2.3. Arylated phenols and Aniline Prepared

Product	mp (°C)	Microanalysis Calc.	Found	MS m/e (70eV)	^{1}H NMR ($CDCl_3$/TMS) δ, (mult., *J* Hz)
40a*	62-65	-	-	-	-
40b	47-49	C, 76.59 H, 4.28	76.37 4.33	282 (M^+, 100)	5.37 (s, 1 H, OH), 7.12 (m, 3 Harom) 7.28-7.51 (m, 8 Harom).
40c[30]	35	- -	- -	306(M^+, 100),	3.86 (s, 6 H, MeO), 5.38 (s, 1 H, OH), 6.90-7.06 (m, 5 Harom), 7.23 (d, 2 Harom, *J* =7.94 Hz), 7.49 (d, 4 Harom, *J* = 8.8 Hz).
41a	98-99	C, 81.80 H, 4.96	82.01 5.01	264 (M^+, 100)	5.17 (s, 1 H, OH), 6.86 (d, 1 Harom), 7.36-7.49 (m, 10 Harom).
41b	56	C, 81.80 H, 4.96	81.46 4.81	264(M^+, 100)	5.38 (s, 1 H, OH) 7.05-7.13 (m, 1 Harom), 7.27-7.37 (m, 4 Harom), 7.54-7.67 (m, 7 Harom).
41c	115	C, 82.58 H, 5.84	83.12 5.92	276 (M^+, 100)	3.87 (s, 3 H, OMe), 5.40 (s, 1H, OH),7.04 (t, 3 Harom), 7.27 (d, 2 Harom), 7.39-7.61 (m, 7 Harom).
48[31]	36	- -	- -	532(M^+, 49.9), 262(100).	1.74(s, 6 H, Me), 5.29 (s, 1 H, OH), 7.21 (s, 4 Harom) 7.36-7.56(m, 20 Harom).
52	74 -75	C, 88.13 H, 6.16	88.41 6.22	245 (M^+, 100)	3.85 (s, 2 H, NH_2), 6.90 (t, 1 Harom), 7.15 (d, 2 Harom), 7.51 (m, 10 Harom)

* Product is identical to an authentic sample.

References:

(1) Plesek, J., *Chem Listy* , **1956**, 50, 252.

(2) Bodroux, D., *Ann. Chim.*, (Paris), **1929**, 11, 511. Hennion, G.F., *J. Am. Chem. Soc.*, **1944**, 66, 1801.

(3) Hay, A. S. and Clark, R. F., *Macromolecules*, **1970**, 3, 533.

(4) Dana, D. E. & Hay, A. S. *Synthesis*, **1982**, 2, 164.

(5) Barton, D. H. R., Bhatnagar, N. Y., Blazejewski, J-C., Brigitte, Charpiot, B., Finet, J-P., Lester, D. J., Motherwell, W. B., Papoula, M. T-B., & Stanforth, S. P. *J. Chem. Soc. Perkin Trans.* I, **1985**, 2657.

(6) Barton, D. H. R., Finet, J-P., Giannotti, C., & Halley, F., *J. Chem. Soc. Perkin Trans.* I, **1987**, 241.

(7) Wittig, G., Clauss, K. Liebigs *Ann. Chem.*, **1952**, 578, 136.

(8) Heck, R. F., "*Palladium Reagents in Organic Synthesis*" Academic Press, **1985**, Chapter. 6.

(9) Ossor, H. and Pfeffer, M., *J. Chem. Soc. Chem. Commun.*, **1985**, 21, 1540.

(10) Heck, R. F. *Acc. Chem. Res.*, **1979**, 12, 146. ; Patel, B. A., Ziegler, C. B., Cortese, N. A., Plevyak, J. E., Zebovitz, T. C., Terpko, M. & Heck, R. F., *J. Org. Chem.*, **1978**, 43, 2941.

(11) Tilley, J. W. and Zawoiski, S., *J. Org. Chem.*, **1988**, 53, 386.

(12) Widdowson, D. A. and Zhang, Y. Z., *Tetrohedron*, **1986**, 42, 2111.

(13) Kumada, M., *Pure Appl. Chem.*, **1980**, 52, 699.

(14) Miyaura, N., Yanagi, T., & Suzuki, A. *Synth. Commun.*, **1981**, 11, 513.

(15) Sharp, M. J. and Snieckus, V., *Tetrahedron Letters*, **1985**, 5997.

(16) Sharp, M. J., Chen, W. and Snieckus, V., *Tetrahedron Letters*, **1987**, 28, 5093.

(17) Jendralla, H. & Chen, L-J., *Synthesis*, **1990**, 827.

(18) Wolfe, J. F. & Arnold. F. E., *Macromolecules*, **1981**, 14, 909.

(19) Dana, D. E., *Ph.D Thesis*, **1982**.

(20) Edgar, A, et al., *J. Chem. Soc.*, **1957**, 1083; Kosowar, E. and Wu, J., *J. Org. Chem.*, **1963**, 28, 633.

(21) Mahmoud, S. K., *J. Org. Chem.*, **1974**, 39, 2126.

(22) Roberts, R. M. and Ali, A. K., *Friedel-Crafts Alkylation Chemistry*, Marcel Dekker, New York, **1984**.

(23) Khan, S. A., Munawar, M. A. & Siddiq, M., *J. Org. Chem.*, **1988**, 53, 1799.

(24) Merkushev, E. B., *Synthesis*, **1988**, 12, 923.

(25) Wing-Wah, S., Lodge, B. A., & Arnold, W. B., *Synth. Commun.*, **1990**, 20, 877; Wing-Wah., S. & Lodge, B. A. *Tetrahedron Letters*, **1989**, 30, 3769.

(26) Tashiro, M., Watanabe, H., and Oe, K., *J. Prakt. Chem.*, **1985**, 327, 998.

(27) Pearson, D. E. , Wysong, R. D. & Breder, C. V., *J. Org. Chem.*, **1967**, 32, 2358.

(28) Kelly, T. R., Chandrakumar, N. S. & Saha, J. K., *J. Org. Chem.*, **1989**, 54, 980.

(29) Hergenrother, P. M.., Havens, S. J., and Connell, J. W., *Polym. Prepr.* **1986**, 408.

(30) Dana, D. E., and Hay, A. S., *Synthesis*, **1982**, 2, 164.

(31) Wang, Z. Y., and Hay, A. S., *Synthesis*, **1989**, 6, 471.

CHAPTER 3. OXIDATIVE POLYMERIZATION OF 2,6-DIARYLPHENOLS

3.1. MECHANISM OF OXIDATIVE POLYMERIZATION

Theoretically any bifunctional molecules can be potential candidates for synthesizing high-molecular weight polymers. Whether the product is low-molecular weight oligomer or high molecular weight polymer depends on the reactivity of the reactants and whether the side-reactions will interfere with the polymerization reaction.

The initial attempts by Allan S. Hay and coworkers[1] in 1956 to oxidize phenol with amine-copper complex as catalyst gave only a dark brown tar as products which are highly crosslinked materials. This is not surprising because there are four available reactive sites on the phenol and the intermediates formed in the reaction will actually be oxidized more easily than the starting phenol.

Scheme 3.1

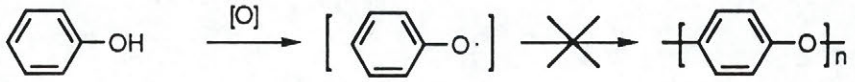

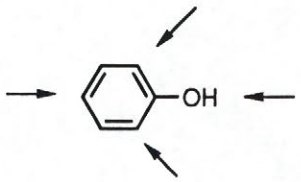

On the assumption that the first step in the reaction involves coordination of the copper catalyst with the phenol, some relatively bulky ligands for the copper catalyst complex were used in an attempt to block out the unwanted reactions at the ortho positions, shown schematically in scheme 3.2[1], so that the desired selective C-O coupling could proceed to yield linear polymer. Some success in the oxidative polymerization of phenol and o-cresol were achieved, however the branching due to the reaction at additional reactive sites was never excluded completely[2].

Scheme 3.2

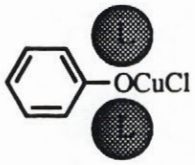

To eliminate the side reactions, Hay[3] used 2,6-dimethylphenol as monomer in which the ortho positions are occupied by methyl and the high molecular weight linear polymer was obtained with only minor amounts of the diphenoquinone byproduct from C-C coupling .

Scheme 3.3

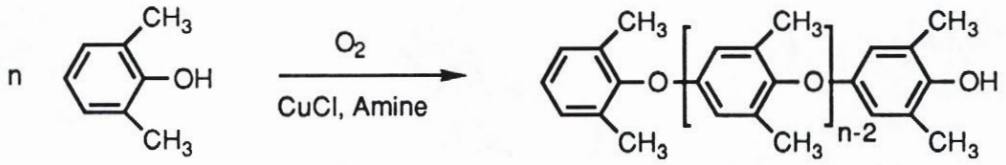

2,6-Dimethylphenol PPO

Because of the industrial significance of this polymer and the novelty of the polymerization reaction, much effort has been made to understand the mechanism of this polymerization reaction[4,5]. Initially it seemed that this reaction mechanism could be categorized as a chain growth propagation mechanism by simple radical addition of one unit to the growing polymer chain which is similar to vinyl type polymerizations. But the molecular weight - conversion profile does not correspond to the chain growth pattern. In fact, high molecular weight polymer is only formed at the latter stage of the reaction. It is apparent , therefore, that mechanistically the polymerization behaves as a typical step reaction rather than a chain reaction. Two prevailing mechanisms, redistribution mechanism[6] and rearrangement mechanism[7] have been proposed based on the experimental evidence. Both mechanisms are similar in that both require the initial formation of phenoxy radicals that couple to produce a quinone ketal intermediate (scheme 3.4).

Scheme 3.4

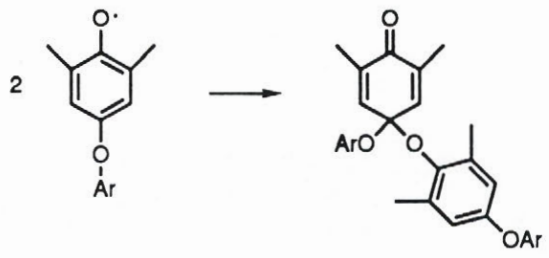

In the redistribution mechanism it is suggested that the ketal intermediates are not stable and dissociate to either their precursors or form a pair of new oligomeric radicals. This process is demonstrated in scheme 3.5 in which the ketal formed from two dimer radicals dissociates to a trimer radical and a tetramer will be produced whenever trimer radical couples with the monomeric radical co-product of the dissociation.

Scheme 3.5

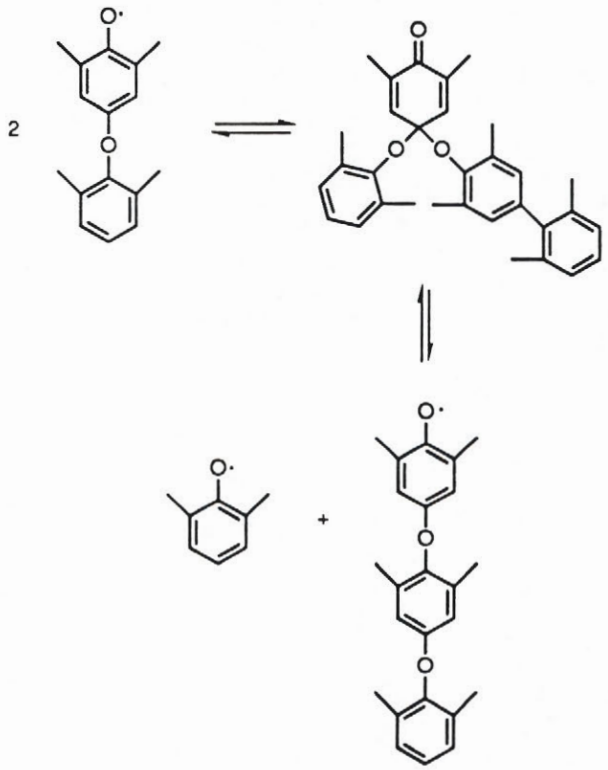

White[8] and others[9] have provided experimental evidence to show the equilibrium nature of the redistribution mechanism and applied this knowledge to synthesize some sub-

stituted hydroxyphenyl ethers from the redistribution of substituted phenols with xylenol high polymer.

Scheme 3.6

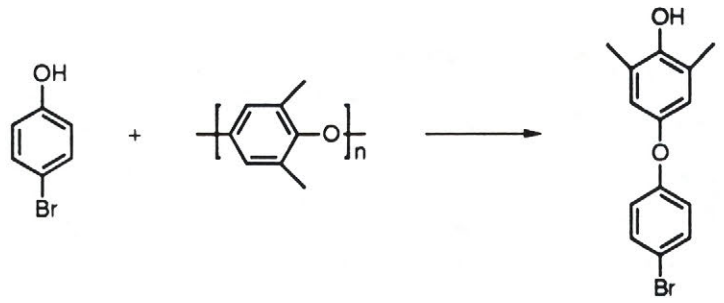

The second mechanism, quinone ketal rearrangement, also required that the first step proceeded by coupling of two phenoxy radicals to generate a quinone ketal intermediate. Molecular modeling of this intermediate suggested that the carbonyl oxygen atom of the quinone ketal lies within the bonding distance of the para carbon of one of the ketal aromatic rings providing the possibility of rearrangement by simultaneously breaking and forming an ether linkage. It was suggested that this process occurs concurrently with the redistribution reaction and becomes dominant at lower temperature. The reason is that at a higher temperature, the ketal intermediate may dissociate before reaching the end of the chain.

Scheme 3.7

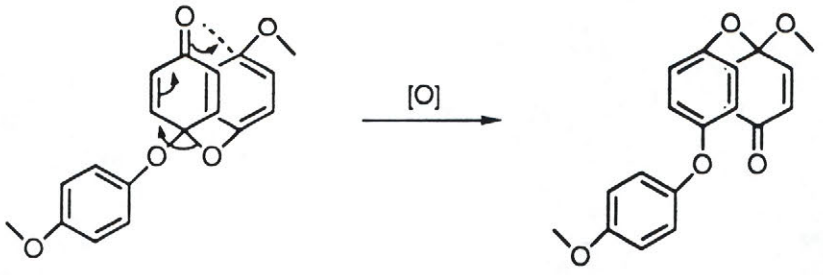

This mechansim was supported by experimental evidence. In the oxidation of dimer at 5 °C, a good yield of tetramer was obtained[5] without detectable monomer or trimer present and this agreed with the prediction from the rearrangement mechanism that only even numbered oligomers can be formed.

Scheme 3.8

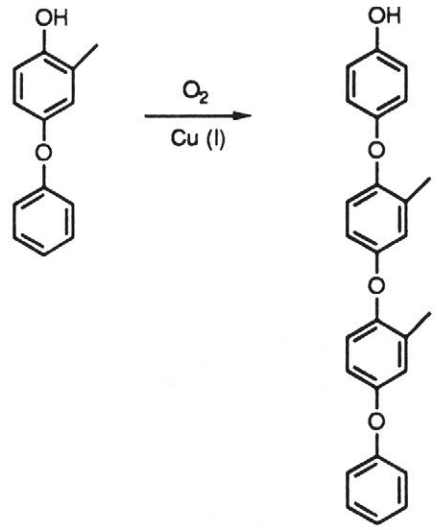

3.2. CATALYSIS SYSTEM AND REACTION VARIABLES

The oxidizing agent for the polymerization of phenols is usually molecular oxygen and a transition-metal catalyst such as copper or manganese compound combined with ligands. The role of oxygen in the reaction is to keep the copper catalyst at the higher oxidative potential and provide the access for electron transferring from phenol to catalyst. Most of the work in the literature on oxidative polymerization of phenols has been limited to a study of the polymerzation of 2,6-dimethylphenol and much of this work has been performed with copper(I) halide as catalyst and pyridine as ligand. Other ligands that have been used are diethylamine, dibutylamine[10], N,N,N',N'-tetramethylethylenediamine[11], morpholine[12] or dimethylaminopyridine[13]. The amine function to solubilize the metal salt in the organic medium and increases the pH, thereby lowering the oxidation potential of the phenol, as well as a role of ligands. Sometimes, a drying agent such as anhydrous magnesium sulfate or molecular sieve is added to the reaction mixture to avoid hydrolysis of the catalyst by the water generated from the oxidation reaction. The catalysts are believed to have the following structures with the trans conformation for monodentate amine ligands and cis for bidentate amines:

Scheme 3.9

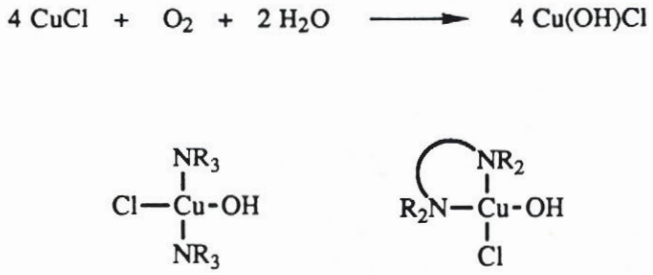

The electron transfer from oxygen to copper in the copper-amine complex would give a aryloxy radical. The overwhelming preponderance of C-O coupling over C-C coupling in the polymerization suggested that copper-amine complex remains bound to the reacting phenoxy radical and the coupling of these radicals would then give the dimer:

Scheme 3.10

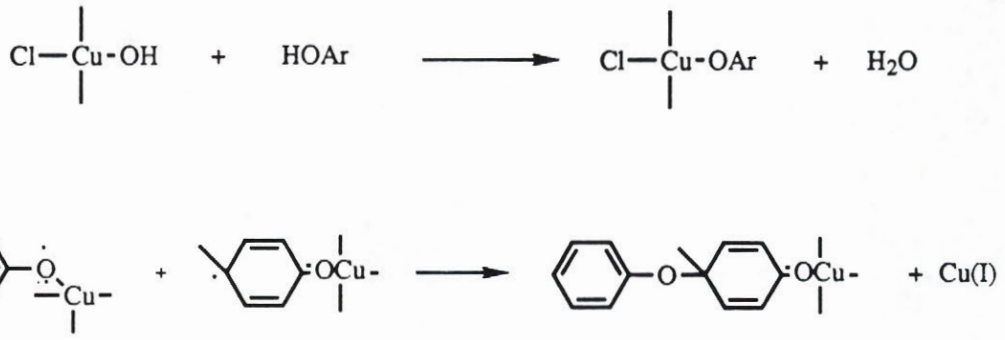

The major side-product from the reaction is the diphenoquinone from C-C coupling. The course of the polymerzation can be affected by minor changes of the reaction variables[4,14]. In the copper-amine system, the polymer:diphenoquinone ratio is increased by increase of amine:copper ratio, reducing temperature, and the slow addition of monomer to the mixture.

3.3. INFLUENCE OF MONOMER STRUCTURE ON POLYMERIZATION

It was found that under a constant set of reaction conditions, the reaction products were largely determined by the nature of the substituents. The effects can be through either

steric effect or electronic effects.

In the following table, the results clearly indicate that the course of the reaction directly depends on the degree of steric hindrance of the hydroxyl group of phenols. The presence of bulky groups at the ortho position of phenol will suppress the C-O coupling and increase the C-C coupling which leads to the diphenoquinone side product. If one of the substituents is as large as t-butyl, or both are as large as isopropyl, then the diphenoquinone is preferentially formed[4,15].

Table 3.1. Products from Oxidation of Substituted Phenols

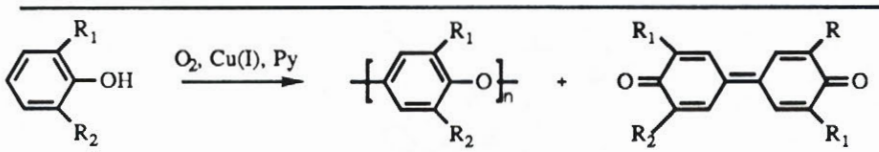

		Principal product	
R_1	R_2	Polymer	Diphenoquinone
methyl	methyl	X	
methyl	ethyl	X	
methyl	iso-propyl	X	
methyl	phenyl	X	
phenyl	phenyl	X	
methyl	t-butyl		X
iso-propyl	iso-propyl		X
t-butyl	t-butyl		X

Electronic effects also affect the polymerization because of the resulting variation in the oxidation potential of the phenols[16]. For instance, 2,6-dimethylphenol will readily give high molecular weight polymer at room temperature. But a temperature in the neighborhood of 60 °C is required to polymerize 2-chloro-6-methylphenol because of the higher oxidation potential[17]. In the polymerization of 2,6-diphenylphenol which has a higher

oxidation potential and increased steric hindrance, the diphenoquinone side product can be largely eliminated by using bidentate amine N,N,N',N'-tetramethylethylenediamine (TMEDA) as ligand at a temperature of 80 °C. Under these conditions, high molecular weight polymer was successfuly obtained[18].

3.4. SYNTHESIS OF P3O HOMOPOLYMERS

Poly(2,6-diphenylphenylene ether) P3O has a Tg of 235 °C and a melting begins at 480 °C. It can be cast into films or spun into fibers and has excellent electrical properties. However, the high melting point of P3O has limited the scope of potential applications since it cannot be molded. Attempts have been devoted to modify this polymer by changing the substitutents on the pendant rings of P3O. It has been demonstrated that the substituents at either meta or para position will not inhibit the polymerization and the success of the polymerization is then mainly dependent on whether the polymerization can proceed in a homogenous phase throughout reaction without saperating from solution because of insolubility due to crystallization[19,20].

Our principal objective was the synthesis of symmetrically-substituted polymers with substituents in the para or meta position of the pendant phenyl rings. It appeared unlikely that the substituents would affect the polymerization because of steric factors. In terms of oxidation potential of the substituted monomers, the monomers with strong electron withdrawing groups would be expected to have increased oxidation potential and so the reactivity of the monomer would decrease. However, these electronic effects would be expected to be sufficiently small due to the remoteness from the center phenolic moiety. In addition, the substituents we chose are all expected to be chemically inert toward to the conditions used in the oxidative polymerization.

The major concern to us was the solubility of the polymerization intermediates. In order to achieve high molecular weight, the reaction has to remain homogenous throughout the reaction. It was previously demonstrated that when the substituents are 4-methoxy or 4-

phenyl groups that a crystalline solid precipitated out of the reaction solution before high molecular weight polymer was obtained. So the success in making high molecular weight polymer depends totally on the nature of the monomeric structures. We hoped by choosing a wide spectrum of various-substituted monomers, we could obtain some polymers with good solubility which would still maintain inherent crystallizability in the bulk state and have lower melting points which would allow them to be melt processed. The substituents we selected can be basically divided into two categories: nonpolar groups, such as t-butyl and phenoxy group, and polar groups such as fluoro, chloro, bromo, iodo, phthalimidyl and cyano groups with increasing polarity. The results of the polymerization reactions are listed in table 3.2.

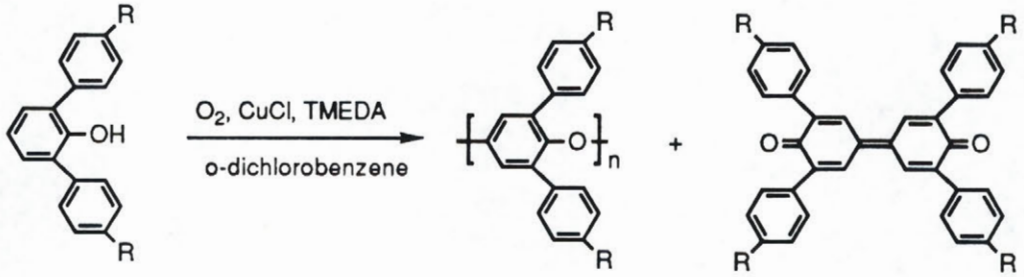

Table 3.2. Homopolymers from 2,6-Diarylphenols

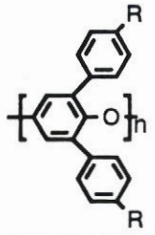

Substitutent	η_{inh}, dL/g[a]	Reaction Time	Yield%
H	0.58	8 h	72
F	0.68	10 h	69
Cl	insol.	2 h (40 min[b])	56
Br	insol.	2 h (30 min[b])	54
I[c]	insol	-	-
CN[c]	insol	-	-
t-Butyl	0.53	20 h	67
Phenoxy	0.29	4 h	66
OMe[d]	0.39	10 h	70
CN[d]	0.48	7 h	69
Phthalimidyl[d]	insol.	8 h (4 h[b])	64

a. All the viscosities were measured in $CHCl_3$ except the t-Butyl derivative which was measured in o-dichlorobenzene. The test were conducted at room temperature at a concentration of 0.5 weight %.

b. When intermediate precipitates from solution.

c. Polymer precipitates immediately.

d. Mono substituted derivatives.

The polymerization of t-butylated 2,6-diphenylphenol DPP proceeds to high molecular weight in o-dichlorobenzene solution without any solubility problem. However, the isolated polymer does not dissolve in the common organic solvents such as chloroform, benzene and dichloromethane as P3O does. This seems unusual considering that the t-butyl group is a very bulky group which generally improves polymer solubility[21,22]. We assume that this is due to the very symmetrical arrangement of t-butyl groups on the polymer which actually results in a more rigid backbone instead of an irregular chain conformation obtained by t-butylation in other systems.

As expected, phenoxy substituted DPP is soluble throughout the reaction. This apparently is due to the introduction of this bulky but flexible ether linkage in the polymer which would make crystallization difficult.

The second group of monomers contain polar groups with varying polarity. We were not successful in synthesizing high molecular weight polymer from symmetrically substituted monomers with chloro, bromo, iodo and cyano substituents since the oligomers are highly crystalline and precipitated out of the solution at an early stage of the reaction before high molecular weight could be obtained. The oxidative polymerization of iodo and cyano substituted monomers rapidily yield insoluble oligomers which precipitated out of the solution in about 10 to 20 minutes. The polymerization of bromo and chloro substituted monomers proceeds for a relatively longer time before precipitation and presumably higher molecular weights than the cyano and iodo derivatives were obtained.

There is no problem in the synthesis of fluoro-substituted P3O and high molecular weight polymer was readily obtained. The solubility of this polymer is surprising since it is not only soluble in common organic chlorinated solvents and aromatic hydrocarbons, but also soluble in some ketonic solvents which is rather unusual for such a rigid aromatic polymer.

The polymerization of unsymmetrically substituted mono-substituted monomers with cyano and methoxy groups readily yields high molecular weight polymers which are soluble in common organic solvents. However, the phthalimidyl-substituted monomer reaches a relatively high molecular weight and finally precipitates out of the reaction solution. The insolubility of this polymer can be caused by the strong chain interactions from the very polar imidyl rings.

3.5 SYNTHESIS OF RANDOM COPOLYMERS

It has been shown previously by Hay and Dana that monomers that are difficult to polymerize due to the insolubility of the intermediates, can be copolymerized with other monomers to yield soluble random copolymers[20]. Low solubility prevents the homopolymer of 3,4,5-tritribromo-2,6-dimethylphenol from attaining high molecular weight, in contrast to its copolymers with 2,6-dimethylphenol, which are more soluble and can be built up to high molecular weight[23]. Since some of the monomers, e.g. with cyano and iodo substituents, failed to give high molecular weight polymer, we planned to prepare the corresponding copolymers with sufficiently high molecular weight. The resulting copolymers would provide a much wider property spectrum with the variation of comonomer structures and the compositions.

The copolymerization reaction are conducted by simultaneous oxidation of both comonomers under identical conditions used for preparing homopolymers. The reaction time used was 12 hours for all the polymerization reactions. The data for copolymers are listed in table 3.3. The inherent viscosities of the copolymers ranges from about 0.3 to 0.5.

Table 3.3. Copolymers of 2,6-Diarylphenols with 2,6-Diphenylphenol[a]

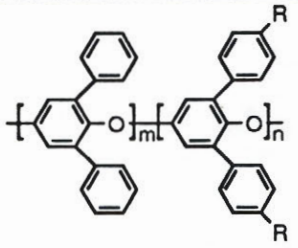

A B

Comonomer B R	A % (mole) (Feed)	η_{inh}, dL/g[b]	Yield (%)
Bu	7.0	0.42[c]	71
Bu	9.09	0.39[c]	65
Bu	16.7	0.44	70
Bu	50.0	0.54	72
Bu	83.3	0.45	80
Bu	90.9	0.41	74
Bu	93.0	0.46	68
Br	16.7	0.26[c]	74
Br	23.1	0.42[c]	66
Br	50.0	0.37	76
Br	83.3	0.44	81
Br	90.9	0.54	86
Cl	16.7	insol.	80
Cl	23.1	0.33	69
Cl	50.0	0.45	70
I	50.0	0.33	82
CN	50.0	0.41	73

a. The reaction time for all entries is 12 hours.

b. The viscosity measurements were conducted at room temperature at a concentration of 0.5% in $CHCl_3$ at 25 °C.

c. The measurements were conducted in o-dichlorobenzene.

Table 3.4. Copolymers of 2,6-Diarylphenols with 2,6-Diphenylphenol[a]

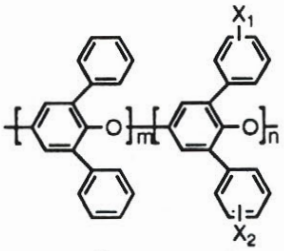

A B

X_1	X_2	A % (mole) (Feed)	η_{inh}, dL/g[b]	Yield (%)
4-F	4-F	23.1	0.46	83
4-F	4-F	28.6	0.36	79
4-F	4-F	50.0	0.38	76
4-F	4-F	62.5	0.38	81
4-F	4-F	71.4	0.45	84
4-F	4-F	76.9	0.49	69
4-F	4-F	83.3	0.46	67
4-F	4-F	90.9	0.51	81
3-F	H	7.0	0.44	83
3-F	H	13.0	0.40	79
3-F	H	23.1	0.29	80
3-F	H	37.5	0.36	68
3-F	H	50.0	0.36	85
3-F	H	62.5	0.38	76
3-F	H	76.9	0.37	74

a. The reaction time for all entries is 12 hours.

b. The viscosity measurements were conducted at room temperature at a concentration of 0.5% in $CHCl_3$ at 25 °C.

Structure of copolymers

There is a possibility of formation of a block structure due to the expected difference in reactivity of comonomers which bear substituents with varied electronegativity. However, the formation of block copolymers appeared unlikely in view of the rapid redistribution reactions which accompany the polymerization[6,24]. The preparation of block copolymers can only be made using some specific conditions, such as sequential addition of the different comonomers and adjusted reaction temperature[25].

For the copolymers that we have made by simutaneous oxidation of comonomers, a random structure is apparent from their nmr spectra. We chose two copolymers to study, the first one is copolymer DPP/$DPPF_2$ (molar ratio 1:1) in which the fluoro group is electron-withdrawing in nature, the second one is copolymer DPP/$DPPBu_2$ (molar ratio 1:1) in which the t-butyl group is electron-donating in nature.

In the nmr spectra of the homopolymers, the two chemically identical protons of the central phenylene ring give a singlet due to the same chemical environment of monomeric units along the polymer chain. In figure 3.1, the spectrum at the top is from a mixture of homopolymer P3O and para fluoro substituted P3O homopolymer in which the two singlets at δ 6.24 and δ 6.26 correspond to the protons on the phenylene rings for the two individual homopolymers. The spectrum at the bottom is for the corresponding copolymer with molar ratio of 1:1, and the envelope of mutiple peaks reveals clearly the multiple environments of random distributed comonomers along the molecular chains.

In figure 3.2, the mixture of P3O homopolymer and copolymer DPP/$DPPBu_2$ with block length of $DPPBu_2$ as 8 (since the homopolymer is not soluble in chloroform, copolymer with sufficient block length was used to represent the corresponding homopolymer) is shown at the top in which two singlets at δ 6.45 and δ 6.26 correspond to the individual homochain sequence. The random structure of the copolymer with molar ratio of 1:1 (bottom) is reflected by the multiple peaks in the range of δ 6.24 - 6.43 which correspond to various environments along the length of the polymer chain.

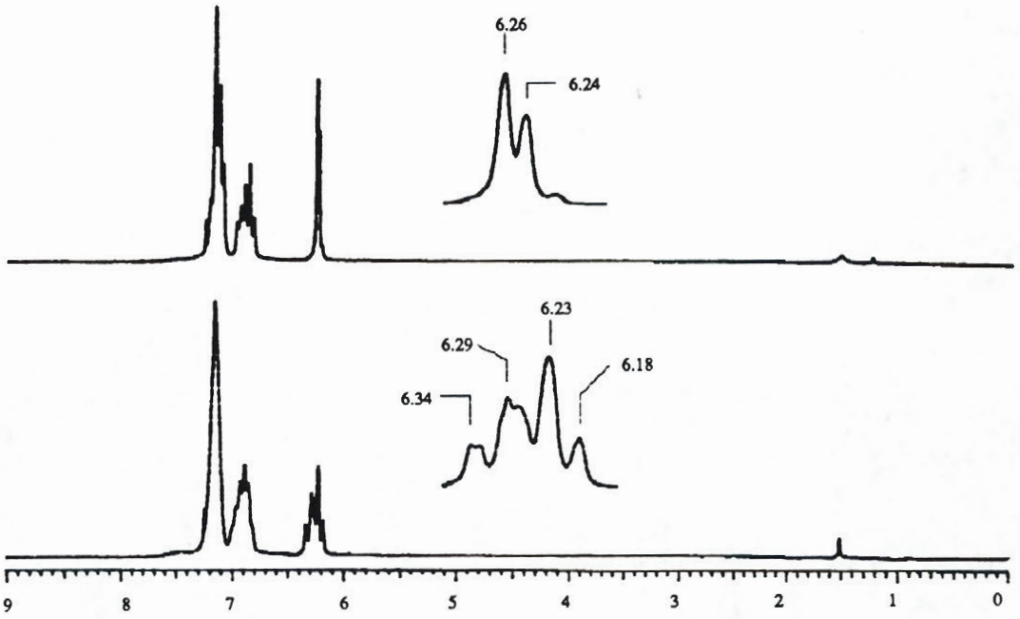

Fig. 3.1. Proton nmr spectra of copolymer DPP/$DPPF_2$
Top: mixture of homopolymers P_3O and P_3OF_2. Bottom: random copolymer (molar ratio, 1:1)

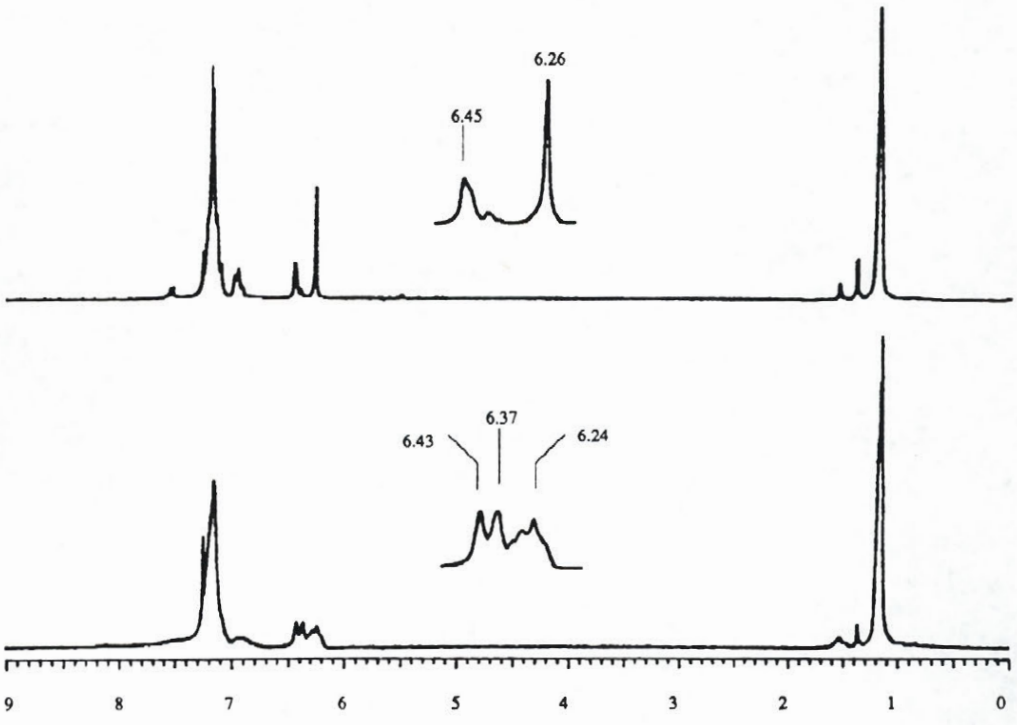

Fig. 3.2. Proton nmr spectra of copolymer DPP/$DPPBu_2$
Top: mixture of homopolymer P_3O and copolymer DPP/$DPPBu_2$ (molar ratio 10:2).
Bottom: random copolymer (molar ratio, 1:1)

3.6 EXPERIMENTAL

a. Homopolymer

General Procedure. To a test tube there was added 8.2 mg of CuCl, 6.2 mg of TMEDA , 0.4 g of anhydrous magnesium sulfate and 7 mL of o-dichlorobenzene. The test tube was put in an oil bath at 65 °C and the mixture was agitated with a magnetic stirrer. Oxygen was bubbled into the mixture for 10 min. When the solution became green colored, a solution of 1 g of the substituted 2,6-diphenylphenol in 8 mL of o-dichlorobenzene was added slowly over 20 min. A dark red color developed instantly. The reaction was continued for the time indicated in table 3.2. When the reaction was finished, the mixture was diluted with 10 ml of chlorobenzene and several drops of anhydrous hydrazine were added to the reaction mixture to reduce the diphenoquinone byproduct whereupon the deep red-orange color of the diphenoquinone disappeared. The inorganic solids were removed by filtration through a layer of celite (1 cm) and the solution was added dropwise to 200 mL of methanol containing several drops of hydrazine. After stirring for several hours, the polymer was collected by filtration. The polymer was dissolved in about 20 mL of chloroform and precipitated in 200 mL of methanol. The polymer was collected again by filtration and dried in a vacuum oven at 80 °C for 24 h. The yields and viscosities of the polymers are listed in table 3.2.

b. Random Copolymers:

The random copolymers were made by the same procedure as decribed above with the molar ratios of monomers indicated in table 3.3 and 3.4. The reaction time is 12 hours for all the copolymerizations and the reactions were performed on a 0.5 g scale.

References:

(1) Hay, A. S. in "High Performance Polymers: Their Origin and Development" *Proceedings of the Symposium of the History of High Performance Polymers at the American Chemical Society Meeting helded in New York*, **1986**, April 15-18, 209.

(2) Hay, A.S. and Endres, G. F., Polymer Letters, 1965, 3, 887.

(3) Hay, A. S., Blanchard, H. S., Endres, G. F., and Eustance, J. W., *J. Am. Chem. Soc.*, **1959**, 81, 6335.
Hay, A. S., **U.S.** 3,306,874; 3,306,874 (GE).

(4) Aycock, D., Abolins, V., and White, D. M., *Encyclopedia of Polymer Science and Technology*, Wiley, New York, **1985**, 13, 1.

(5) Buanu, V. A. and Kishore, K., *Chem. Rev.*, **1991**, 91, 103.

(6) Cooper, G. D., Blanchard, H. S., Endres, G. F., and Finkbeiner, H. L., *J. Am. Chem. Soc.*, **1965**, 87, 3996.

(7) Mijs, W. J., von Lohuizen, O. E., Bussink, J. and Vollbracht, L., *Tetrahedron* **1967**, 23, 2253.
White, D. M., *Polym. Prepr. Am. Chem. Soc. Div. Polym. Chem.* **1968**, 9, 663.

(8) White, D. M., *J. Org. Chem.*, **1969**, 34, 297.

(9) Bolon, D. A., *J. Org. Chem.*, **1967**, 32, 1584.
Cooper, G. D., Gilbert, A. R., and Finkbeiner, H. L., *Polym. Prepr. Am. Chem. Soc. Div. Polym. Chem.* **1966**, 7, 166.

(10) Bennett, J. G. and Cooper, G. D., **U.S.** 3,661,848, **1972** and **U.S.** 3,639,656, **1972**.

(11) Meinders, H. C., Van Bolhuis, F. and Challa, G., *J. Mol. Catal.*, **1976**, 5, 225.

(12) Kotas, J., Pospisil, L., and Kolar, V. *Chem. Prum.*, **1976**, 26, 645. *Chem. Abstr.* **1976**, 86, 107092.

(13) Verlaan, J. P., Alferink, P. J. T., and Challa, G., *J. Molecular Catal.*, **1984**, 24, 235.

(14) Endres, G. F., Hay, A. S., and Eustance, J. W., *J. Org. Chem.*, **1963**, 28, 1300.

(15) Hay, A. S., *J. Polym. Sci.*, **1962**, 58, 581.

(16) Suatoni, J. C., Snyder, R. E., and Clark, R. O., *Anal. Chem.*, **1961**, 33, 1894.

(17) Sen, S, Kisakurek, D, Turker, L., Toppare, L., and Akbulut, U., *New Polymeric Mater.*, **1989**, 1, 177.

(18) Hay, A. S., *Macromolecules*, **1969**, 2, 107; Hay, A.S., **U.S. 1969**, 3,432,466.

(19) Hay, A. S., and Clark, R. F., *Macromolecules*, **1970**, 3, 533.

(20) Hay, A. S., and Dana, D. E., *J. Polym. Sci. Polym. Chem. Ed.*, **1989**, 27, 873.

(21) Risse, W. R., and Sogah, D.Y., *Macromolecules*, **1990**, 23, 4029.

Mohanty, D. K., Lin, T. S., Ward, T. C., and McGrath, J. E., *Int. SAMPE Symp. Exp.* **1986**, 31, 945.

(22) Fenoglio, D.J. and Foster, J.J., *J. Polym. Sci. Polym. Chem. Ed.*, **1990**, 28, 2753.

(23) Price, C. C., Semsarzadeh, M. A., and Nguhen, T. B. L., *Appl. Polym. Symp.*, **1975**, 26, 861.

Yoshida, S., and Hawahara, H., *Polym. Prepr. Am. Chem. Soc. Div. Polym. Chem.*, **1979**, 20, 861.

(24) Cooper, G. D., *Ann. N. Y. Acad. Sci.*, **1969**, 159, 278.

(25) Bennett, J. G., and Cooper, G. D., *Macromolecules*, **1970**, 3, 102.

CHAPTER 4. THERMAL PROPERTIES OF P3O HOMOPOLYMERS

4.1. INTRODUCTION

A. Crystalline Polymers

Solid polymers can exist in an amorphous state characterized by a disordered arrangement of molecules similar to a liquid, and in a crystalline state characterized by three-dimensional order. The major characteristic of crystalline polymers that distinguishes them from small molecule crystals is that they are normally semicrystalline. The density of crystalline polymers normally falls between that of amorphous polymers and that expected for fully crystalline polymers due to the presence of amorphous regions. Also, the x-ray diffraction patterns of crystalline polymers generally show both the sharp features associated with crystalline regions as well as the scattered patterns which are characteristic of disordered substances with liquid-like arrangements of molecules. The coexistence of crystalline and amorphous phases is typical behavior of crystalline polymers.

The existence of crystalline regions in polymers causes dramatic changes in polymer properties, such as density, optical clarity, modulus and mechanical response and the polymers are no longer subject to the rules of linear visco-elasticity, which apply to amorphous polymers. Because of the two-phase nature of crystalline polymers, the glass transition in the amorphous region, the melting transition in the crystalline region and the crystalline content in the samples are the most important parameters which determine the polymer properties. Polymer properties are related to their structural features and enormous efforts have been made to understand the correlation between polymer structure and their physical properties. These correlations are not understood in all detail, however, some general guiding principles linking the properties to the molecular structure have been well developed and have been very useful tools for chemists in synthesizing polymeric materials with desired properties[1-3]. The three most important properties for crystalline polymers: the amount of crystallinity, melting point and glass transition tempera-

ture will be briefly discussed in the following sections.

B. Structural Features of Crystalline Polymers[4-6]

(1) Chain Regularity: Since the efficient parallel alignment of molecular chains is required in the long range, three-dimensional ordered crystal lattice, this determines the essential requirement for crystallizable polymers, i.e. that the polymer should have a regular sequence in chain structure, either chemically regular or geometrically similar. Irregularities in structure tend to inhibit crystallization due to the difficulty of packing in the crystal lattice. Polyethylene has the simplest chain structure and can assume a very regular zigzag conformation with a short identity period along the length of the molecular chain. A high degree of crystallinity in this polymer can be very readily achieved. Other examples, such as polyformaldehyde and its aromatic analog polyphenylene ether, for the same reason, can readily assume a planar zigzag crystal conformation and have high crystallinity. Another striking example is polystyrene. There is not any detectable crystallinity in its atactic form, produced by radical, ionic or anionic polymerization, in which the bulky phenyl side groups are in a largely random attachment to the main chain. In contrast, polystyrenes prepared using special catalysts have the bulky phenyl group attached to the backbone in a regular order, isotactic or syndiotactic, and are readily crystallizable[7].

(2): Chain Interaction: When a polymer is crystallizable due to a regular chain structure, the degree of crystallinity will depend on the stability of the crystal lattice. The stability is provided by cohesion between neighboring chains in the crystal lattice through specific groups which provide intermolecular attraction forces. For a polymer with nonpolar molecular chain, such as polyethylene, the chain interaction originates from dispersion forces. For polymers which carry dipoles (such as Cl, CN or carbonyl groups), the dipole interactions in the polymers also contribute to the chain interactions. The extreme case of this type of bonding is hydrogen bonding. The high crystallinity and insolublity of

cellulose is attributed to strong lateral hydrogen bonding due to the presence of many hydroxyl groups on the polymer chains.

C. Melting and Structural Dependence[4-6]

(1) Melting: The melting process involves the destruction of the ordered crystal structure that leads to the disordered liquid state when the temperature reaches the point where the crystal lattice vibration is large enough and the crystal lattice falls apart. The melting process is accompanied by discontinuous changes in the density, refractive index, heat capacity, transparency, and other properties. The crystalline melting point can be detected by monitoring one or more of these properties for a discontinuous change.

In classical thermodynamics, melting is considered to be a first order transition in which both crystal and liquid phase coexist and so the change in free enthalpy on melting must be zero:

$$\Delta G^\circ = \Delta H_f^\circ - T_m^\circ \Delta S_f^\circ = 0$$

$$T_m^\circ = \Delta H_f^\circ / \Delta S_f^\circ \qquad (1)$$

This concept of fusion has been extended to the fusion of polymeric crystalline structures. But the melting behavior of polymers deviates from the ideal significantly because of the polymer crystallization kinetics which is a result of the macromolecular nature and the polydispersity of the polymer molecules.

From statistical mechanics which based on a lattice model, the following relation is used to describe the melting behavior of polymeric materials from the lattice model[8] :

$$\frac{1}{Tm} - \frac{1}{Tm^\circ} = \frac{R}{\Delta Hm}\left(\frac{1}{\chi W} + \frac{1}{\chi - \xi + 1} \right) \qquad (2)$$

W is the weight fraction of noncrystalline material, ξ is a parameter associated with crystallite size, χ is the degree of polymerization, R is the gas constant, and ΔHm is the

heat of fusion per mole of (crystalline) chemical repeat units. Since the degree of polymerization χ and the crystallite size ξ cover a finite range of values for a polymer, the polymer melting will not have a well-defined melting temperature like small molecules, rather the melting takes place in a finite temperature range. The relation gives a general description of polymer melting behavior associated with the lack of sharpness of melting caused by the broad molecular weight distribution, variety of crystallite sizes and imperfections.

(2) Tm - Structure relation: Referring to thermodynamic equation (1), a higher melting temperature should be related to either a large heat of fusion or a small entropy change during the melting. The heat of fusion is related to the crystal lattice energy which is associated with molecular cohesion and is intermolecular in nature. The entropy term describes the changes in molecular disordering during the melting which involves positional, orientational and conformational disordering. For macromolecules, a large part of the entropy is due to the conformational disordering associated with free rotation of polymer chains occurring after melting which is restricted in the crystal lattice. More often, people use chain flexibility to describe this conformational disordering.

From equation (1), no such general statements can be made to explain the observed specific changes without detailed information about the solid and liquid state. However, by appropriate estimation of entropy, it is possible to link through the heat of fusion with the melting temperature. High melting points of polymers can be obtained by having crystals either with high heats of fusion, which usually involves strong interactions between polymer chains, or by reducing the conformational disordering by stiffening the molecules, which limits the free rotation of polymer chains. One example for a high melting - high heat of fusion correlation is the strong chain interaction from hydrogen bonding in cellulosic polymers which results in a high melting transition temperature. The entropy contribution to the melting can be illustrated in the following polymer pairs whose melting points differ from one another as a result of the presence of steric hindrance to rotation in one member of the pair, but not in another[9].

Influence of rotation hindrance on Tm

Polymer	Tm (°C)
Ethylene	137
Propylene (isotactic)	176
o-Methylstyrene	>360
m-Methylstyrene	215
o-Allyltoluene	290
m-Allyltoluene	180

D. Tg and Structural Dependence[10-12]

The most familiar property change in the glass transition range is that the polymer changes from a hard, brittle solid below the Tg to a viscous or flexible material above. The Tg is associated with the onset of segmental motion in the amorphous phase of a amorphous or semicrystalline polymer. There are a number of specific properties which undergo discontinuous changes at the glass transition, such as volumetric, thermodynamic, mechanical and electromagnetic properties and the related techniques can be used to detect glass transition temperatures.

In general, intermolecular forces, flexibility and chain geometry are the three principal parameters that govern the glass transition temperature of polymers. Since these molecular structure parameters affect the glass transition in much the same way as the melting point, a correlation between the glass transition temperatures and melting points can often be found in crystalline polymers. For a large number of linear homopolymers, the ratio of Tg/Tm is found to be around 0.5 for unsymmetrically substituted polymers and about 0.8 for symmetrically substituted polymers.

4.2. GENERAL COMMENTS ON P3O MODIFICATION

The reduction of melting temperature and maintenance of sufficient crystallinity by structural modification of P3O are the major objectives in this thesis. The high melting

temperature and the efficient crystallization of P3O is related to its unique structural features. The crystal structure of P3O was obtained by Boon and Magre[13] and is shown in Figure 4.1. It shows that the pendant phenyl rings are arranged in a regular pattern along the length of chain axis and thus an efficient packing can be readily achieved. The chain motion is largely inhibited due to the presence of bulky phenyl rings along the polymer chain and this results in a very high melting temperature[14].

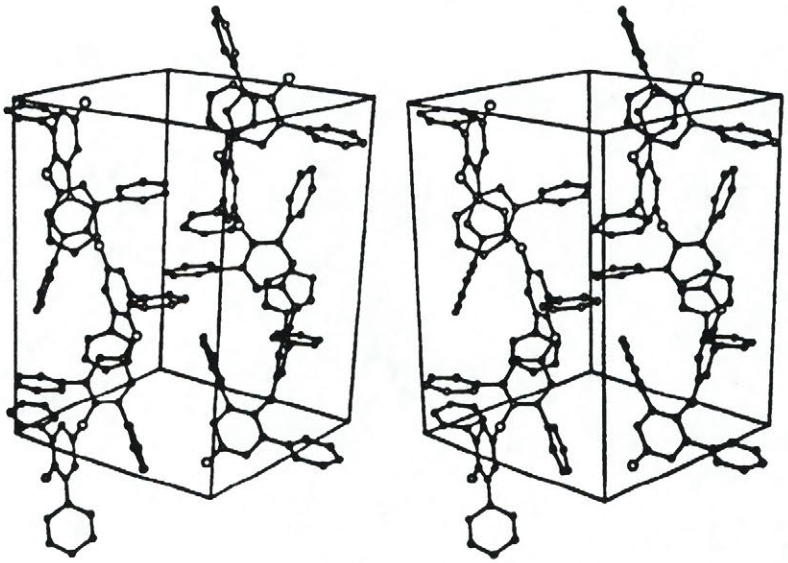

Fig. 4.1. Stereoscopic illustration of P_3O crystal

P3O assumes a helical conformation with 1/4 repeats. The C-O-C angle of the ether linkage in **P3O** is 127°, 3° higher than the unsubstituted polyphenylene ether (PhO-1,4)n. This is attributed to the steric hindrance caused by the bulky phenyl side groups[15]. The pendant phenyl rings are nearly perpendicular to the center phenylene ring. Van der Waals forces provide the cohesion between the neighboring polymer chains.

The P3O crystal structure indicates that the pendant phenyl rings are in close contact between the neighboring chains. The P3O polymers that we made with substituents on the pendant phenyl rings would be expected to affect chain packing and chain cohesion, therefore, the properties, such as transition temperatures and crystallization behavior.

In this study, we intend to investigate the thermal properties of polymers with various substituents on the pendant phenyl rings. By differential scanning calorimetry analysis, we will attempt to study the influence of these substitutions on the transition temperatures, i.e. Tg and Tm, and their crystallization behavior. By thermogravimetric analysis, we attempt to study the influences of the substituents on the thermal stabilities of the resulting polymers. The resultant structure-property relationships should help us to design a system with a reduced melting point which remains crystallizable. The structures of the polymers involved in this study are shown below.

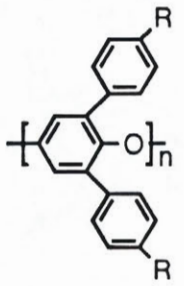

X = H, t-Bu, OPh, CF_3, F, Cl, Br, I, CN

4.3. EXPERIMENTAL

Differential scanning calorimetry (DSC, Seiko 220 analyzer) was used to measure glass transition temperatures Tg, melting transition temperatures Tm, crystallization temperatures Tc, heats of fusion ΔHm, heats of crystallization ΔHc and heat capacity change ΔCp at Tg. As shown in figure 4.2, the Tg was taken as the mid-point of the slope of the Tg deflection. Tc and Tm were taken as the tip of the corresponding peak. The related thermal properties, such as ΔCp, ΔHc and ΔHm, were obtained by programmed automatic integration.

The thermograms were recorded with a programed heating and cooling accessory. Typically, 8-15 mg polymer samples were pressed into pellets and were scanned at 10 °C/min between 60 and 540 °C with dry nitrogen as the purging gas. The DSC output was digitized and stored in the computer for subsequent data analysis.

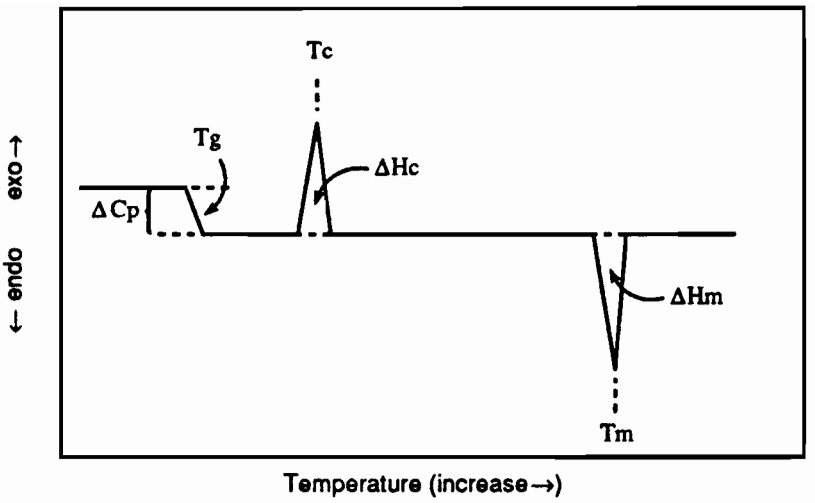

Fig. 4.2. General schematic of DSC curve of P_3O polymers.
ΔCp: heat capacity change at Tg; ΔHc: heat of crystallization; ΔHm: heat of melting.

Thermogravimetric analysis (TGA) was performed on a Seiko 220 system using 8 -15 mg samples as pressed pellets. The samples were scanned at 10 °C/min between 60 and 600°C with dry nitrogen or air as the purging gas. The thermal analyzers have been calibrated according to recommended procedures[18].

4.4. RESULTS AND DISCUSSION

4.4.1. Substitution Effects on Polymer Crystallinity

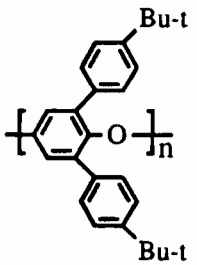

P_3OBu_2: Introduction of t-butyl groups into polymer chains is a widely used method to depress polymer crystallinity[19,20]. The presence of the bulky t-butyl groups on polymer backbones is usually considered to inhibit the efficient packing of polymer chains in a crystal lattice. A recent example is that an inherently highly crystalline and insoluble poly(ether ketone) became totally amorphous and soluble by introducing t-butyl groups into this polymer[19]. This morphology change was considered to be a result of loss of chain regularity due to the unsymmetrical arrangement of t-butyl groups along the polymer chain.

The first DSC scan of P_3OBu_2 (curve e), shown in figure 4.5, to gives a Tg of 248 °C

the polymerizations.

Mono substituted P3O: P3O(OMe); P3O(CN); P3O(phthalimidyl):

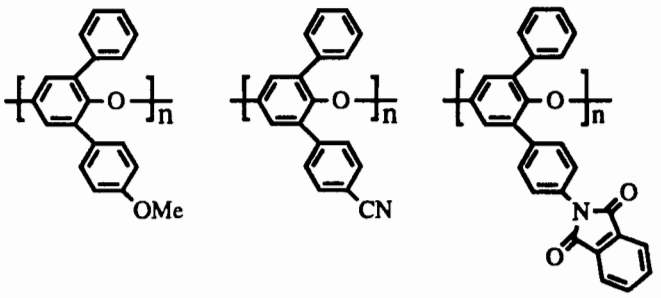

The DSC scan of P3O(OMe) and P3O(CN) gave only a glass transition without any detectable crystallization or melting. This reveals an interesting difference from the symmetrically substituted analogs $P3O(OMe)_2$ and $P_3O(CN)_2$ which are insoluble and highly crystalline. Annealing failed to introduce any crystallinity in these two polymers. The irregular arrangements of the the substituents along the polymer chains are believed to contribute to the difficulty in crystallization of these polymers. A 13 °C increase in Tg is observed for P3OCN which is believed to be a result of induced dipole interaction by the cyano substitution. As expected, an increase of nearly 50 °C in the Tg was obtained from phthalimidyl substitution which is apparently related to the induced rotation barrier from this bulky group substitution.

It is known that polymers with a greater efficiency to crystallize usually have lower crystallization temperatures. However, more often the ΔT, the difference between Tc and Tg, has been used to evaluate polymer crystallizability. Since ΔT represents the difference between the temperature where the crystallization and the segmental motion of the polymer actually take place, it provides a better criterion for crystallizability [20].

Table 4.1. Properties of P3O Polymers and Monomers

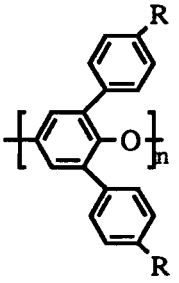

Substituent	Monomer	Polymers			
	m.p. °C	Tg °C	Tm °C	Tc °C	Tc-Tg °C
F	62 - 5	213	351	300	87
Methyl[a]	91-2	221	321	-	-
H	101-2	228	501	270	42
Methoxy[a]	109-10	220	356	-	-
Phenoxy	118-20	141	-	-	-
CF3	125-6	-	384	-	-
Cl	136-7	232	420	347.2	115[e]
t-Butyl	137-8	248	483	300	52
Br	147-8.5	243[c]	404	275	46
I	151-3	262	d	-	-
Phenyl[a]	242-3	265a	>500	-	-
CN	262-2.5	298a	d	-	-
OMe[b]	115	217	-	-	-
CN[b]	185-6	241	-	-	-
Imidyl[b]	210-2	275	-	-	-

a: data from reference 17.

b: mono para-substituted P_3O.

c: calculated from copolymer with DPP.

d: low M.W. polymer, decomposition.

e: data from the sample quenched from melt.

According to the data in table 4.1(ΔT: Tc-Tg), t-butyl and bromo substituted derivatives have crystallizability similar to P3O as determined by DSC. The much larger ΔT value observed for fluorinated P3O indicates that this polymer is much more reluctant to crystallize.

A significant dependence of Tm's and Tg's on the substituents on P3O polymers was observed in the above investigation. The latter section contains a detailed discussion of this correlation.

4.4.2. Crystallization upon Annealing

Crystallinity is one of the critical parameters for polymer properties on which the thermal stability and the mechanical response are dependent. Crystallinity in the polymer samples is usually introduced by melt crystallization or annealing at either fixed or variable temperatures. Other methods such as solution crystallization or crystallization introduced by mechanical treatment are also common. Since some of the polymers we have synthesized decompose in their melting temperature range, crystallinity was therefore introduced using a cold crystallization method. The samples were held at the crystallization temperature, Tc, for a period of time and the resultant crystallinity development in the samples was detected in subsequent DSC scans.

The crystallinities developed in the polymers are shown in figure 4.6. Polymers with Cl, Br and t-Bu substituents were shown to reach a high degree of crystallinity as revealed by the complete disappearance of the glass transitions except for a DSC trace in the chloro substituted polymer which shows a small deflection around 300 °C. No crystallization exotherm was observed in these DSC scans. The fluoro-substituted P3O shows significantly less tendency to crystallize compared with other samples. A limited increase in crystallinity was indicated by the increased fusion heat while Tg is still evident and remains in the same range.

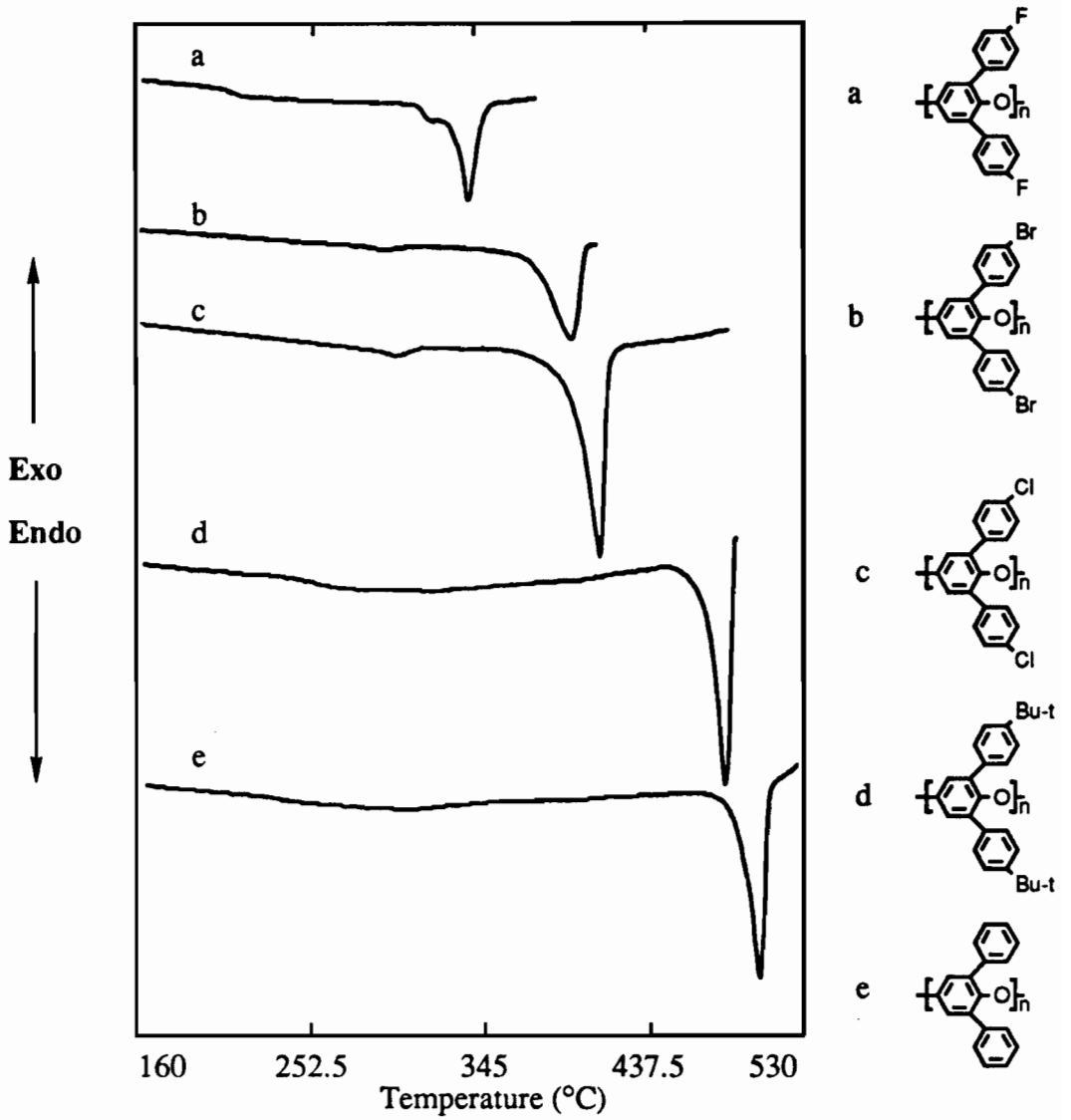

Fig. 4.6. DSC traces of samples from annealing treatment.

a: annealing at 300 °C. b: annealing at 290 °C. c: annealing at 290 °C.

d: annealing at 300 °C. e: annealing at 270 °C.

Annealing time: 30 minutes. Heating rate: 20 °C/min.

4.5. STRUCTURE-TRANSITION TEMPERATURE

4.5.1. Structure-Tg

From table 4.1, we notice that there is a general trend, monomers with higher melting points correlate with polymers with higher Tg's. Koleske and Lundberg[21] observed a similar correlation between the Tg of aliphatic lactone monomers and the Tg of their corresponding polymers. When we compiled all the melting point data of the monomers and the Tg's of the corresponding polymers that we synthesized along with those reported previously, we found that the Tg's of the polymers increase as the melting points of the corresponding monomers increase. This suggested that the structural parameters which affect the melting points of monomers would also significantly affect the Tg of the polymers.

The chain flexibility and chain interactions are known to be the principal parameters that govern the glass transition temperature of polymers. In this series of polymers, the only structural variable is the substitution at the para position of pendant rings of P3O with substituents ranging from small to bulky, and polar to nonpolar. The substitution of P3O with bulky groups would lead to less flexible or more rigid chain structures by a Crankshaft effect. Introduction of polar groups should lead to a variation in chain interactions. One might expect that the variation in Tg's in this series of polymers could be attributed to either dimensional factors or the variation in chain interactions, or an interrelated contribution from both factors.

Figure 4.7 shows the correlation between the melting point of monomers and the Tg of polymers. The cyano-substituted P3O has the highest Tg in the series. This is apparently related to the strong chain interaction from the cyano dipole which has the highest dipole moment (PhCN; D: -2.54) in the series. The chloro (PhCl; D: -1.47), and bromo (PhBr; D: -1.57) substituted polymers presumably also involve dipolar interactions which lead to

higher Tg's than the parent P3O. The significantly higher Tg of t-butyl and phenyl substituted derivatives would be mainly due to the rigidized chain due the bulkiness of the substituents. it is unusual that the group dipole moment of PhF (PhF; D: -1.40) is comparable to its halogen analog and similar size to hydrogen, but the Tg of fluorinated P3O is the lowest in the series.

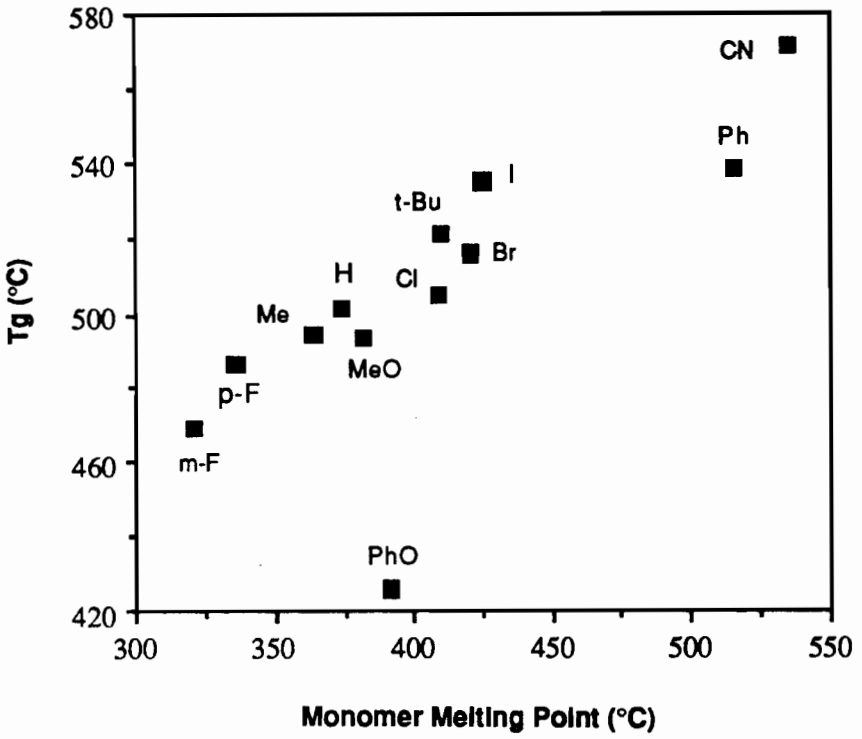

Fig. 4.7. Correlation between polymer Tg's and monomer melting points

4.5.2 Structure-Tm

From the rule of thumb which describes a simple correlation between the Tg and Tm for linear homopolymers, and the correlation between the melting points of monomers and the Tg of polymers we observed, we would expect a similar correlation between the melting points of monomers and the corresponding Tm's of polymers. In figure 4.8, we plot the melting points of monomers against the Tm's of polymers and observed that the Tm of polymers increase as the melting points of the corresponding monomers increase.

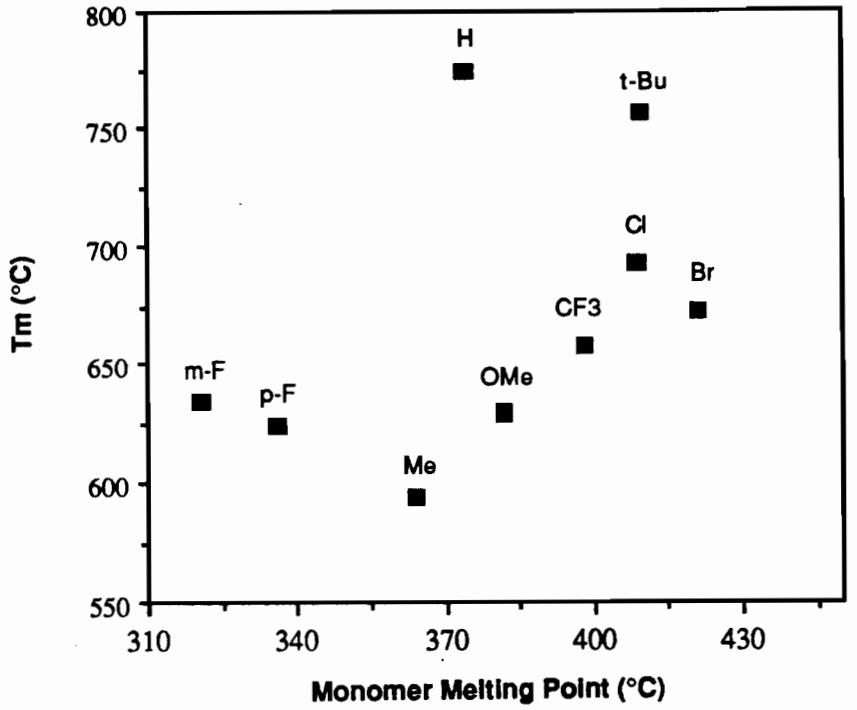

Fig. 4.8. Correlation between polymer Tm's and monomer melting points

It is difficult to rationalize this correlation through a single structural parameter by considering either substituent polarity which would affect the chain cohesion, or dimensional factors which would affect the crystal packing. The van der Waals radius and dipole moments for various substituted groups are shown in table 4.2.

Table 4.2. Physical Data of Substituents [22,23]

X	Me	H	OMe	I	F	Br	Cl	CF_3	CN
van der Waals Radii	2.0	1.2	-	2.15	1.35	1.95	1.80	-	-
Dipole moment (D) (Ph-X)	0.37	0	1.28	-1.40	-1.47	-1.57	-1.59	-2.54	-4.05

It is shown in figure 4.8 that the polar substituents fit better into the correlation while the nonpolar substituents such as t-butyl group and P3O itself significantly deviate from this correlation. We can see that although the bromo and chloro have a comparable size

with methyl group, their Tm's are considerably higher. This could be attributed to the considerably higher dipole monoments of bromo and chloro which attribute to the increased chain interaction, and increased Tm. Again, the fluorinated P3O has the lowest Tm in the series. This will be discuss in detail in the next chapter.

4.6. THERMAL STABILITY

The variations in the thermal stabilities of the polymers in this series would be expected to depend on the only structural variable: the para substituent on the pendant rings of P3O. We found that the stability shows a correlation with the bond strength which links the substituents. The thermogravemetric profiles obtained by TGA of the derivatives we synthesized are shown in table 4.3. The fluoro and chloro substituted P3O are shown to have higher stability in air or nitrogen, which we assumes is most likely due to the higher bond energy (C-F: 124.8 kcal/mol, C-H: 103 kcal/mol, C-Cl: 94.1 kcal/mol)[24] plus the strong inductive effect which further stabilizes the aromatic moiety. The bromo derivative and t-butyl substituted derivative show significantly lower stability than the parent polymer. This could be a result of the relatively weak bond strength of C-Br (79.9 kcal.mol)[24] and alkyl C-C bonds. Their thermolysis would further accelerate decomposition.

Table 4.3. Thermogravimetric Analysis of P3O Polymers[a]

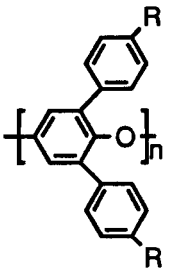

Substituent	Nitrogen		Air	
	$T_5(T_{10})$ (°C)	T_{max} (°C)	$T_5(T_{10})$ (°C)	T_{max} (°C)
H	518(528)	544	528(545)	561
F	540(548)	560	532(554)	578
Cl	502(537)	-	503(545)	-
Br	484(518)	537	456(489)	516
t-Butyl			477(502)	529
Phenoxy	498(520)	557	521(548)	584
OMe[b]	473(493)	528	474(512)	524
CN[b]	511(525)	542	505(520)	524
Imidyl[b]	420(455)	484	402(436)	523

T_5: temperature with 5% weight loss, T_{10}: temperature with 10% weight loss.

T_{max}: first maximum decomposition temperature.

a: heating rate: 10 °C/min. b: Mono substituted derivatives.

References:

1. Seymour, R. B., and Carraher, C. E., *Structure-Property Relationship in Polymers, Plenum Press*, **1984**.
2. Van Krevelen, D. W., *Properties of Polymers, Their Correlation with Chemical Structure; Their Numerical Estimation and Prediction from Additive Group Contribution.*, Elsevier Sci. Pub. Comp. Inc., New York., **1990**.
3. Margolis, J. M., *Engineering Thermoplastics: Properties and Applications*, Marcel Dekker, Inc., **1985**.
4. Young, R. J., and Lovell, P. A., *Introduction to Polymers*, Cambridge Uni. Press, **1991**, Chapter. 4.
5. Wunderlich, B., *Macromolecular Physics*, Academic Press, **1980**
6. Wunderlich, B., Ch. 2 in *Thermal Characterization of Polymeric Materials*, Ed. by Turi, E. A., Academic Press. Inc., **1981**, Chapter 2, p143.
7. Pasztor, Jr. A. J., Landes, B. G., and Karjala, P. J., *Thermochimica Acta*, **1991**, 177, 187.
8. Billmeyer, Jr. F. W., *Textbook of Polymer Science*, 3rd., A Wiley-Interscience Publication, John Wiley & Sons, **1984**, p285.
9. Miller, M. L., *The Structure of Polymers*, Reinhold Book Corporation, New York, 2nd., **1968**, p531.
10. Shen, M. C., and Eisenberg, A., *Glass Transitions in Polymers*, Reprinted from *Rubber Chem. & Technology*, Vol. 43, No. 1, **1970**. p126.
11. Shalaby, S. W., *Thermal Characterization of Polymeric Materials*, Edited by Turi, E. A., Academic Press. Inc., **1981**, Chapter 3, p245.
12. Lee, C. J., *JMS-Rev. Macromol., Chem. Phys.*, **1989**, C29, 431.
13. Boon, J., and Magre,E. P., *Die Makromolekulare Chemie*, **1970**, 136, 267.
14. Cassidy, P. E., *Thermally Stable Polymers*, Marcel Dekker, Inc., **1980**. p48.
15. Boon, J., and Magre,E. P., *Die Makromolekulare Chemie*, **1969**, 126, 130.
16. Natta, G., *Die Makromolekulare Chemie* , **1959**, 35, 94.
17. Hay, A. S., and Dana, D. E., *J. Polym. Sci. Polym. Chem. Ed.*, **1989**, 27, 873.
18 Seiko 220 Thermal Analysis Manaul.
19. Risse, W. R., and Sogah, D.Y., *Macromolecules*, **1990**, 23, 4029.

Fenoglio, D.J. and Foster, J.J., *J. Polym. Sci. Polym. Chem. Ed.*, **1990**, 28, 2753

20. Kiyotsukuri, T., Tsutsumi, N., and Sandan, T., *J. Polym Sci. Part A: Polymer Chemistry*, **1990**, 28, 315.

21 Koleske, J. V. and Lundberg, R. D., *J. Polym. Sci. Polym. Phys. Ed.*, **1972**, 10, 323.

22. Minkin, V. I., Osipov, O. A., and Zhdanov, Y. A., *Dipole moments in organic chemistry*, Translated by Hazzard, B. J., Plenum Press, New York-London, **1970**.

23. Gordon, A. J., and Ford, R. A., *The Chemist's Companion, A Handbook of Practical Data, Techniques and References*, John Wiley & Sons, **1972**, p109.

24. Kapuscinska, m., Pearce, E. M., Chung, H. F. M. and Ching, C. C., *J. Polym, Sci, Chem. Ed*, **1984**, 22, 3999.

CHAPTER 5. FLUORO SUBSTITUTION EFFECTS ON POLY(2,6-DIPHENYLPHENYLENE ETHER)

5.1. INTRODUCTION

The general approach to highly thermal stable polymers is to build molecular backbones with rigid structural features. Generally any attempt to improve the thermal stability is detrimental to the tractability of the polymers due to the insolubility and high softening point of the polymers which results in difficulty in synthesis, processing and applications[1]. In the past decades, much attention has been directed toward the syntheses of polymers which retain as much stability as possible while introducing solubility or moldability. There are several developed concepts for structural modifications to achieve solubility and reduce softening temperatures, such as the addition of bulky substituents[2], noncoplanar biphenylene moieties[3,4], kinked and double-kinked comonomers[5,6] and flexible spacers or side chains[7,8].

We have previously demonstrated that fluoro substitution on P3O can lead to a substantial reduction in crystallinity and melting point and improved solubility while the thermal stability remains very high. The understanding of the mechanism of this fluoro substitution effect on polymer properties would be of particular interest for designing high temperature polymers with increased solubility and tractability.

Fluorine containing polymers are very important in industrial applications mostly because of their related properties, such as low dielectric constant, low moisture absorption, enhanced thermooxidative stability and high optical transparency[9,10]. This has resulted in extensive research on the properties of fluorinated polymers, such as softening point, morphology, solubility, processibility, etc. It is especially desirable to incorporate fluorine structural units in high temperature polymers due to the highly stable C-F linkages. The molecular structure features of various fluorine-containing polymers which usually

are highly rigid aromatic system, can be classified into the following three categories:

1. Introduction of fluorinated alkyl segments as spacers into polymer chains, in most cases these attempts were focused on the hexafluoroisopropylidene moiety[11].
2. Introduction of fluorinated alkyl segments as side chains such as perfluoroalkyl or alkoxy segments[12].
3. Fluorine directly attached to aromatic rings of polymer chains[13-15].

The first two categories are often based on the introduction of flexibility to improve solubility, lower the softening temperature and improve dielectric properties. But the third category, direct attachment of fluorine to aromatic backbones has been less studied due to the unavailability of systematically varied polymer structures.

There have been many attempts to modify highly crystalline aromatic polyesters (14) and polyamides[15] to achieve improved processibility. The results indicated that the attachment of fluorines to the aromatic moieties in these polymers can lead to significant property changes, such as melting point and crystallinity.

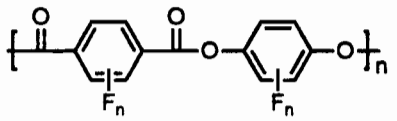

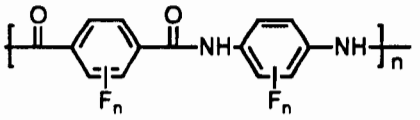

However, the property variations do not correlate with the structural variation by fluoro substitutions. We assume that the lack of property-structure correlation could be a result of interrelated contribution from effects of both dipolar or hydrogen bonding and fluoro substitutions.

In this section, we describe the synthesis of a series of fluoro substituted P3O polymers

with systematically varied structures as shown below and the characterization of these polymers. These results should help us to accomplish two things. First, the variation in properties with structural variations, mainly variations in transition temperatures and crystallinity, should allow us to have a better understanding of the effects due to fluoro substitution and the possible mechanism of fluoro substitution effects on polymer properties. Secondly, more attractive property profiles will hopefully be found in this series of polymers, i.e. Tm in the melt-processible range while maintaining higher crystallinity than the fluorinated P3O polymer described previously in chapter 4.

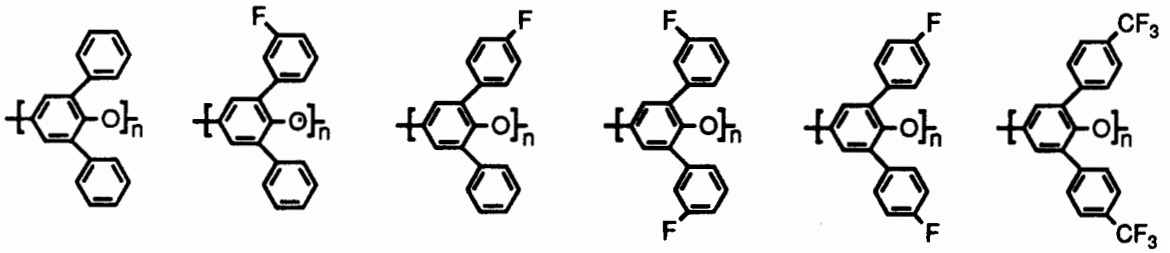

P_3O P_3OmF P_3OpF P_3OmF_2 P_3OF_2 $P_3O(CF_3)_2$

5.2. POLYMER PREPARATION

The polymerization reactions were carried out by identical procedure described in chapter 3[16]. All the monomers listed in table 5.1 give high molecular weight polymers except $P_3O(CF_3)_2$ which precipitated out of the reaction mixture before a high molecular weight polymer was obtained. Attempts to measure the molecular weight of these polymers by GPC failed to give reliable data because of the significantly different behavior of the fluorinated polymers on the column from the reference polystyrene. Inherent viscosities were determined in chloroform (0.5 % w) at 25 °C. The results are shown in table 5.1.

Table 5.1. Fluorinated P3O Polymers

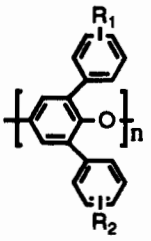

Polymers	R_1	R_2	η_{inh}, dL/g[a]	Reaction time	Yield %
P_3OpF	p-F	H	0.58	14h	81
P_3OmF	m-F	H	0.86	24 h	90
P_3OmF_2	m-F	m-F	0.48	9h	87
P_3OF_2	p-F	p-F	0.68	10h	83
$P_3O(CF_3)_2$	p-CF_3	p-CF_3	-[b]	10h	54

a: Determined in $CHCl_3$ (0.5 w%) at 25 °C. b: not available, insoluble.

5.3. RESULTS AND DISCUSSIONS

5.3.1 Experimental

Differential scanning calorimetry (DSC) and thermogravimetric analysis (TGA) were used to characterize the thermal properties of these polymers, i.e. crystallization behavior, transition temperatures and stability. The samples were prepared by precipitation of chloroform solutions into excess methanol, stirring for 2 h, collected and dried in a vacuum oven at 80 °C for 24 hours. Sample **$P_3O(CF_3)_2$** is insoluble and precipitated out of the reaction mixture, and was collected by filtration followed by thoroughly washing with excess methanol and dried.

For DSC measurements, 8 to 15 mg samples were used, the heating scan was conducted at 10 °C/min and the cooling rate was 5 °C/min. TGA measurements were conducted under both nitrogen and air atmosphere, using 8-15 mg samples. The scans were conducted from 60 °C to 600 °C with a heating rate of 10 °C/min.

5.3.2. Crystallization Behavior

A. Crystallization During Heating Scans

The DSC scans for the polymers and **P3O** are shown in figure 5.3. The most remarkable difference in crystallization behavior is revealed between the di-substituted and mono-substituted fluoro derivatives. The di-substituted derivatives **P3OmF2** and **P3OF2** are much more reluctant to crystallize than mono-substituted derivatives as indicated by the significantly higher crystallization temperatures Tc's (fig. 5.1, curve a, b). The di-substituted derivatives also show considerably broader crystallization exotherms than the mono-substituted derivatives. This indicates that the polymers with higher contents of fluorine crystallize much slower than the mono-substituted derivatives. The double melting for **P3OmF2** might suggest either different crystal forms or a meta stable crystal form which recrystallizes with a small exotherm between the two melting peaks (fig. 5.1 curve b). The mono-substituted derivatives **P3OpF** and **P3OmF** readily crystallize which is indicated by the significantly lower crystallization temperatures (Tc) and sharp crystallization exotherms (fig. 5.1, curve c, d).

The difference in crystallization behavior between the position is less significant than the variation in number of substituents by comparison of the pairs **P3OF2** - **P3OmF2** (curve a - b) and **P3OpF** - **P3OmF** (curve c - d) shown in figure 5.1. By using the ΔT interval (Tg-Tc in table 5.2) as a measure of the crystallizability of polymers[17], the tendency to crystallize for the polymers gives the following order: **P3O** ≈ **P3OmF** ≈ **P3OpF** >> **P3OmF2** ≈ **P3OF2**. It appears from these results that the higher amount of fluoro substitution renders crystallizations more difficult.

Significantly different from the above fluorinated derivatives, the trifluoromethyl substituted derivative $P_3O(CF_3)_2$ shows only a melting transition at 364 °C without a detectable glass transition in the DSC scan. This suggests that a highly crystalline material was obtained and it would explain the low molecular weight of the polymer obtained because of the insolubility of this polymer during the polymerization.

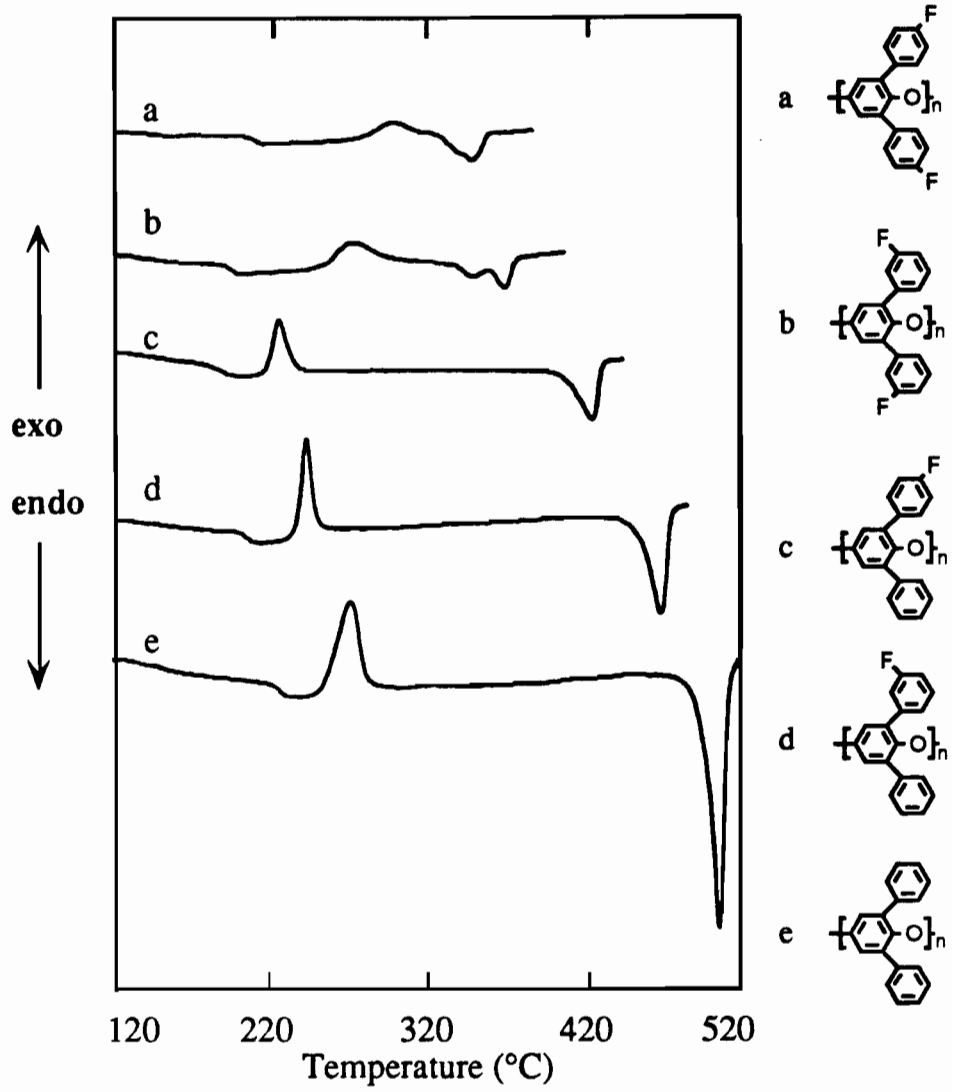

Fig. 5.1. DSC curves showing the effect of fluoro substitution on polymer crystallization and thermal transition temperature.

Table 5.2. Thermal Properties of Fluorinated P3O Polymers[a]

Polymers	Tg, °C	Tc, °C	Tm, °C	ΔCp (J/mol, °C)	ΔHc (J/mol)	ΔHm (J/mol)	Tg-Tc (°C)
P_3O	228	270	501	41.1	-2804	5437	43
P_3OmF	208	247	474	47.5	-2693	5570	39
P_3OpF	196	228	427	42.2	-2376	4118	32
P_3OmF_2	192	275	352(372)[b]	36.7	-3497	3497	83
P_3OF_2	212	300	350	36.7	-2792	3158	88
$P_3O(CF_3)_2$[c]	-	-	364	-	-	-	-

a: Heating rate: 10 °C/min. b: Doublet melting peak.

c: Low Mw.

B. Crystallization During Cooling Scans

For this series of polymers, high thermal stability and reduced Tm which is well below the decomposition temperature range allowed us to investigate their melt crystallization behaviors. The samples **P3OmF**, **P3OpF**, **P3OmF2** and **P3OF2** were heated to 30 °C above their Tm's followed by a cooling scan (cooling rate: 5 °C/min) to trace their crystallization behavior. The samples were then subjected to another heating scan to detect the crystallinity developed from the cooling. Again we see that a remarkable difference between the di-substituted and mono-substituted derivatives. The di-substituted derivative **P3OmF2** and **P3OF2** failed to show any crystallization at the indicated cooling scan from melt. However, mono-substituted derivative **P3OmF** and **P3OpF** give sharp crystallization exotherms peaking at 400 °C and 360 °C respectively (fig. 5.2 curve b & fig. 5.3. curve b). Since polymers which are difficult to crystallize have a longer delayed crystallization upon cooling, the meta isomer **P3OmF** with higher Tc appeared more crystallizable than the para isomer **P3OpF** which did not crystallize until cooling to a relatively lower temperature.

The samples **P3OmF** and **P3OpF** which crystallized during above cooling gave singlet melting exotherms peaking at 440 °C and 400 °C respectively in the subsquent heating scans (curve c in fig. 5.2 & 5.3). Both samples from rapid cooling (100 °C) gave double melting endotherms in the subsquent scans. The significant decreased intensity of the glass transition and the disappearance of further crystallization (curves c in fig 5.2 and 5.3) indicates that high crystallinity has been developed from the melt crystallization for both **P3OmF** and **P3OpF**. The corresponding thermal property data are listed in table 5.3.

Table 5.3. Thermal Properties of Fluorinated P3O Polymers from Melt Crystallization[a]

Polymer	Tc(°C)	Tm(°C)	Tg(°C)	ΔHc(J/mol)[b]	ΔHm(J/mol)
P_3OmF	397	444	212	-4488	4594
P_3OpF	365	409	-	-3828	3934

a Data from heating scan (curve c in figure 5.2 & 5.3) after melt crystallization, heating rate: 10 C/min.

b ΔHc data from cooling scan (curve b in figure 5.2 & 5.3).

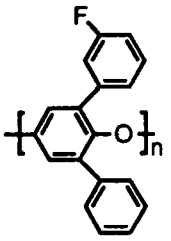

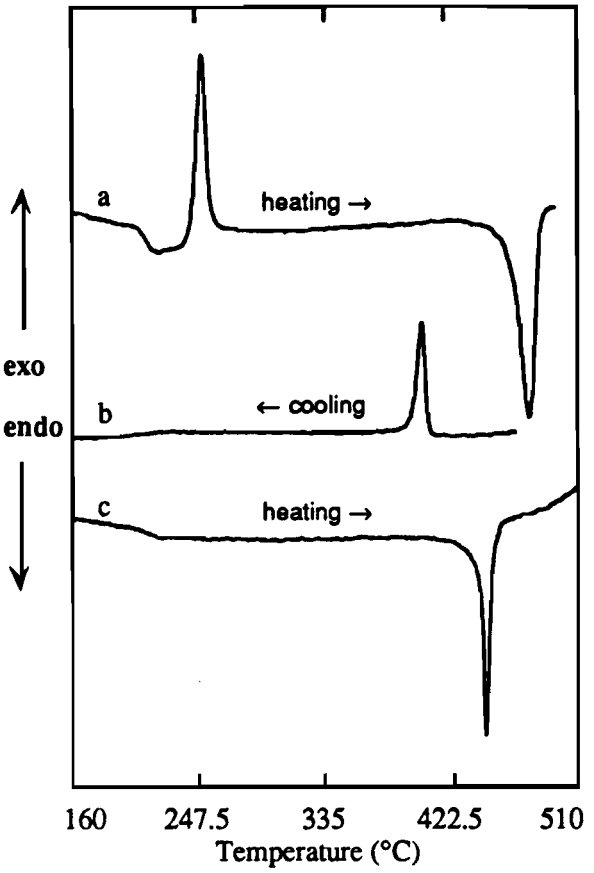

Fig. 5.2. DSC curves for sample **P3OmF:** Scanning sequence: (a): sample as made, from 80 to 510 °C, heating rate 10 °C/min. (b): cooling from 510 to 80 °C, cooling rate 5 °C/min. (c): follow b, from 80 to 510 °C, heating rate 10 °C/min.

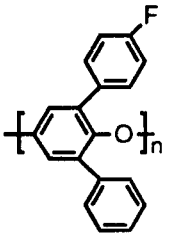

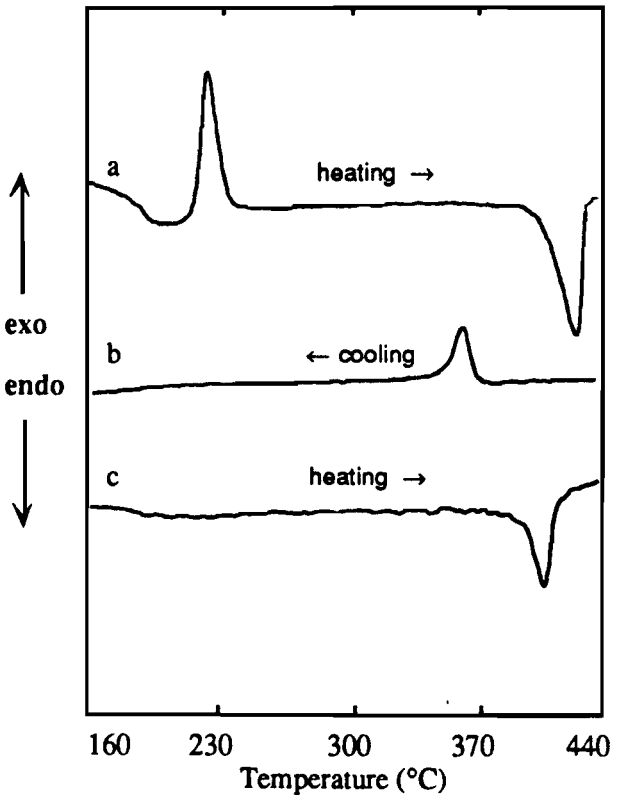

Fig. 5.3. DSC curves for sample **P3OpF:** Scanning sequence: (a): sample as made, from 80 to 460 °C, heating rate 10 °C/min. (b): cooling from 460 to 80 °C, cooling rate 5 °C/min. (c): follow b, from 80 to 460 °C, heating rate 10 °C/min.

C. Crystallization upon Annealing

In the above experiments, the samples **P3OF2** and **P3OmF2** do not crystallize when cooled from the melt, so we attempted to study their isothermal crystallization in the temperature range between Tg and Tm. We found that relatively narrow and well-defined melting can be obtained by isothermal crystallization at a temperature close to their Tm's. The lower crystallization temperatures tend to give broad and multiple melting peaks which are likely due to the intensive nucleation at lower temperature which leads to wide distribution of crystal size.

A comparison of DSC traces between the as made samples and the isothermally crystallized samples for **P3OF2** and **P3OmF2** at 350 °C for 1 h are shown in figure 5.4. A significant enhancement of crystal perfection from isothermal crystallization is indicated by the narrower and well defined melting peaks. The disappearance of the crystallization exotherms for both samples (fig. 5.4, curve b, d) is believed to be result from the increased crystallinity in the samples which limits the necessary mobility for further crystallization. A 21 °C increase in Tg was observed for sample **P3OmF2** by the annealing treatment. The thermal property changes from annealing are listed in table 5.4.

Table 5.4. Thermal Properties of Fluorinated P3O Polymers from Annealing[a]

Polymer	as made				after annealing			
	Tg (°C)	ΔCp (J/mol °C)	Tm (°C)	ΔHm (J/mol)	Tg (°C)	ΔCp (J/mol °C)	Tm (°C)	ΔHm (J/mol)
P_3OmF_2	196	36.7	352(372)[b]	3497	217	22.6	350	3694
P_3OF_2	212	36.7	350	3158	213	25.4	348	4484

a: Samples were annealed at 350 °C for 1 h; Cooling rate: 2 °C/min.; Heating rate: 10 °C/min.

b: Doublet melting peak.

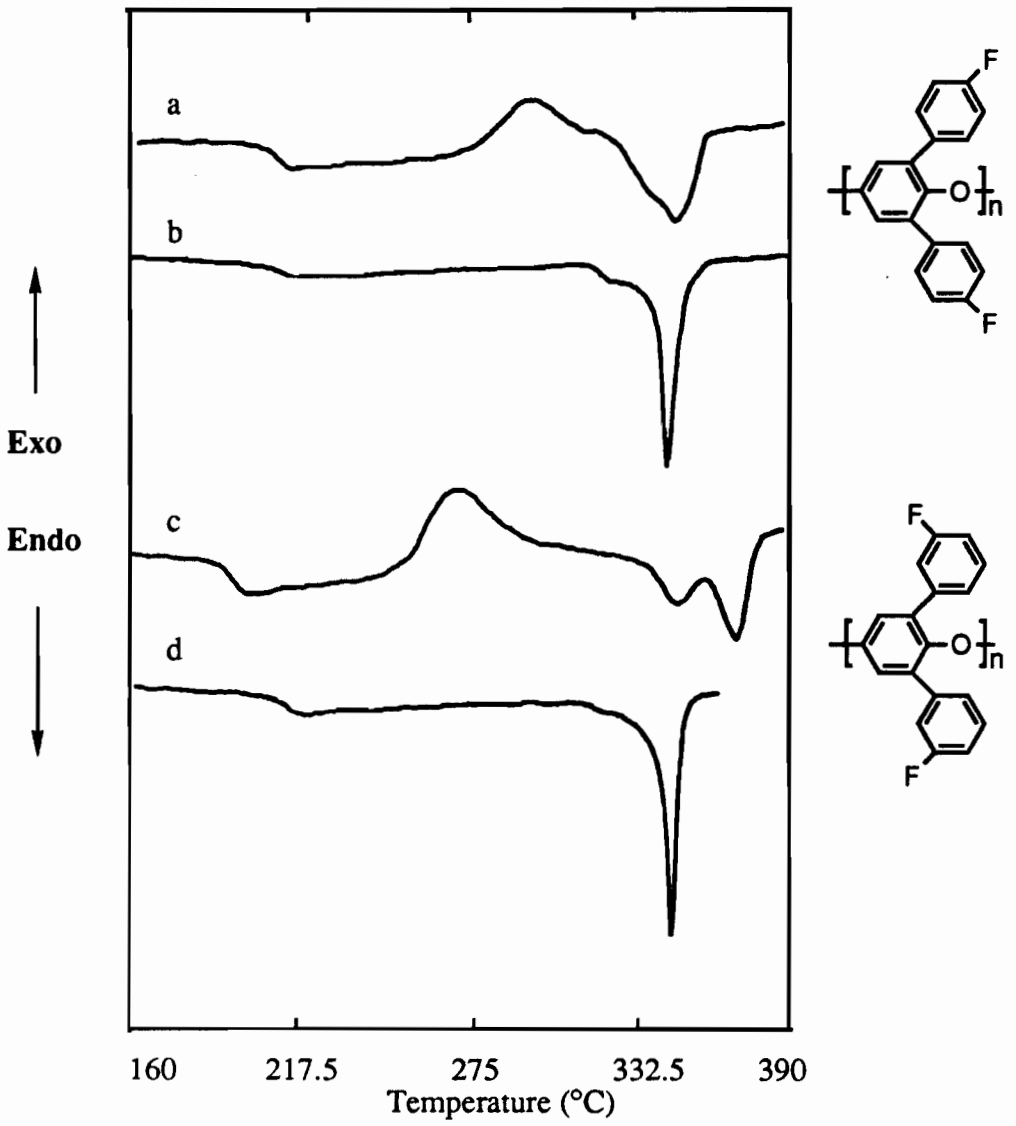

Fig. 5.4. DSC curves showing the effect of annealing on polymer properties.

a, c: sample as made; b, d: sample annealed. Heating rate: 10 °C/min.

5.3.3. Structure -Tm Relationship

The melting temperatures appear to clearly correlate with the structural variation:

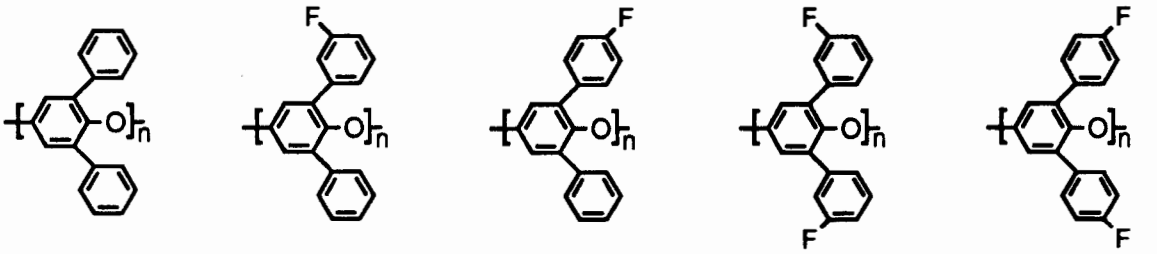

P_3O	P_3OmF	P_3OpF	P_3OmF_2	P_3OF_2
Tm: 501 °C	Tm: 474 °C	Tm: 427 °C	Tm: 352 °C	Tm: 350 °C

The above results indicate that the Tm tends to decrease significantly with increasing content of fluorine in P3O polymer. Para fluoro substitution tends to depress Tm to a larger extent than the meta substitution. The Tm depression effect from fluoro substitution appears to follow the following order:

Disubstitution >> Monosubstitution; Para substitution > Meta substitution

5.3.4. Consideration of Tm and Crystallinity Depression by Fluoro Substitution

The main structural factors favoring the crystallizability of polymers are considered to be the high regularity in the polymer chain and efficient chain interaction. However, the dimensional factor induced by fluoro substitution cannot explain the observed property changes because the di-substituted derivatives with more symmetrical structural features actually show significantly less tendency to crystallize than the mono-substituted derivatives with unsymmetrical substitution. Therefore it would suggest that the presence of fluorine functions to deter the chain interaction and therefore depresses the crystallizability of the resulting polymers. This would also explain the Tm reduction by fluoro substitution described above which could be a result of the decreased chain interaction which is responsible for the crystal lattice energy.

It has been shown that in polyarylates and polyamides in which the lattice energy, which is responsible for the melting enthalpy, is mainly based on the interactions between the aromatic rings and dipolar interaction between the functional groups. While in nonpolar aromatic molecules without strong dipoles present, the chain interaction is mainly attributed to the interaction between aromatic rings[18,19]. Aromatic-aromatic attraction force is considered to be the energetically favorable interaction between electron deficient hydrogen and the electron rich and polarizable π electron on the aromatic ring[19,20]. For example, such an interaction has been proposed in miscible poly(2,6-dimethylphenylene oxide)/polystyrene blends in which the miscibility results from the interaction between the electron deficient methyl group on poly(2,6-dimethylphenylene oxide) and polarizable π electron on the phenyl ring on polystyrene. Other examples for such interactions are found in many aromatic side chains in protein structures in which the interaction between hydrogen on one aromatic ring and the π electron on another aromatic ring functions to stabilize the conformations of protein molecules[21,22].

If such an electrostatic attraction is indeed significant in our system, the presence of electronegative fluorine should decrease the polarizability of π electron on aromatic rings therefore reduces the aromatic-aromatic attractive force.

A similar behavior was observed in the crystal structure of DPP[23], with a hydrogen bonding between the π electron of the pendant phenyl ring and hydrogen from the hydroxyl group. This bonding causes a 8 degree difference in the dihedral angle between the two pendant rings to the center ring which is shown in figure 5.5. However, our x-ray results from 2,6-bis(p-fluorophenyl)phenol crystals[24] in figure 5.6 revealed that the dihedral angles between the two pendant rings and the center ring are very close, only 2 degrees difference was observed (50° & 48 °). This indicates that the strong electronegative fluorine atoms decrease the π electron polarizability of the phenyl ring and lead to the elimination of the hydrogen bonding observed in DPP crystals which resultes in the similar dihedral angle of the pendant phenyl rings and center phenyl ring.

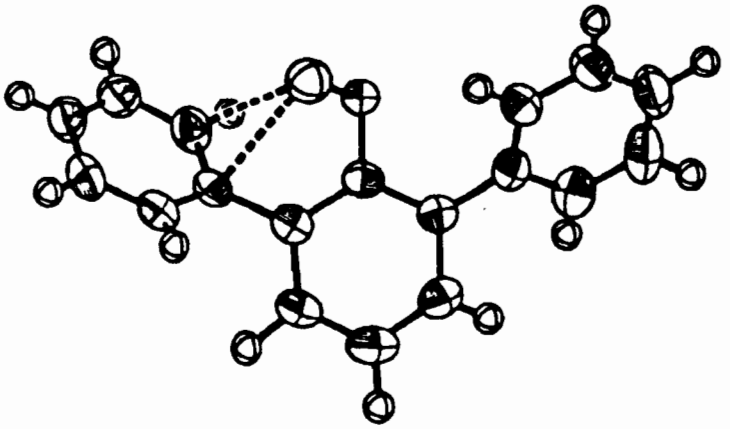

Fig. 5.5. Crystal structure of DPP. dihedral angle of left pendant ring - center ring: 52 °;

dihedral angle of right pendant ring - center ring: 44 °;

O-H bond is nearly coplanar with the C-C bond which is involved in the hydrogen bonding.

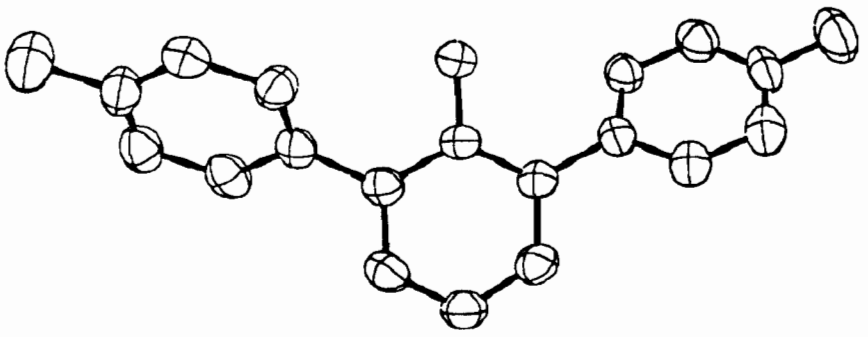

Fig. 5.6. Crystal structure of $DPPF_2$. Dihedral angle of left pendant ring - center ring: 43 °;

Dihedral angle of right pendant ring - center ring: 45 ° .

The above observation would lead us to assume that the presence of fluorines on the pendant phenyl rings of P3O would reduce the aromatic-aromatic attraction forces by decreasing polarizability of the π electrons of the aromatic rings, therefore, leading to reduced Tm and crystallizability.

5.4. THERMAL STABILITY OF FLUORO SUBSTITUTED P3O POLYMERS

The TGA profiles of the polymers are shown in table 5.5 and P3O is included for comparison. Fluorinated polymers show improved or comparable with P3O stability in both nitrogen and air. This is apparently related to the introduction of the strong C-F bond into the polymers and the strong electronegative nature of fluorine which tends to stabilize the aromatic systems.

Table. 5.5. Thermogravimetric analysis of fluorinated P3O[a]

Polymer	Nitrogen		Air	
	$T_5(T_{10})^b$	T_{max}^c	$T_5(T_{10})^b$	T_{max}^c
P_3OmF	540(550)	561	535(553)	577
P_3OpF	525(540)	560	520(541)	560
P_3OmF_2	529(541)	555	500(544)	*
P_3OF_2	540(548)	560	532(554)	578
P3O	518(528)	544	528(545)	561

[a] Heating rate 10 °C/min. [b] 5% weight loss (10% weight loss).

[c] First maximum decomposition temperature.

5.5. SOLUBILITY OF FLUORO SUBSTITUTED P3O POLYMERS

The solubility of these fluorinated polymers in a variety of solvents are listed in table 5.6 and the parent polymer P_3O is included for comparison. They all show very good solubilities in common organic solvents. In addition, the fluorinated polymers become soluble in carbonyl containing solvents in which the parent P_3O is not soluble.

Table. 5.6. Solubility of Fluorinated P3O Polymers

	Solvent					
Polymers	Acetone	MeCOEt	Cyclohexanone	EtOAc	Toln	Cyclohexane
P3O	-	-	+	-	+	-
P_3OmF	s	+	+	+	+	-
P_3OpF	s	+	+	+	+	-
P_3OmF_2	s	+	+	+	+	-
P_3OF_2	s	s	+	s	+	-

(+) = soluble, (-) = insoluble, (s) = swollen. The test was done at room temperature.

From the above results, we assume the decreased molecular cohesion of the fluorinated P3O's could likely attribute to the enhanced solubility in the above solvents. Here again the fluoro substitution effect on the polymer solubility is significantly different from its analogues, such as chloro and bromo substituted P3O which are not soluble even in hot organic solvents.

References:

1. a. Cassidy, P. E., *Thermally Stable Polymers*, Marcel Dekker, Inc., New York & Basel, **1980**.

   b. Critchley, J. P., Knight, G. J., and Wright, W. W., *Heat Resistant Polymers*. Plenum Press., **1983**.

2 a. Risse, W. R., and Sogah, D.Y., *Macromlecules*, **1990**, 23, 4029.

   b. Nagata, N., Tsutsumi, N, and Kyotsukuri, T., *J. Polym. Sci. Polym. Chem. Ed.*, **1988**, 26, 235.

   c. Jadhav, J. Y., Preston, J., and Krigbaum, W. R., *J. Polym. Sci. Polym. Chem. Ed.* **1989**, 27, 1175.

3. a. Rogers, H. G., Gaudiana, R. A., Hollinsed, W. C., Kalyanaraman, P. S., Manello, J. S., McGowan, C., Minns, R. A., and Sahatjian, R., *Macromolecules*, **1985**, 18, 1058.

4. Matsuura, T., Hasuda, Y., Nishi, S., and Yamada. N., *Macromolecules*, **1991**, 24, 5001.

5. Preston, J., in *Encyclopedia of Polymer Science and Engineering*, Mark, H. F., Bikales, N. M., Overberger, C. G., and Menges, G., Eds., Wiley, New York, **1988**, Vol. II, 381.

6. St. Clair, T. L., Structure-property relationships in linear aromatic polyimides in *Polyimides*, Edited by Wilson, D., Stenzenberger, H. D., and Hergenrother, P. M., Blakie & Son Ltd., Ch. 3, **1990**.

7. Aharoni, S. M., *J. Polym. Sci. Polym. Phys. Ed.*, **1981**, 19, 281.

8. Ballauff, M., and Schmidt, G. F., *Macromol. Chem. Rapid Commun.*, **1987**, 8, 93.

9. Lupinski, J. H. and Moore, R. S., *Polymeric Materials for Electrics Packing and Interaction*, ACS, Washington D.C., **1989**.

10. Groh, W., Lupo, D. and Sixl, H., *Angew Chem. Int. Ed. Engl. Adv. Mater.*, **1989**, 28, 1548.

11. Cassidy, P. E., Aminabhavi, T. M., and Farley, J. M., *J. Macromol. Sci. - Rev., Macromol. Chem. Phys.*, **1989**, C29, 365.

12. Ichino, T., Sasaki, S. Matsuura, T. and Nishi, S., *J. Polym. Sci., Part A. Chemistry*, **1990**, 28, 323.

13. Kiyotsukuri, T., Tsutsumi, N., Okada, K., and Asai, K., *J. Polym. Sci. Part A. Polym. Chem*, **1988**, 26, 2225.

14. Kiyotsukuri, T., Tsutsumi, N., and Sandan, T., *J. Polym. Sci., Part A., Polym. Chem.*, **1990**, 28, 315.

15. Nagata, M., Tsutsumi, N., and Kiyotsukuri, T., *J. Polym. Sci., Part A., Polym. Chem.*, **1988**, 26, 235.

16. Dana, D. E., and Hay, A. S. *J. Polym. Sci., Polym. Chem.*, **1989**, 27, 873.

17. Kiyotsukuri, T., Tsutsumi, N., and Sandan, T., *J. Polmy. Sci. Part A: Polymer Chemistry*, **1990**, 28, 315.

18. Tashiro, K., Hou, J-A., Kobayashi, M., and Inoue, T., *J. Am. Chem. Soc.*, **1990**, 112, 8273.

19. O'Mahoney, C. A., Williams, D. J., Colquhoun, H. M., and Blundell, D. J. *Polymer*, **1990**, 31, 1603.

20. Kitaigorodsky, A., *Molecular Crystals and Molecules*, Academic Press, New York, **1973**.

21. Burley, S. K. and Petsko, G. A., *Science*, **1985**, 229, 23.

22. Burley, S. K. and Petsko, G. A.,*J. Am Chem. Soc.*, **1986**, 108, 7995.

23. Nakatsu, K., Yoshioka, H., and Kunimoto, K., *Acta Cryst.*, **1978**., B34, 2357.

24. Crystal structure was provided by Dr. Rose Hynes in the Department of Chemistry.

CHAPTER 6: THERMAL PROPERTIES OF RANDOM P_3O COPOLYMERS

6.1 INTRODUCTION

6.1.1 Relation Between Tg and Tm in Homo and Copolymers

In linear homopolymers, the principal structural parameters, such as chain stiffness and chain cohesion, affect the Tg and Tm in very much same way, i.e. rigid chains and strong chain cohesion tend to give both a higher Tg and Tm. It is therefore not surprising that a correlation between glass transition and melting point is found for many crystalline polymers which exhibit both types of transitions:

$$Tm = K\,Tg \qquad (1)$$

This correlation has been described as a rule of thumb, in which Tg is approximately one-half Tm for polymers with symmetrical chains and two-thirds for polymers with unsymmetrical chains. This expression, although obviously oversimplified, represents a reasonable approximation for many linear homopolymers and is shown schematically in figure 6.1. [1]

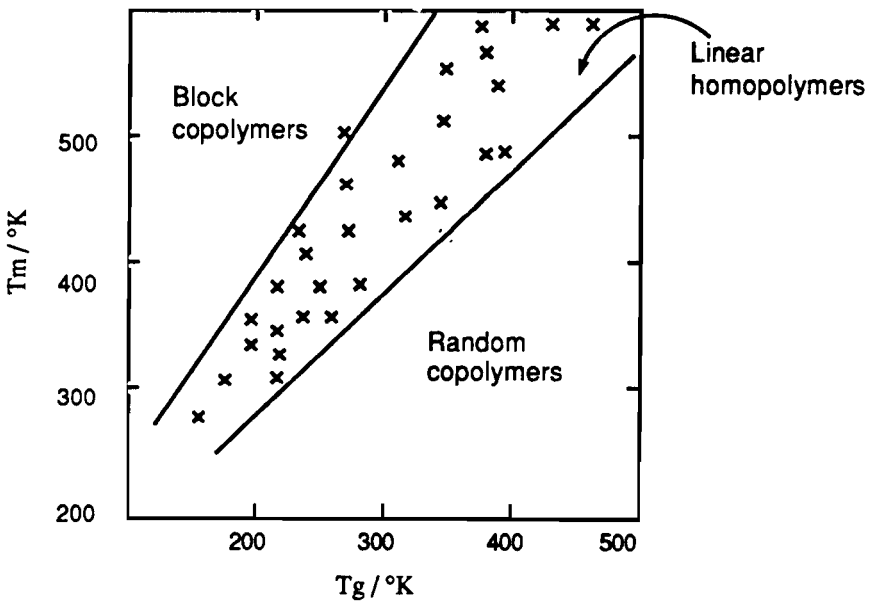

Fig. 6.1 Schematic representation of the relation between Tg's and Tm's of polymers

It has been demonstrated that any attempts to control the glass transition and melting temperatures for linear homopolymers by modifying the structures, will give either a high Tg and Tm or a low Tg and Tm, and it is difficult to control Tg and Tm separately.

Despite this, it is a fact that the requirement of three dimensional order in crystalline phases which determines the melting points of polymers, is more a function of packing efficiency than the glass transition is. Hence, the separate control of Tg and Tm can often been achieved by synthesizing random copolymers. For example, random copolymers from nylon 6.6 and nylon 6.10 give very little change in the Tg[2], because the chain stiffness of the main chain is virtually unchanged. On the other hand, significant reductions in Tm are obtained because of the irregular arrangements of co-units along the copolymer chains which impairs efficient crystal packing. The magnitude of the Tm reduction depends on both the comonomer structures and the compositions. Since random copolymers lead to a lower Tm, usually a narrower gap between Tg and Tm is the result as shown in figure 6.1. While an increased gap between Tg and Tm can be achieved in block copolymers in which a high melting chain segment capable of crystallizing is attached chemically to a lower Tg chain segment which is shown in figure 6.1.

6.1.2. Tg and Tm in Random Copolymers

A. Glass Transitions in Random Copolymers [3,4]

Random copolymers generally exhibit a single Tg with a value between the Tg's of the individual homopolymers. A simple linear relation between Tg's and the composition has been found for some copolymers composed of compatible monomers where a simple mixing rule can be applied (equation 1).

$$Tg^{AB} = Tg^{A} W_A + Tg^{B} W_B \qquad (1)$$

If the comonomer properties differ significantly, a deviation from the above linear relationship can result and the Tg's are usually below the straight line joining the Tg's of individual homopolymers (equation 2).

$$1/Tg^{AB} = 1/Tg^{A} + 1/Tg^{B} \qquad (2)$$

The relationships above have been often used to predict the Tg's of copolymers and compatible blend systems. They have also been frequently used to extrapolate the Tgs of the crystalline homopolymers from their corresponding random copolymers when the Tg is difficult to detect due to high crystallinity.

B. Melting Temperature and Crystallinity in Random Copolymers [5,6]

The usual consequences of random copolymerization is the formation of polymeric materials with reduced melting points, lower crystallinity and increased solubility. The structural features of the comonomer are the over-riding factors which determine the properties of the resulting copolymers.

When a pair of comonomers with very dissimilar structures, i.e. shape, volume and chemical nature, are copolymerized, the co-units will not be able to pack into a common crystal lattice. A dissimilar co-unit at low content will not be included into the main chain crystal lattice, instead it leads to a termination of the crystallizable chain length. The consequences are usually a deep decrease in both melting points and crystallinity at very low concentrations of the comonomers in the copolymers. At higher ratio, the copolymers will lose the crystallinity completely. This is shown schematically as curve Tm in figure 6.2[7].

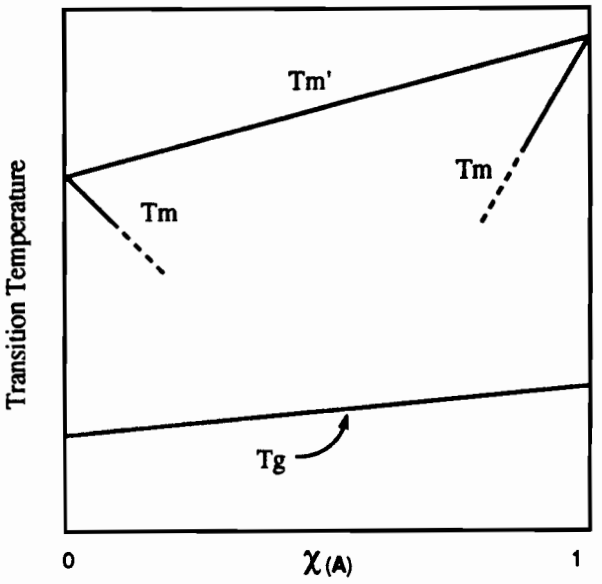

Fig. 6.2. Schematic representation of Tm and Tg as a function of copolymer composition

Flory proposed the following equation to describe this melting point depression at low concentration of comonomer based on the uniform exclusion model[8].

$$1/Tm - 1/Tm^{\circ} = -(R/\Delta Hu)\ln \chi_A \qquad (3)$$

Where Tm refers to the copolymer and Tm° to the corresponding homopolymer, ΔHu is the molar enthalpy of melting of homopolymer A and χ_A is the molar fraction of monomeric units A in the copolymers. In this equation, the foreign unit B is considered to be excluded from crystal lattice of A.

In another extreme case, when a pair of monomers have structures sufficiently alike, comonomers can pack into a common crystal lattice. This generally results in a smooth change in melting points over the composition range as shown in curve Tm' in figure 6.2. This phenomena is called isomorphism[9,10] and is related to the same phenomena in small molecules. The number of this type of copolymer systems is limited because of the strin-

gent requirements for comonomer structures. Other properties, such as crystallinity and crystal lattice parameters also vary regularly over the copolymer compositions.

Copolymer styrene/p-fluorostyrene is a good example of a system showing isomorphism[11] as a result of the small size of fluorine and the noncritical van der Waals contact distance of the fluoro substitution position in the crystal lattice. Over all the composition range, the copolymers exhibit linear variations in melting point between the melting points of the two homopolymers (235° C for polystyrene and 263 °C for p-fluorostyrene). In figure 6.3. it is shown that the copolymers that are richer in styrene have the structure of isotactic polystyrene (threefold helix); those richer in p-fluorostyrene have the structure of poly-p-fluorostyrene (fourfold helix)[12].

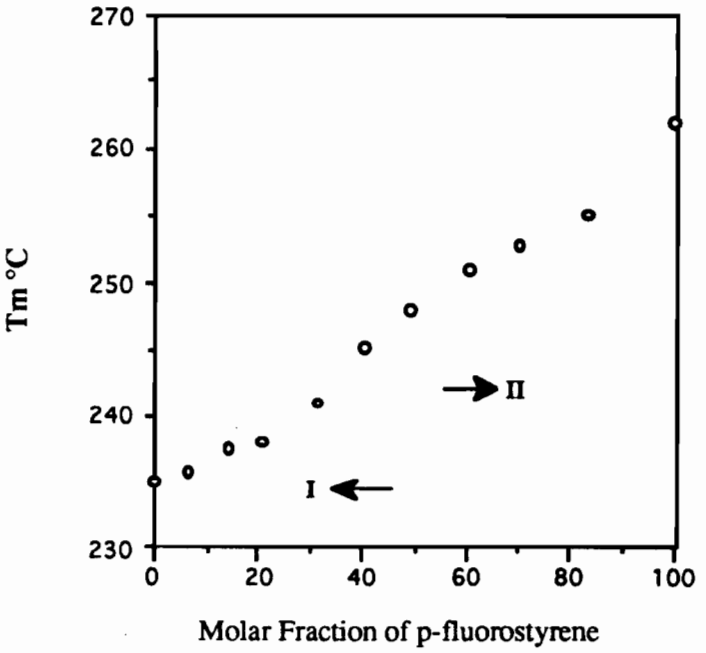

I Crystallites with threefold helix; II Crysatllites with fourfold helix

Fig. 6.3. Tm vs composition of random copolymer styrene/p-fluorostyrene

6.2. RANDOM P_3O COPOLYMERS

Copolymerization generally provides much wider variations in the polymer properties than corresponding homopolymers, such as melting temperatures, crystallinity and solubility. We have demonstrated previously that a series of random copolymers can be made in high molecular weight due to the improved solubility as a result of crystallinity depression. In this study, we intend to study their thermal property variations in relation to the comonomer structures and the compositions. The copolymers subjected to this study are shown in the following scheme in which the various monomeric units bear different substituents with varied van der Waals radii.

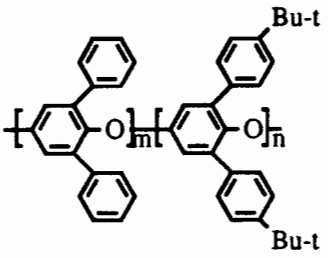

DPP/DPPBu$_2$

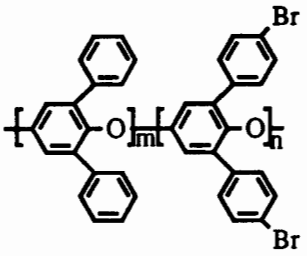

DPP/DPPBr$_2$

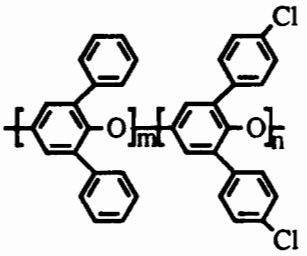

DPP/DPPCl$_2$

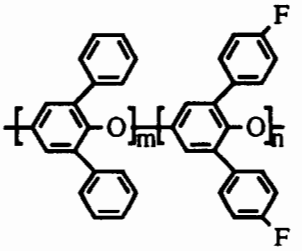

DPP/DPPF$_2$

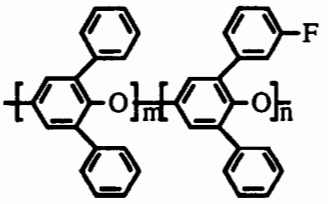

DPP/DPPmF

The property variations would be expected to depend on the similarity of the comonomer structures, either dramatically when comonomer structures are significantly different, or gradually when comonomer structures are sufficiently alike. The substituents in the above copolymers range from very bulky t-butyl groups to very small fluoro groups. Hence we would expect that the thermal properties would change over a rather wide range. We in-

tend to study the influence of the various substitutions in the resulting copolymer on their transition temperature, crystallization behavior and the thermal stability.

6.3. RESULTS AND DISCUSSIONS

A. Copolymers DPP/$DPPBu_2$: The first system consisted of comonomer DPP/$DPPBu_2$ with compositions ranging from 7 % mole to 93 % mole of DPP in the copolymers. The Tm, Tg and ΔHm data are compiled in table 6.1.

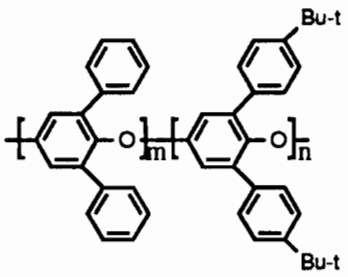

DPP $DPPBu_2$

DSC traces in figure 6.4 show that the copolymers remain crystalline only at composition containing less than 10% mole of either of the co-units (curve b, 9.1 DPP% and curve f, 9.1 $DPPBu_2$%). The copolymerizations lead to significant decreases in crystallinity and crystal perfection, as indicated by the substantial decrease in ΔHm (table 6.1. entry 3, 7) and significant broadening of melting peaks (figure 6.4, curve b, f). In addition, the co-polymerizations also resulted in polymers with significantly decreased melting temperatures. The observed substantial depression in crystallinity and imperfect crystals developed even at very low comonomer compositions must be a result of the bulkiness of the t-butyl substituent. Because of the large difference in comonomer structures, either of the co-units tend to terminate the crystallizable chain length, therefore leading to significant drops in crystallinity and melting temperatures at even very low comonomer compositions.

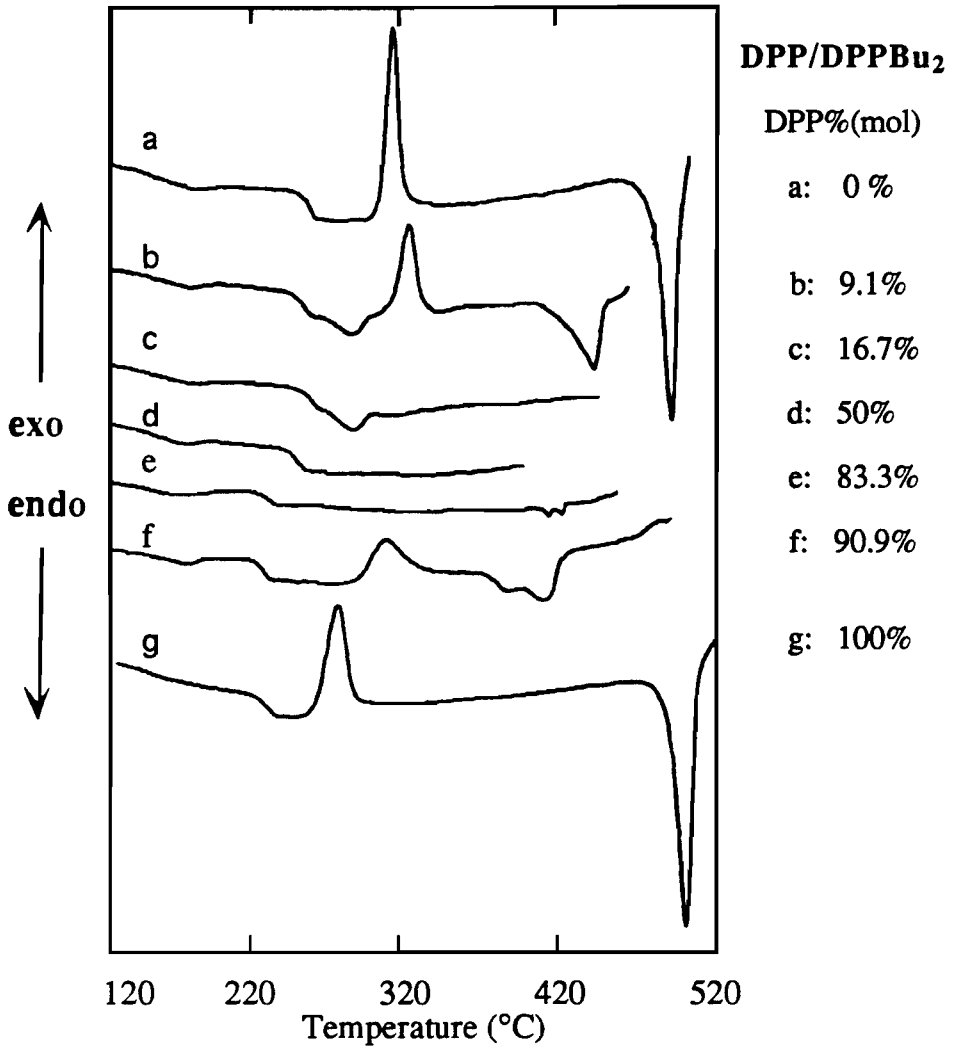

Fig. 6.4. DSC traces of copolymer DPP / $DPPBu_2$.

Figure 6.5 shows that the glass transitions vary relatively linearly over the composition ranges. The Tm however, suffers a sharp decrease at very low comonomer compositions, a typical melting point depression described by the Flory exclusion model. We noticed that the incorporation of a small amount of $DPPBu_2$ co-units into DPP sequences led to a sharper decrease in Tm (Tm variation in the right hand) than that from the incorporation of the same amount of DPP co-units into $DPPBu_2$ sequences (Tm variation in left hand). We assume this could be due to the looser crystal lattice of $DPPBu_2$ sequences which is more tolerable to the introduction of smaller DPP units. This is shown in the DSC traces in figure 6.4 in which the incorporation of 9.1% mole $DPPBu_2$ co-units into DPP sequences leads to a more broad melting peak or more imperfect crystalline phase (curve f) than that of the incorporation of same amount of DPP co-units into $DPPBu_2$ sequences (curve b). This is similar to the observation that the polymers with looser helical crystal lattice are more tolerable to the inclusion of foreign units than the polymers with relatively closed packed, planar zig zag crystal lattice.

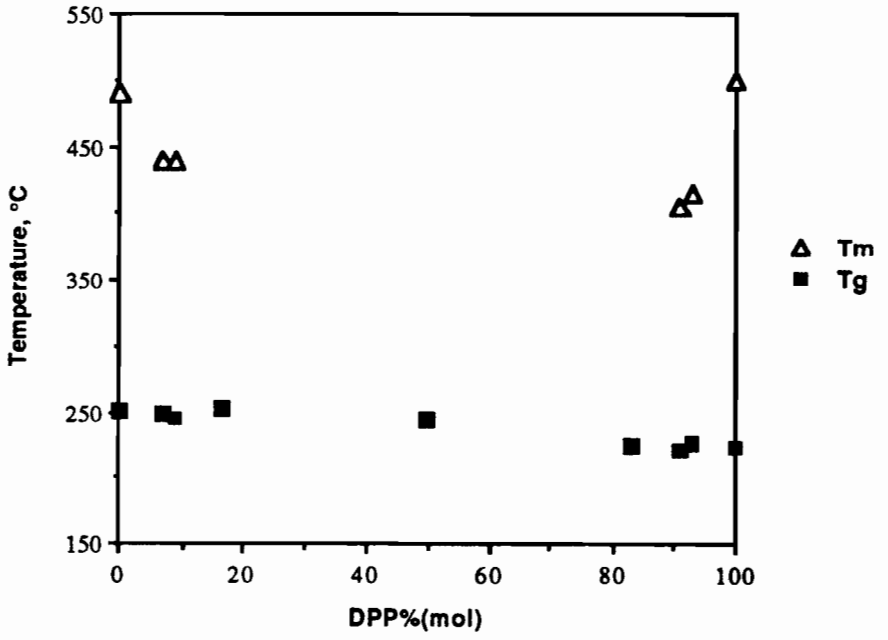

Fig. 6.5. Transition Temperature vs Copolymer Composition. DPP/$DPPBu_2$

Table 6.1. Thermal Properties of Copolymers DPP/DPPBu$_2$[a]

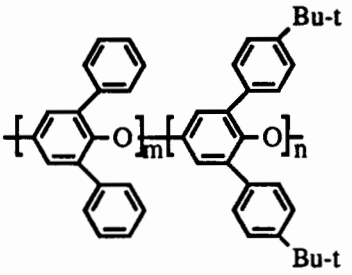

DPP DPPBu$_2$

Entry	DPP %(mol)	η_{inh}, dL/g[b]	Tg,°C	Tc,°C	Tm,°C	ΔHm, J/g
1	0.00	0.53[c]	249.2	305.2	489.9	25.3
2	7.0	0.42[c]	247.4	312.9	438.9	7.9
3	9.09	0.39[c]	245.4	316.5	438.7	10.7
4	16.7	0.44	251.9	-	-	-
5	50.0	0.54	242.8	-	-	-
6	83.3	0.45	223.7	-	-	-
7	90.9	0.41	221.1	301.8	406.2	13.3
8	93.0	0.46	225.4	303.5	415.8	15.2
9	100	0.48	222.9	270.4	500.9	27.6

a: heating rate: 20 °C/min. b: $CHCl_3$(0.5%w), 25 °C. c: obtained in o-$PhCl_2$.

B. Copolymers DPP/$DPPBr_2$ and DPP/$DPPCl_2$:

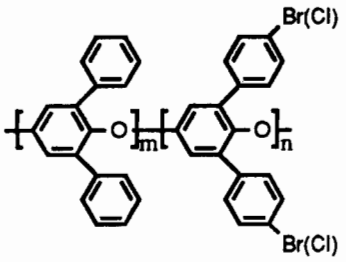

DPP $DPPBr_2(Cl_2)$

The DSC traces for copolymers of DPP/$DPPBr_2$ and DPP/$DPPCl_2$ are shown in figure 6.6 and 6.7 respectively, in which the crystallinity decreases as the DPP content in the copolymers increases. The significant crystallinity depression in the bromo substituted copolymer is revealed by its small and broad melting endotherm in the DSC trace as shown in figure 6.6 (curve b, e). The chlorinated copolymers maintained crystallinity to a even higher DPP content and gave better defined melting peaks than the brominated analogues (fig. 6.7, curve b, c).

The chlorinated copolymers maintain higher crystallinity than bromo analogues which is indicated by the ΔHm values listed in table 6.3 (entry 2, ΔHm 14.6 J/g and entry 3, ΔHm 19.8 J/g). Thus, chloro substituted copolymers provided systems with retained crystallizability, further reduced melting point and desired solubility.

The transition temperature-copolymer composition profiles are shown in figure 6.8. The glass transition temperatures are relatively linearly dependent on the compositions for both bromo and chloro substituted copolymers. Tm's for both series tend to decrease quite sharply at low concentrations of comonomer.

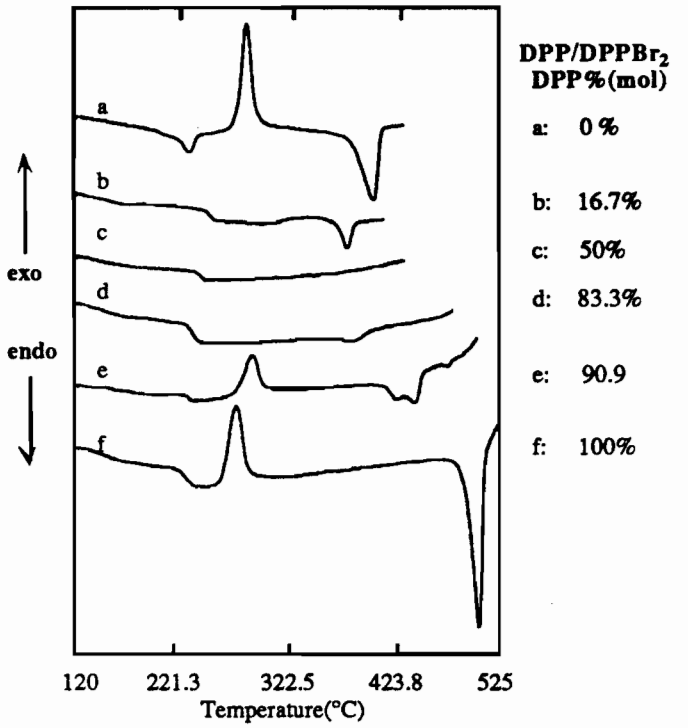

Fig. 6.6 DSC Traces of Copolymer DPP/$DPPBr_2$. Heating Rate: 20 °C/min.

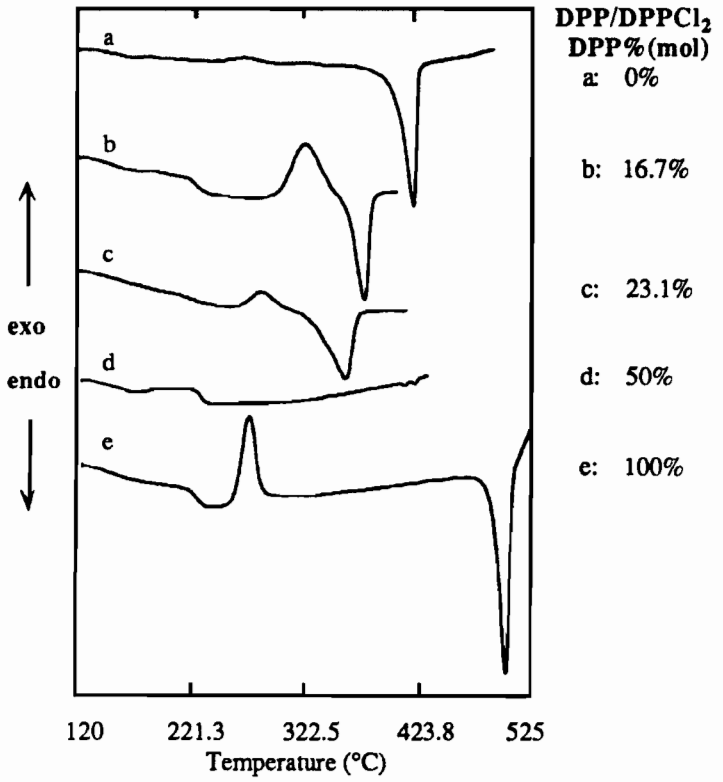

Fig. 6.7. DSC Traces of Copolymer DPP/ $DPPCl_2$. Heating rate: 20°C/min.

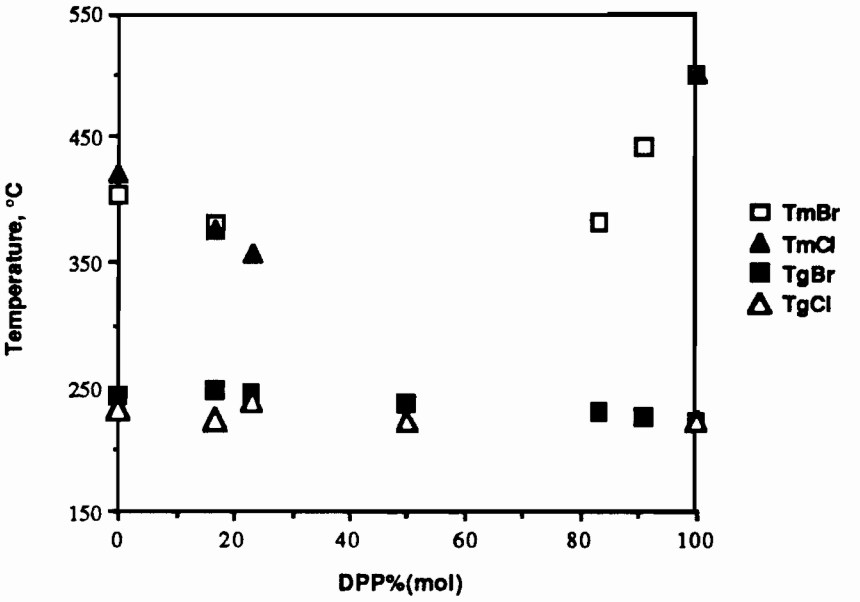

Fig. 6.8. Transition Temperatures vs Copolymer Composition Copolymer DPP/DPPBr$_2$ & DPP/DPPCl$_2$

Table 6.2. Thermal Properties of Copolymer: DPP/DPPBr$_2$[a]

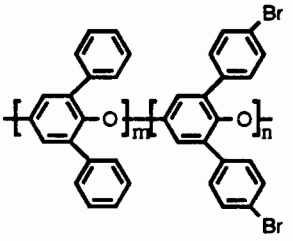

DPP DPPBr$_2$

Entry	DPP%(mol)	η_{inh},dL/g[b]	Tg,°C	Tc,°C	Tm,°C	ΔHm, J/g
1	0.00	insol	243.0[c]	283.4	403.3	21.9
2	16.7	0.26	246.5	340.0	379.2	2.90
3	23.1	0.42	244.7	-	-	-
4	50.0	0.37	237.5	-	-	-
5	83.3	0.44	130.1	-	380.8	1.10
6	90.9	0.54	225.7	287.7	441.8	14.4
7	100	0.48	222.9	270.4	500.9	27.6

a: Heating rate 20 °C/min. b: $CHCl_3$(0.5%w), 25 °C. c: Low Mw.

Table 6.3. Thermal Properties of Copolymers: DPP/$DPPCl_2$[a]

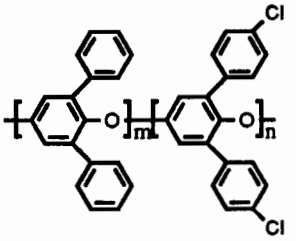

DPP $DPPCl_2$

Entry	DPP%(mol)	η_{inh},dL/g[b]	Tg,°C	Tc,°C	Tm,°C	ΔHm, J/g
1	0.00	inosl.	232.5[c]	-	419.3	28.1
2	16.7	insol	224.2	321.0	375.2	14.6
3	23.1	0.33	-	282.4	356.8	19.8
4	50.0	0.45	222.7	-	-	-
5	100	0.48	222.9	270.4	500.9	27.6

a: Heating rate 20 °C/min. b: obtained in CHCl3 (0.5%w) at 25 °C. c: Low Mw.

C. Copolymers from DPP /$DPPF_2$:

The previous results indicated that when substituted DPP monomers with larger substituents are copolymerized with DPP, a substantial reduction in Tm and improved solubility resulted. However, the Tm reduction was accompanied by a significant crystallinity depression in t-butyl and bromo substituted copolymers. Obviously, the large dimensional variations along the length of the copolymers results in this significant crystallinity decrease.

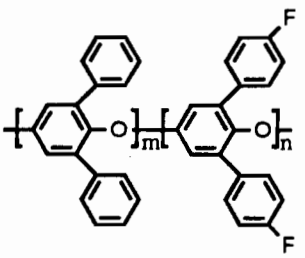

DPP $DPPF_2$

Considering the similar van der Waals radius between fluorine and hydrogen (van der Waals' radius: F: 1.35 Å; H: 1.25 Å. bond length: C-F: 1.10 Å; C-H: 1.35 Å[12]), we expected that the copolymers DPP/$DPPF_2$ would satisfy the structural similarity requirement in cocrystallization and therefore maintain sufficient crystallinity at the higher compositions of comonomer in the resulting copolymers.

DSC traces in figure 6.10 show that the copolymers remain crystalline with increasing content of $DPPF_2$ co-units up to 28.6% (mol) in the copolymers (curve b, c, d, e). The ΔHm listed in table 6.4 indicate that the crystalline copolymers in the series have significant crystallinity (entry 6, 16.0 J/g; 7, 16.9 J/g; 8, 19.2 J/g; 9, 24.8 J/g). With higher concentration of fluoro substituted co-units in the copolymer, amorphous polymers result (fig. 6.10, curve a). The formation of amorphous polymers at higher contents of the fluoro co-units was believed to be a result of the noncrystallizable nature of fluoro co-unit sequence.

The relationship between the Tg's, Tm's, Tc's and the copolymer compositions is shown in figure 6.9, A nearly linear relationship between Tg's and the copolymer compositions was observed. The Tm's tend to decrease sharply with increasing concentration of fluoro co-units in the P_3O chain. With increasing contents of fluoro substituted co-units, the gap between Tm and Tc also tends to decrease which indicates the increasing difficulty in crystallization. However, comparing with bromo or chloro substituted systems, the fluoro substituted copolymers give much more gradual reductions in Tm with the composition changes and maintain higher crystallinity over a wider composition range.

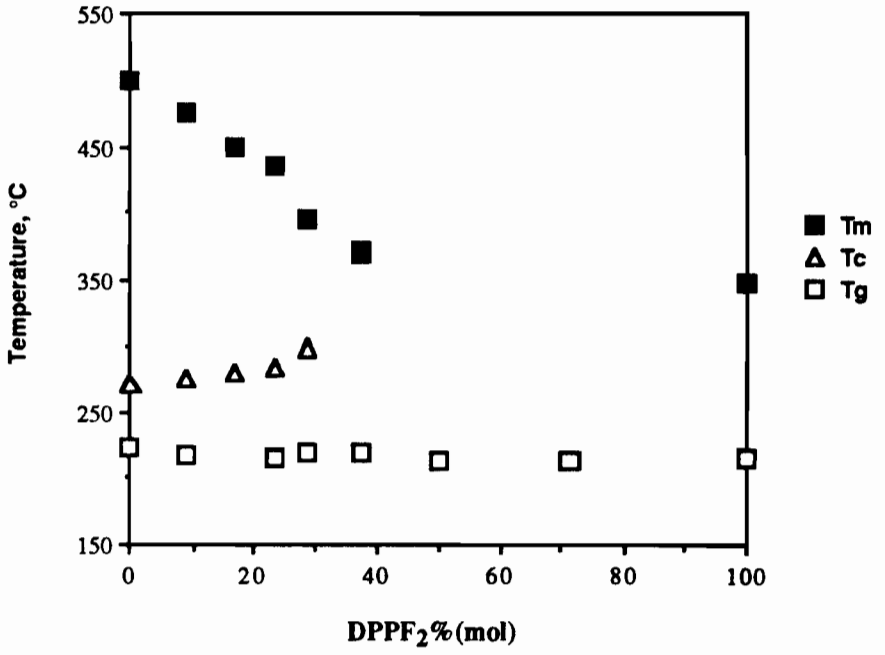

Fig. 6.9. DSC Traces of Copolymer DPP/$DPPF_2$. Heating rate: 20 °C/min.

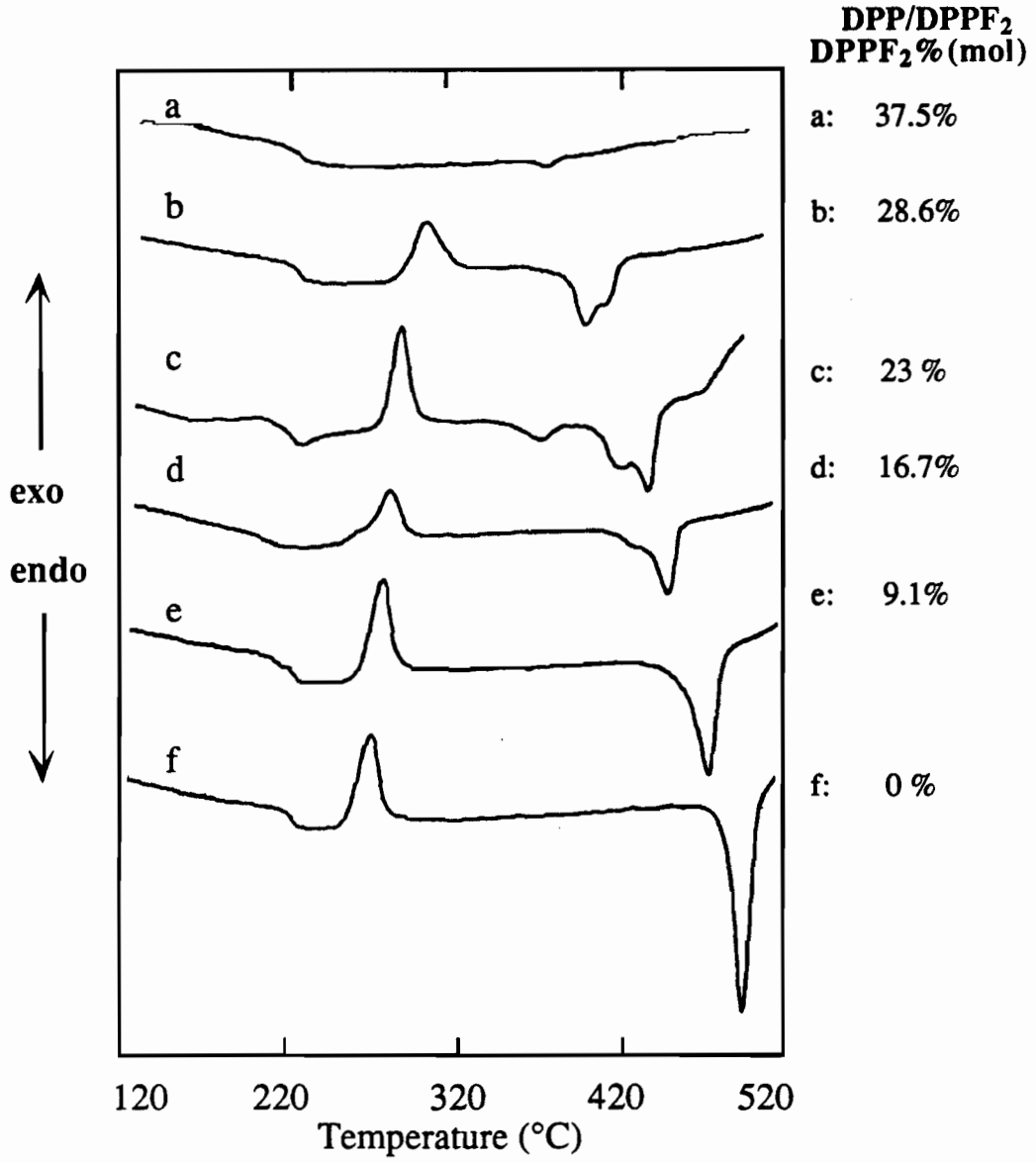

Fig. 6.10. Transition Temperature vs Copolymer Composition DPP/$DPPF_2$

Table 6.4. Thermal properties of copolymer DPP/$DPPF_2$[a]

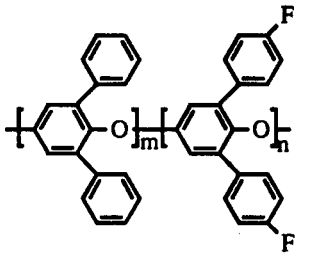

DPP $DPPF_2$

Entry	DPP%(mol)	η_{inh}, dL/g[b]	Tg,°C	Tc,°C	Tm,°C	ΔHm, J/g
1	0.00	0.48	215	300	347	4.7
2	23.1	0.46	210	-	-	-
3	28.6	0.36	213.3	-	-	-
4	50.0	0.38	213.4	-	-	-
5	62.5	0.38	219.6	-	370.3	0.6
6	71.4	0.45	219.5	297.2	395.8	16.0
7	76.9	0.49	214.2	283.7	435.9	16.9
8	83.3	0.46	217.0	279.2	449.5	19.2
9	90.9	0.51	215.8	276.0	476.8	24.8
10	100	0.48	222.9	270.4	500.9	27.6

a: heating rate: 20 °C/min. b: $CHCl_3$(0.5%w).

C. Copolymers from DPP/DPPmF

The previous results show that the dimensional similarity of co-units is the most important factor for the resulting copolymers to maintain sufficient crystallinity. However, as observed in DPP/$DPPF_2$ system, the copolymers became amorphous at the middle composition range due to the noncrystallizable nature of the $DPPF_2$ unit.

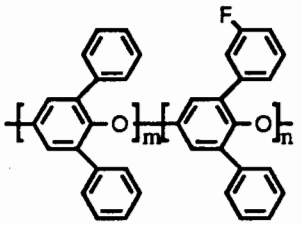

DPP DPPmF

In order to obtain a system which maintains high crystallinity over a wider composition range, in addition to dimensional similarity of comonomers, it requires that both of the comonomers yield crystallizable homopolymers. In this series of copolymer DPP/DPPmF, both comonomers give homopolymers which are readily crystallizable. Hence, this series of copolymers would be expected to have the best chance to maintain high crystallinity over the whole composition range.

The DSC scans of this series of copolymers are shown in figure 6.11. The copolymers over the whole composition range show well defined melting endotherms and the sharpness of the crystallization exotherms indicats that all of these copolymers are readily crystallizable. The degree of crystallinity for all the copolymers is sufficiently high, which is indicated by their fusion heats which are comparable with individual homopolymers (table 6.5). The fact that the degree of crystallinity remains high over the composition range led us to assume that the co-crystallization of the two co-units, which was described previously for polystyrene copolymer, occurs over the entire composition range. We noticed that the melting peak for the copolymer at middle concentrations (fig. 6.11, curve e, 37.5 A%) is broader compared with others. One possible reason for this is that there is a coexist of two types of crystal structures from the individual homopolymers. But this can only be confirmed with further detailed crystal structural information.

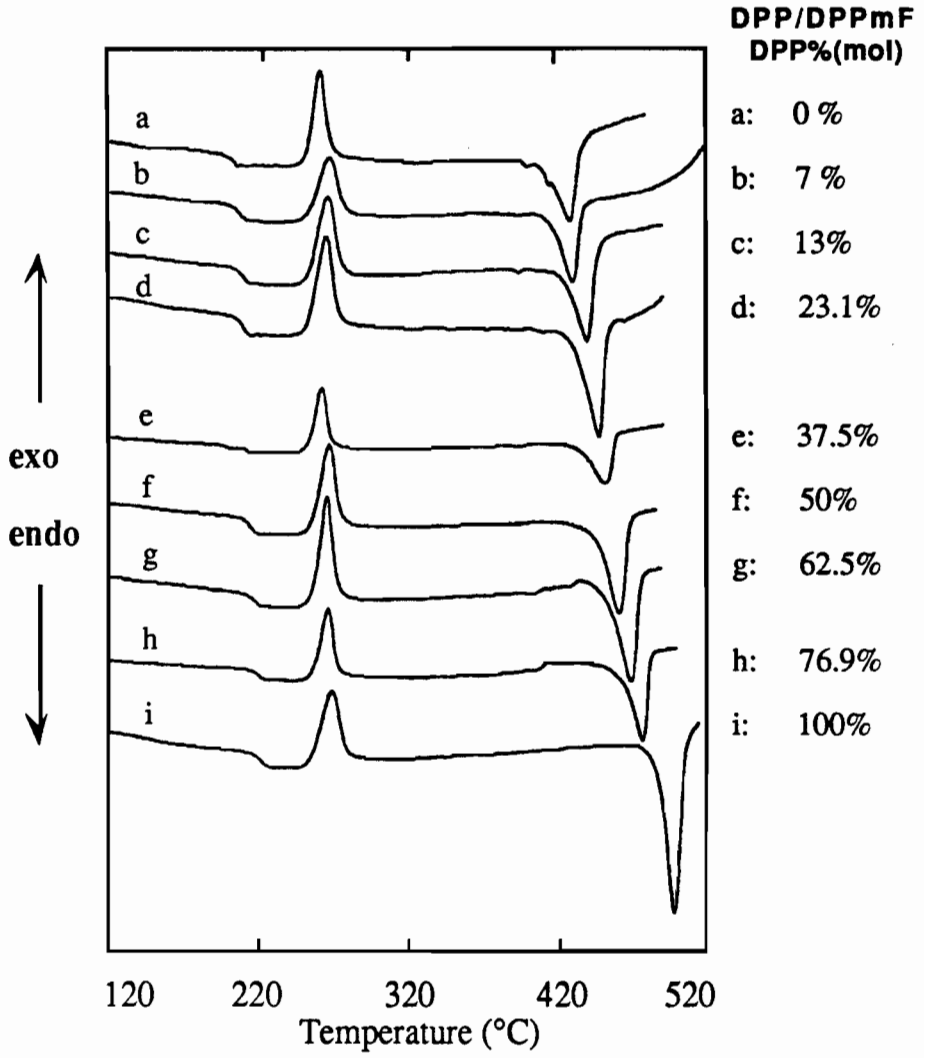

Fig. 6.11. DSC traces of copolymer DPP/DPPmF. Heating rate: 20 °C/min.

In figure 6.12, it is shown that not only glass transition temperatures, but also melting points and crystallization temperatures of the copolymers, vary with composition in a linear way between those of the two homopolymers. No minimum in the melting point-composition relationship is observed, as would be expected if the comonomer crystallized separately.

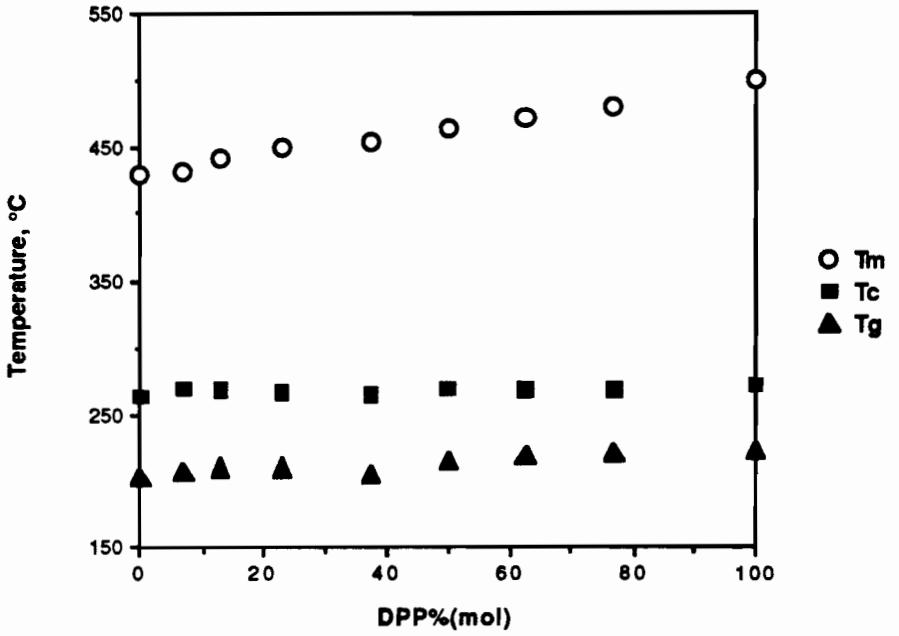

Fig. 6.12. Transition Temperature vs Copolymer Composition: DPP/DPPmF

The gradual variation in the properties of the resulting copolymers observed above presumably is a result of the small size of fluorine and the non-critical van der Waals contact of meta fluoro substitution in the crystal lattice. The fact that the crystallinity remains high over all the composition ranges and the linear variation leads us to believe that co-crystallization occurs in these copolymers.

Table. 6.5. Thermal Properties of Copolymer DPP/DPPmF[a]

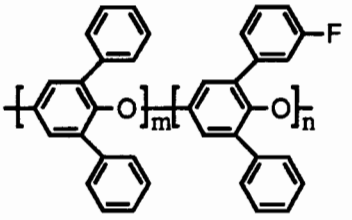

DPP $DPPF_2$

Entry	DPP%(mol)	η_{inh}, dL/g[b]	Tg,°C	Tc,°C	Tm,°C	ΔHm, J/g
1	0.00	0.36	202	261	430	15.0
2	7.0	0.44	208	267	431	14.1
3	13.0	0.40	210	268	440	14.7
4	23.1	0.29	210	266	449	17.9
5	37.5	0.36	212	263	453	13.6
6	50.0	0.36	215	268	463	22.0
7	62.5	0.38	217	267	471	19.6
8	76.9	0.37	223	268	479	23.4
9	100.0	0.48	231	273	509	25.5

a: heating rate: 20 °C/min. b: $CHCl_3$(0.5%w).

Comparsion of Various Substitution on Tm Depression

The influence of the substituents on the Tm's of the resulting copolymers is illustrated in figure 6.13. The magnitude of the melting point depressions clearly correlated with the dimensional variation of substituted co-units. The butylated copolymers suffer a dramatic drop in Tm at very low concentration of $DPPBu_2$ co-units. The smaller bromo substituted copolymer can maintain crystallinity at relatively higher content of bromo substituted co-units. A much more gradual variation of Tm results in the copolymer DPP/$DPPF_2$ system, however, Tm drops sharply at higher content of of $DPPF_2$ units.

Only the copolymers DPP/DPPmF give high crystallinity over the entire composition range, while showing a very smooth variation in Tm. The small size of fluorine, presumably in a non-critical substitution position, and the crystallizability of both co-units likely contributes to this cocrystallization behaviour over the entire composition range.

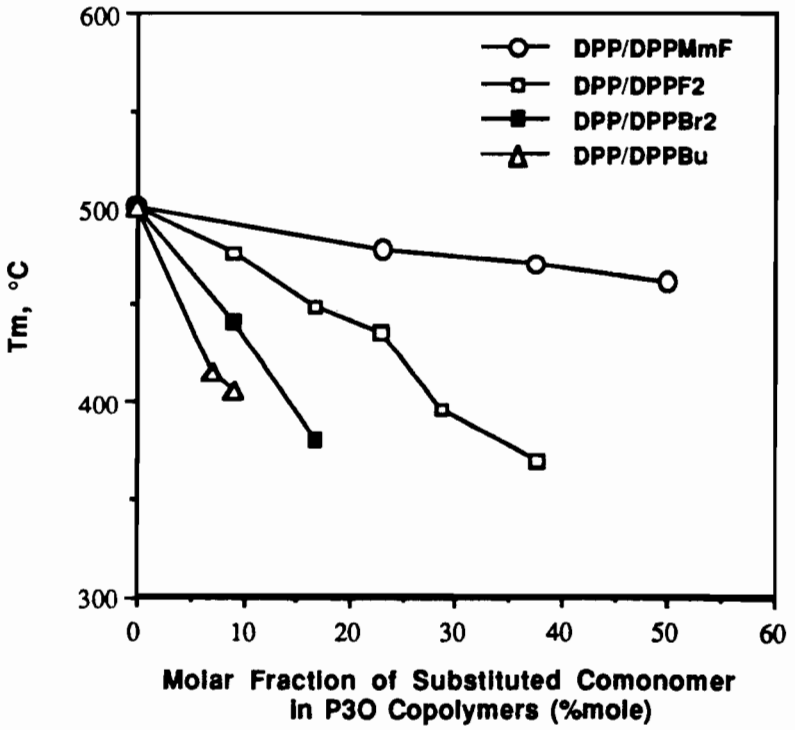

Fig. 6.13. Comparison of Tm Depression of Various Substituted Copolymers

6.4. THERMAL STABILITY OF RANDOM P_3O COPOLYMERS

Among the five series of copolymers, since the only structural variable is the substituents on the pendant phenyl rings, we expected that the thermal stabilities would be related to the bond strength of the Ar-X linkage to which the substituent is attached. The thermal stabilities of the polymers were evaluated by thermogravimetric analysis under nitrogen atmosphere and the temperature at which 5% weight loss occurs and the decomposition onset temperature are given in table 6.6 as a measure of the stability. The results indicate that the thermal stability in halogenated copolymers appeare related to the bond strength of the Ar-X linkage. The stabilities basically follow the order of F > Cl >> Br . This order corresponds to the order of the dissociation energies, C-F: 124.8, C-H: 103 cal/mol, C-Cl: 94.1 cal/mol, C-Br: 79.9[14]. Copolymers containing aliphatic t-butyl show the least stability among these copolymers.

A comparison of the overall decomposition profile for the five copolymers with comonomer ratio of 1:1 is illustrated in figure 6.14. Only fluoro substituted copolymers (DPP/$DPPF_2$ and DPP/DPPmF) show higher stability than the parent polymer P3O. This could be due to the high bond strength of Ar-F and the inductive effect of fluorine which would tend to further stabilize the aromatic systems. The bromo derivative appeares to be the least stable polymer in the series which is probably related to the weaker bond strength and the bond cleavage which would accelerate the decomposition process. The t-butyl substituted polymer appears to decompose at a slighly higher temperature than the bromo derivative but tends to give more extensive decomposition over a wide temperature range. The chloro derivative shows a maximum decomposition peaking at the same range as P3O, but begins to decompose at rather lower temperatures.

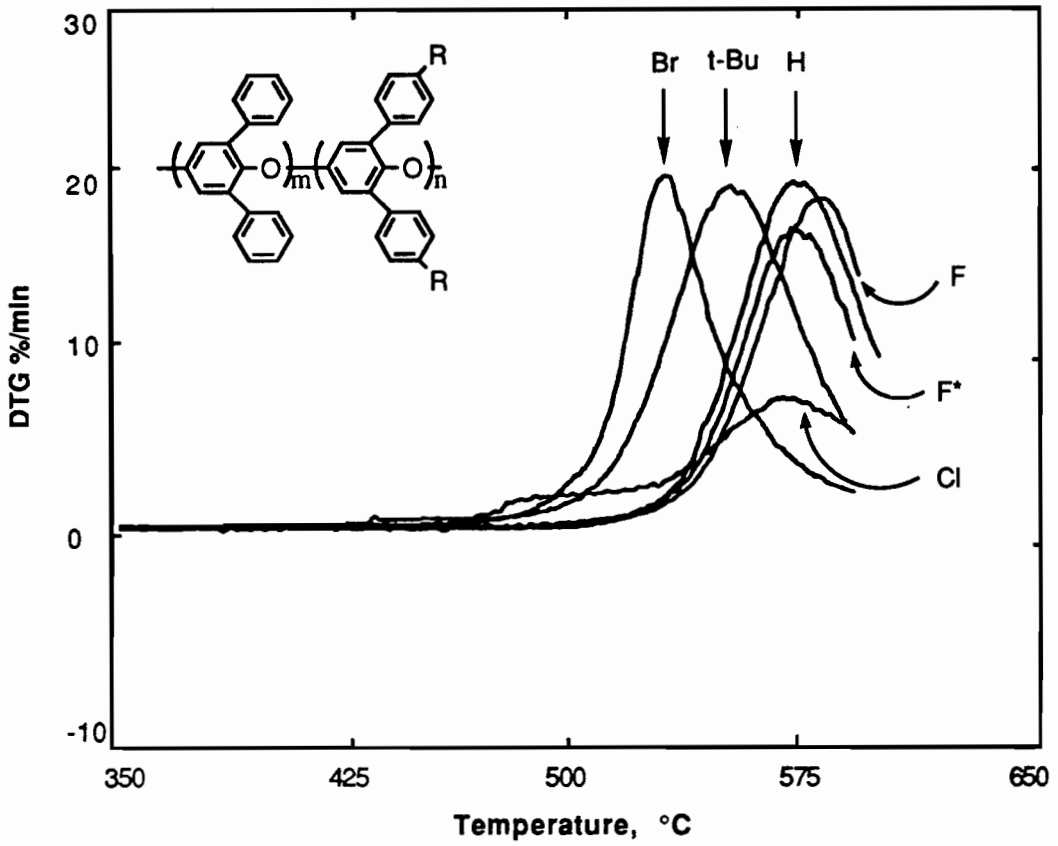

Fig. 6.14. DTG curves of coplymer DPP/substituted DPP (molar ratio: 1:1)
F*: mono meta fluoro substituted DPP
Heating rate: 20 °C/min. Atmosphere: nitrogen.

Table 6.6. Thermogravimetric Results of Copolymers*

Copolymer	DPP%(mol)	W5% loss(°C)	T(°C, onset)
DPP/DPPBu$_2$	7.0	472.0	503.3
	9.09	484.1	506.6
	16.7	495.0	513.3
	50.0	513.0	520.6
	83.3	484.1	516.6
	90.9	523.9	533.8
	93.0	481.6	531.5
DPP/DPPBr$_2$	16.7	506.0	500.8
	23.1	498.6	512.1
	50.0	508.3	511.8
	83.3	518.0	515.7
	90.9	498.6	507.8
DPP/DPPCl$_2$	16.7	537.2	544.8
	23.1	534.8	529.1
	50.0	513.2	523.1
DPP/DPPF$_2$	23.0	536.2	543.2
	28.6	528.7	546.4
	50.0	546.9	552.2
	62.5	549.4	550.5
	71.4	544.5	546.5
	76.9	514.2	542.7
	83.3	528.8	547.4
	90.9	547.0	551.8
DPP/DPPmF	7.0	534.9	540.0
	13.0	528.9	531.5
	23.1	537.2	535.6
	37.5	504.7	542.8*
	50.0	545.8	544.5
	62.5	537.3	543.9
	76.9	539.6	547.0

*heating rate: 20 °C/min., purging gas: nitrogen

References:

1. Cowie, J. M. G., *Polymers: Chemistry & Physics of Modern Materials*, 2nd, Chapman and Hall, New York, **1991**. p325.
2. Young, R. J. and Lovell, P. A., *Introduction to Polymers*, Chapman & Hall, **1991**. p297.
3. Cowie, J. M. J., *Polymers: Chemistry & Physics of Modern Materials*, Chapman & Hall, **1991**, p269.
4. Shen, M. C. and Eisenberg, A., Glass Transitions in Polymers, Reprinted from *Rubber Chem. & Tech nology*, Vol. 43, No.1, **1970**, p285.
5. Wunderlich, B., *Macromolecular Physics*, Academic Press, **1980**, Vol. 3., Ch. X, p254.
6. Miller, M. L., *The Structure of Polymers*, Reinhold Book Corp., **1968**, p534.
7. Cowie, J. M. J., *Polymers: Chemistry & Physics of Modern Materials*, Chapman & Hall, **1991**, p268.
8. Flory, P. J., *Trans. Faraday Soc.*, **1955**, 51, 848.
9. Natta, G., *Die Makromolekulare Chemie*, **1959**, 35, 94.
10. Allegra, G and Bassi, I. W., *Adv. Polym. Sci.*, **1969**, 6, 549.
11. Natta, G., Corradini, P., Sianesi, D. and Morero, D., *J. Polym. Sci.*, **1961**, 51, 527.
12. Natta, G., Allegra, G., Bassi, I. W., Sianesi, D. and Caporiccio., and Torti, E., *J. Polym. Sci.*, **1965**, 3, 4263.10.
13. Kapuscinska, M., Pearce, E. m., Chung, H. F. M., Ching, C. C. and Zhou, Q. X., *J. Polm, Sci, Chem. Ed.* **1984**, 22, 3999.

substituted 2,6-diphenylphenols in hand, from which a series of substituted tetraphenyl-p,p'-biphenols through path B could be readily prepared (scheme 7.1). The preparation of the corresponding polymers from these substituted monomers would allow us to examine their properties. Of particular interest would be the property variations induced by fluoro substitution which we observed previously in the P3O system, and the properties of the t-butylated system which was unexpected in the P3O series.

Scheme 7.1

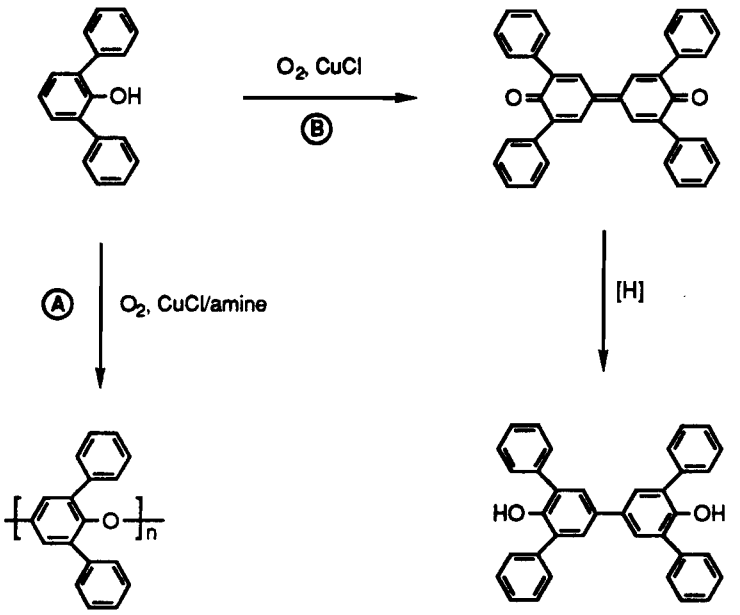

7.2. RESULTS AND DISCUSSIONS

7.2.1. Preparation of Substituted 2,2',6,6'-Tetraphenyl-4,4'-biphenols

The synthesis of substituted tetraphenylbiphenols was carried out by using the published procedure for the preparation of tetraphenyl-p,p'-biphenol[5]. The precursors, substituted 2,6-diphenylphenols were prepared by the procedures described in chapter 2. The substituents studied are t-butyl and fluoro group. The experimental details are outlined in the experimental section.

Scheme 7.2

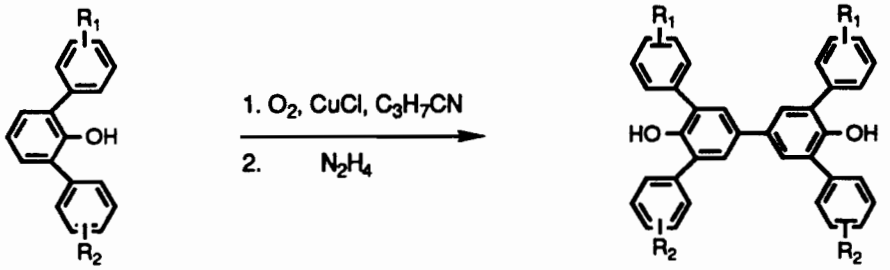

7.2.2. Polymer Preparation and Properties:

The polymerization of these substituted tetraphenyl-p,p'-biphenols was carried by the reported procedure[6]. The poly(ether sulfone)s were prepared by reacting the biphenols with 4,4'-difluorophenylsulfone and poly(ether ether ketone)s by reacting the biphenols with 4,4'-difluorobenzophenone, respectively (scheme 7.3). The identical reaction conditions were used for both poly(ether sulfone)s and poly(ether ether ketone)s. The concentration of reactants used was 20 % by weight and the reactions were carried out on 2 mmole scale, using 30% excess of base with NMP as solvent. Because of the high steric hindrance of the phenoxide ion in this system, higher temperature and much longer reaction time must be used than for unhindered phenol systems in order to obtain high molecular weights. The experimental procedure is described in the experimental section.

Homogeneous solutions were maintained throughout the polymerization reactions for all of the attempted polymerizations. The relatively lower molecular weight of the t-butylated polymers (table 7.1) might be caused by insufficient purity of the monomers which are not readily purified by crystallization.

Scheme 7.3

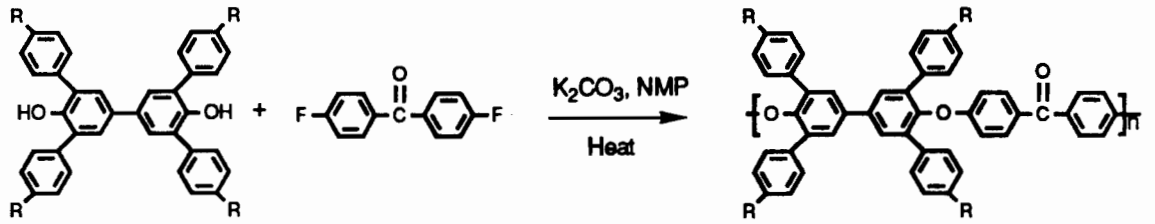

Poly(ether ether ketone) **PEEK**

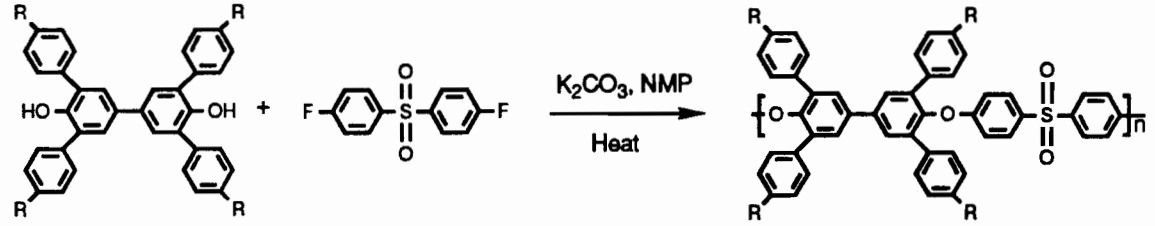

Poly(ether sulfone) **PS**

The DSC results showed that all the Tg's of the **PS** are about 20 °C higher than those of **PEEKs**. The Tg's of the t-butylated polymers are about 30 °C higher than those of the fluorinated polymers which is most likely due to a crankshaft effect due to the large t-butyl groups.

Table 7.1. Substituted Poly(ether sulfone)s and Poly(ether ether ketone)s[a]

Polymer	R	X	Tg, °C[b]	η_{inh}, dL/g[c]	Reaction Temp.°C	Reaction Time	Yield, %
P1	t-Bu	SO_2	299	0.24	175	3 days	67
P2	F	SO_2	272	0.71	185	4 days	65
P3	t-Bu	CO	282	0.18	175	45 h	64
P4	F	CO	253	0.45	185	3 days	53

a:

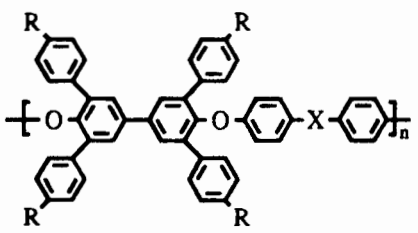

b: Heating rate: 10 °C/min.

c: Tested at 25 °C in 0.5% $CHCl_3$ solution.

In view of the insolubility and high crystallinity of the unsubstituted poly(ether ether ketone)s from unsubstituted tetraphenylphenol[4], the most interesting observation is that the poly(ether ether ketone)s from both fluoro and t-butylated biphenol are very soluble. This effect from t-butylation is expected and is well documented in the literature[7,8], and has been interpreted to steric effects. Obviously, steric factors would not be the case for fluoro substitution due to very similar size of fluorine and hydrogen. In both cases there is a profound property change since totally amorphous polymers result from fluoro and t-butyl substitution. Steric factors can explain the result from t-butyl substitution which leads to significantly structural variation, however fluoro substitution must involve a different mechanism since the very small size of fluorine would not likely account for such dramatic property change. Even annealing the polymer failed to induce any crystallinity in fluorinated **PEEK**. The above observation led us to assume that the weakened chain interaction resulting from the presence of fluorine described previously could result in the elimination of the crystallinity due to the fluoro substitution.

We further studied this fluoro substitution effect on the properties of poly(ether ether ketone)s by designing fluorinated polymers **P5** and **P6** as structural derivative of **P4** as shown in scheme 7.4.

Scheme 7.4

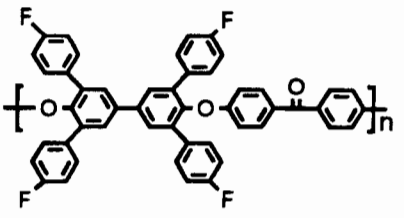

P 4

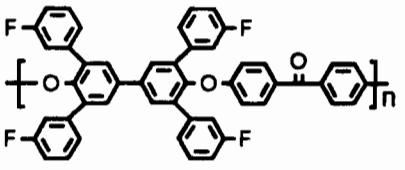

P 5

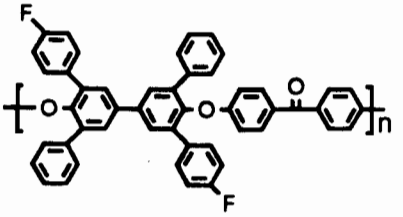

P 6

Table 7.2. Fluoro Substituted Poly(ether ether ketone)s

Polymer	Tg, °C[a]	Tm, °C[a]	η_{inh}, dL/g[b]	Reaction Temp.°C	Reaction time	Yield, %
P4	253	amorph.	0.45	185	3 days	53
P5	221	amorph.	0.18	185	4 days	62
P6	-	392	insol.	185	20 h	69

a: Heating rate: 10 °C/min. b: Tested at 25 °C in 0.5% $CHCl_3$ solution.

The results are listed in table 7.2 and **P4** is also included for comparison. The attempted preparation of **P5** only gave low molecular weight polymer which remained soluble throughout the reaction. In the preparation of **P6**, oligomer precipitated from solution at an early stage of reaction. DSC studies indicated that **P5** is an amorphous material which is similar to **P4** described previously. However **P6** is highly crystalline without a detectable glass transition but a melting endotherm. This explains the insolubility of the material. The results indicated that the effects of enhancing solubility and depressing crystallinity occur when fluorine is in the meta or para positions on all four pendant rings. When only two of the four pendant phenyl rings are substituted with fluorine, the polymer remains highly crystalline.

7.3. SOLUBILITY BEHAVIOR

The fluorinated polymers prepared are not only soluble in the reaction medium but also in common organic solvents, and even in some ketone solvents which is unusual for this type of highly rigid polymer system. A brief solubility test was conducted for the fluoro substituted polymer **P2**, **P4** and **P5** and the unsubstituted poly(ether sulfone)[4] and poly (ether ether ketone)[4] was included for comparison.

Table 7.3. Solubility of Fluorinated Poly(ether sulfone)s and Poly(ether ether ketone)s*

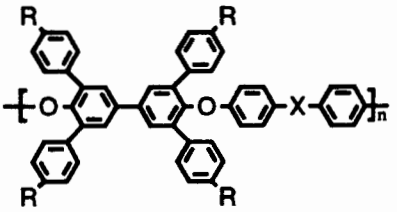

	Unsubstituted Polymers		Fluoro Substituted Polymers		
	1	2	3	4	5
Solvent	R=H, X=CO	R=H, X=SO_2	R=p-F, X=SO_2	R=p-F, X=CO	R=m-F, X=CO
chloroform	-	+	+	+	+
toluene	-	-	s	s	+
acetone	-	-	s	s	+
MeCOEt	-	-	+	+	+
ethyl acetate	-	-	s	+	+
nitromethane	-	-	s	-	-
MeCN	-	-	-	-	-
2-propanol	-	-	-	-	-
hexane	-	-	-	-	-

* Test was conducted at room temperature. (+) = soluble, (-) = insoluble, (S) = swollen.

The results tabulated in the above table show that the fluorinated polymers generally have better solubility than their unsubstituted analogs. The fluorinated polymers in this series are more soluble in ketone solvents, such as acetone and ethyl acetate. This behavior is similar to what we have already observed in the fluorinated P3O series. The introduction of solubility into the highly crystalline **PEEK** by fluoro substitution corresponds with the elimination of the crystallinity in the polymer. However, the comparison of unsubstituted poly(ether sulfone) and the fluoro substituted poly(ether sulfone), both of which are amorphous, revealed that the fluoro substitution improves solubility considera-

bly (table 7.3. colum 2 & 3).

7.4. THERMAL STABILITY

Table 7.4 listed the results of thermal stability of the prepared polymers from thermopgravimetric analysis. The fluoro substituted polymers show higher stability in either inert gas or air. This is apparently related to the high C-F bond strength. The aliphatic t-butyl substituted polymers tend to undergo thermolysis or oxidation at lower temperatures and show lower stability than fluoro substituted polymers.

Table 7.4. Stability of Substituted Poly(ether sulfone)s and Poly(ether ether ketone)s[a]

R	t-Bu	t-Bu	p-F	p-F
X	SO_2	CO	SO_2	CO
T5, °C(N_2)	509	517	528	543
T5, °C(Air)	477	489	512	540

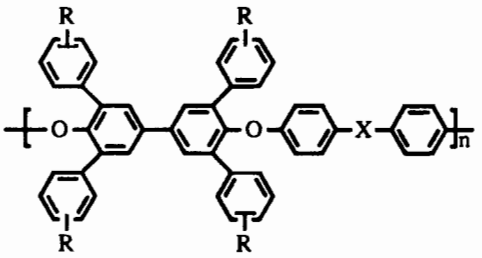

T5: Temperature at 5% weight loss

a: Heating rate: 10 °C/min.

7.5. CONCLUSION

In this study, we have observed that a highly crystalline and rigid polymer becomes totally amorphous by attaching fluorine onto the pendant phenyl rings. The presence of fluorine on the pendant phenyl rings also leads to considerable improvement in solubility. These profound property changes could not be explained by dimensional factors from fluoro substitution since fluorine is only slightly larger than hydrogen. Therefore, we assume the effect is due to the weakened chain cohesion by the presence of fluorine which leads to crystallinity depression and solubility improvement.

7.6. EXPERIMENTALS

Monomer Synthesis

General Procedure: 2,2',6,6'-tetra-(4-fluorophenyl)-p,p'-biphenol 2 To a three neck 250 mL flask equipped with oxygen inlet and magnetic stirrer, were combined 2,6-bis(4-fluorophenyl)phenol (8.46 g, 30 mmole), butyronitrile (100 mL) and CuCl (0.75 g). With magnetic stirring and oxygen bubbling, the temperature was raised to 100 °C . A red color rapidly developed and a brown colored solid separated out of the solution during the reaction. The reaction was allowed to continue overnight and TLC showed complete conversion of the phenol. The mixture was cooled and the solid was collected by filtration and redissolved in chloroform (100 mL) and anhydrous hydrazine (0.5 mL) was added. The mixture was refluxed for 10 min to give a light yellow colored solution. The inorganic solid was removed by filtration. The solution was washed with hydrochloric acid (20%, 150 mL) and water (2x100 mL) and dried ($MgSO_4$). The solvent was removed at reduced pressure and the yellow solid was dissolved in hot chloroform-hexane and put in the refrigerator overnight. The product was collected by filtration and dried in a vacuum oven at room temperature to afford the product as light yellow crystals. The yields, reaction conditions and analytical data are listed in table 7.5 and table 7.6.

Table. 7.5. Substituted 2,2',6,6'-Tetraphenyl4,4'-biphenols from 2,6-Diarylphenols

Biphenol	R_1	R_2	m.p. (°C)	Reaction Time	Yield, %	Purification*
1	p-t-Bu	p-t-Bu	>300	16 h	50	AcOH-$CHCl_3$
2	p-F	p-F	219-220	16 h	79	$CHCl_3$-Hexane
3	m-F	m-F	176-177	30 h	46	$CHCl_3$-Hexane
4	p-F	H	179-180	30 h	37	$CHCl_3$-Hexane

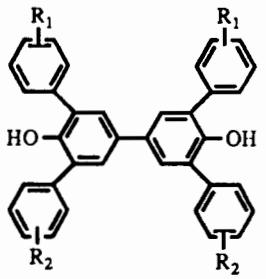

* Crystallization solvents.

Table 7.6. Analytical Results for Substituted Tetraphenyl-4,4'-biphenols

Biphenol	Microanalysis		MS m/e (70eV)	^{1}H NMR ($CDCl_3$/TMS)
	Calc.	Found		δ, (mult., *J* Hz)
1	C, 87.35	C, 87,29	715(M+, 20.8)	1.37(s, 36 H, t-Bu), 5.48(s, 2 H, OH),
	C, 8.18	H, 8.17	357(1/2M^+,)	7.51(d, 20 Harom).
2	C, 76.85	C, 76.55	562(M^+, 100),	5.24(s, 2 H, OH), 7.47(s, 4 Harom),
	H, 3.94	H, 3.89	281(1/2M+, 18.9).	7.13-7.25 (m, 8 Harom),
				7.52-7.59 (m,8 Harom).
3	C, 76.86	C, 76.19	562 (M^+, 100),	5.38(s, 2 H, OH),
	H, 3,94	H, 4.08	281 (1/2M^+, 18.5)	7.06-7.51(m, 20 Harom).
4	C, 82.11	C, 82.56	526(M^+, 100),	5.35(s, 2 H, OH),
	H, 4.59	H, 4.87	263(1/2M^+, 5.17).	7.11-7.62(m, 22 Harom).

General Procedure for Polymerization:

Poly(ether sulfone) P_2 from fluorinated biphenol **2** In a three neck 25 mL round bottom flask equipped with a Dean Stark trap, argon inlet and condenser, were combined 2,2,6,6-tetra-(4-fluorophenyl)-4,4'-biphenol (1.124 g, 2 mmole), 4,4'-difluorodiphenylsulfone (0.509 g, 2 mmole), NMP (6 mL, distilled) and toluene (6 mL, degassed). The flask was put in an oil bath . To the yellow colored solution, anhydrous potassium carbonate (0.36 g, 30% excess) was added and the temperature raised. A dark green color developed in the solution and when the temperature reached 160 °C, reflux began. In the next 4 hours, the temperature was raised to 180 C° and three portions of toluene (5 mL, degassed) were added to remove the water completely. The reaction temperature was maintained at 185 °C. In the first day, only a fine powder was obtained by precipating a small portion of polymer solution dropwise into methanol. At the second day, the solution viscosity began to increase and at the third day, a high molecular fibrous polymer was obtained by adding the solution into methanol. The reaction was stopped at the 4th day and the mixture was

cooled to 80 °C and diluted with $CHCl_3$ (15 mL). The resultant solution was added to methanol-dilute hydrochloric acid solution (3:1, 100 mL) dropwise and stirred for 2 hours. The polymer was collected by filtration and redissolved in 20 mL of $CHCl_3$. The solution was filtered through celite (1 cm) and the filtrate was added to methanol (100 mL) and stirred for 2 hours. The polymer was collected by filtration and dried at 110 °C under vacuum for 1 day. 1.0 g of polymer with a light brown color was obtained (65%).

References:

1. Hay, A. S., *Macromolecules*, **1969**, 2, 107.

2. Hay, A. S., *J. Polym. Sci.*, **1962**, 58, 581.

3. Endres, G. F., Hay, A. S. and Eustance, J. W., *J. Org. Chem.*, **1963**, 28, 1300.

4. Kim, W. G., and Hay, A. S., *Polym. Prepr.*, **1991**, 32, 389.

5. Hay, A. S. *J. Org. Chem.*, **1971**, 36, 218.

6. Viswanathan, R., Johnson, B. C. and McGrath, J. E., *Polymer*, **1984**, 25, 1827.

7. Mohanty, D. K., Lin, T. S., Ward, T. C., and McGrath, J. E., *Int. SAMPE Symp. Exp.* **1986**, 31, 945.

8. Fenoglio, D.J. and Foster, J.J., *J. Polym. Sci. Polym. Chem. Ed.*, **1990**, 28, 2753.

CHAPTER 8

MODIFICATION OF P3O BY THERMAL CROSS-LINKING REACTIONS

8.1. INTRODUCTION

Poly-2,6-diphenylphenylene ether (P3O) is characterized by very high thermal stability due to the totally aromatic polymer backbone, excellent electric properties, high impact strength, and a high softening temperature[1]. But many potential applications of this material are largely limited due to the very high melting point which is close to the decomposition temperature making melt processing impossible[2]. In the previous studies, we demonstrated that substitution on the pendant phenyl rings can reduce the melting point of the polymers to such an extent that melt processing is feasible around 400 °C.

Here we describe an alternative approach to obtaining bulk state processable P3O through a controlled thermal cross-linking reaction. Considering the two phase nature of P3O, a logical approach to reduce the softening point appears to be the elimination of crystallinity. The resulting amorphous form of P3O would be amenable to melt processing. However, with the elimination of crystallinity, loss of mechanical properties would occur near the glass transition temperature and the solvent resistance imparted by crystallinity would be eliminated. By analogy to the physical cross linking in the presence of crystalline domains in a polymer matrix, the inter-molecular chemical cross-link has been recognized as having similar effects in terms of strengthening the polymer matrix at elevated temperature and improving solvent resistance[3-5].

So a possible solution would be to start with an inherently amorphous P3O in which there is incorporated thermally cross-linkable functionality which would be melt processable followed by thermal cross-linking. To design such a system, two requirements must be met: elimination of most or all of the crystallinity to ensure adequate softening and processability above Tg; the cross-linking reaction should occur above the melt processing temperature (for amorphous materials, processing temperature is usually 100 °C above the Tg). From previous results on P3O copolymers, it is indicated that approximately 10 % mole of foreign units incorporated into the P3O backbone will be sufficient

to give an essentially amorphous polymer. So it was expected that incorporating 5 to 10 % mole of a monomer bearing a cure site into P3O polymer would largely eliminate crystallinity in the resulting copolymers.

The temperature range of cross-linking is a more critical parameter. Among the variety of cure functionalities used in thermosets, the acetylene group has been employed to cross-link and/or extend polymer chains for many different polymer classes including polyimides[6,7] , poly(aryl ether sulfones)[8,9] , polyesters[10], and poly(phenylquinoxalines)[11].

Table 8.1. Curing Temperature of Model Compounds

Model Compound	Endothermic peak (°C)	Exothermic peak (°C)	ΔH (kcal/mole)
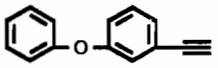	Liquid at 26°C	259	-37.0
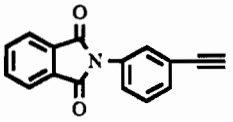	212	255	-38.6
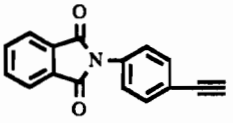	170	249	-37.4
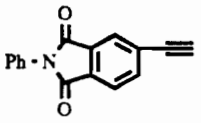	217	239	-38.8
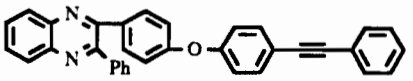	155	385	-
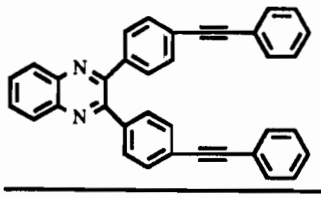	220	403	-

One of the advantages of the acetylenic moieties as cure sites is that no volatile by-products are evolved during it's cure cycle, resulting in a void-free polymer structure. The thermally induced reaction of an alkyne group is extremely complex and can yield a variety of products such as aromatics, dimers and polymeric materials[12]. But the cross-linking reaction temperatures generally correlate with the type of alkyne moiety used, which has been described in a review by Hergenrother[13] (table 8.1). It was shown that ethynyl-substituted compounds give exothermic maxima in a range from 240 to 280 °C while phenylethynyl-substituted derivatives give exothermic maxima near 400 °C.

Based on the above considerations, we attempted to design a P3O polymer incorporating a certain amount of monomer bearing either an ethynyl or phenylethynyl group as shown below. The resultant polymers could be cured at a variety of temperatures based on the correlation described in table 8.1. We intended to incorporate a small percentage of these functional monomers (5 & 10 %mole) into P3O. The content of functional co-unit in this range hopefully will be enough to eliminate crystallinity and at the same time avoid extensive cross-linking due to high content of cure sites which would result in brittleness of the resultant polymers and thus maintain the inherent high impact strength of P3O.

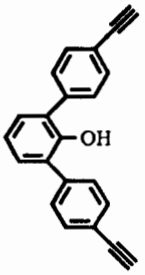

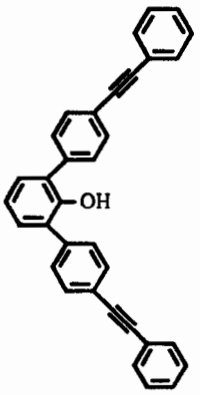

8.2. POLYMER PREPARATION

A. Monomers

The introduction of ethynyl and phenylethynyl groups onto 2,6-diphenylphenol was carried out by reacting 2,6-di(p-iodophenyl)phenol with trimethylsilylacetylene or pheny-

lacetylene by a palladium catalyzed coupling reaction which is outlined in scheme 8.1.

Scheme 8.1

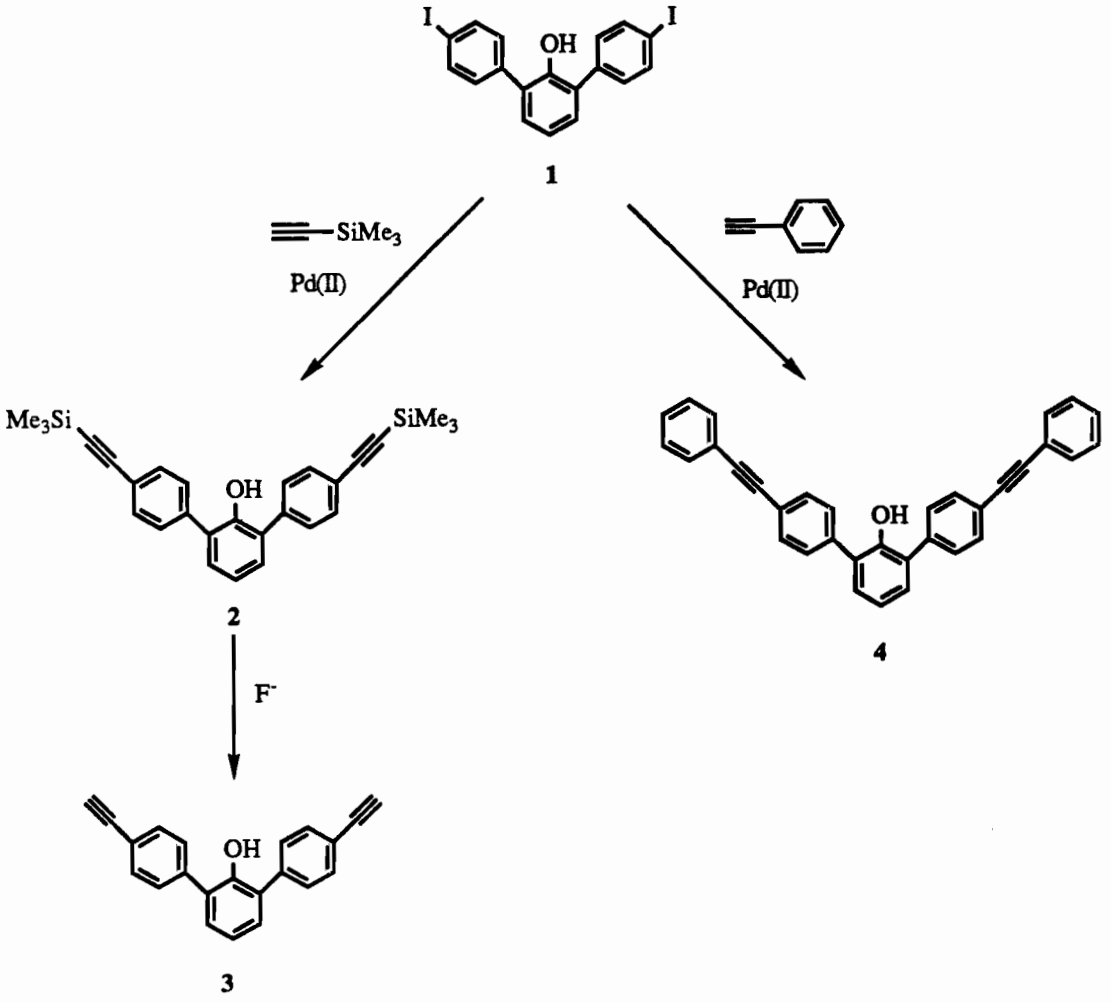

B. Polymers

The alkynyl functionalized monomers were incorporated into P3O by copolymerization with 2,6-diphenylphenol, **DPP**. Either 5 or 10 % mole of the functional monomers were used in the copolymers.

Since the ethynyl group will interfere with the polymerization, **TMS** protected monomer **2** was subjected to copolymerization with **DPP**. The protecting group was subsequently removed by treating the resultant copolymers with tetrabutylammonium fluoride in THF yielding cure precursors **PE5** (5% mole of ethynyl-substituted monomer) and **PE10** (10% mole of ethynyl-substituted monomer).

Scheme 8.2

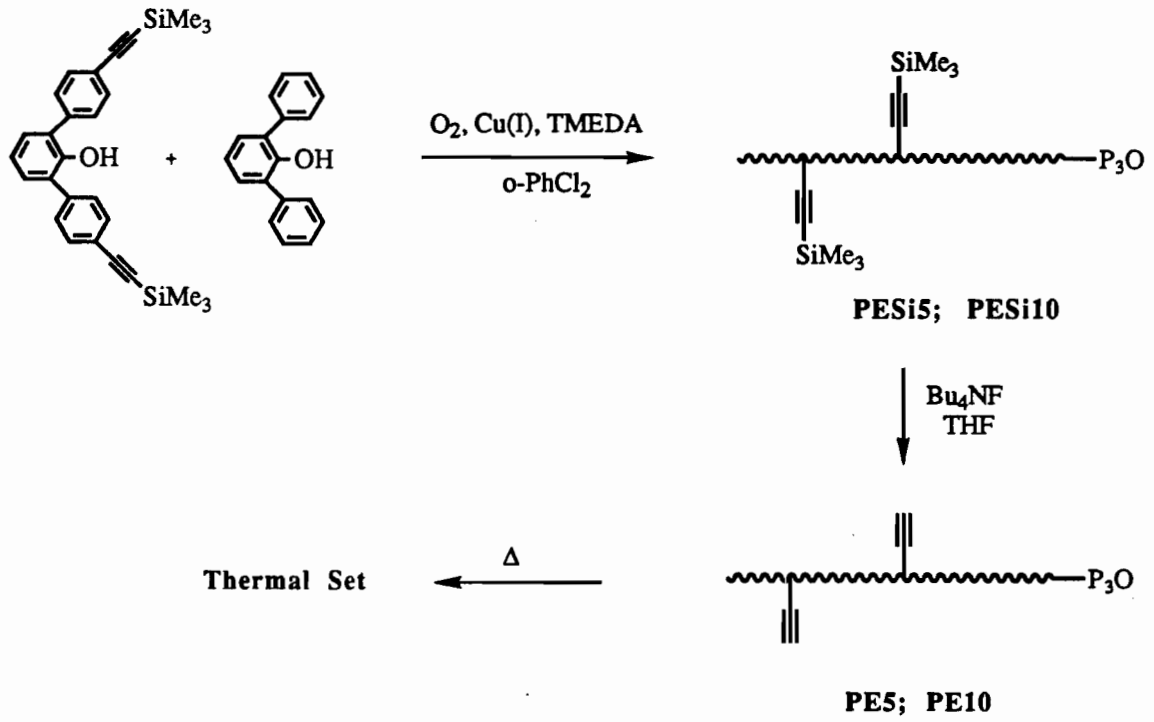

The phenylethynyl-substituted monomer can be directly incorporated into P3O by simultaneous oxidation of a mixture of 2,6-diphenylphenol (**DPP**) and phenylethynyl-substituted monomer **4** and the resulting copolymers **PϕE5** (5% mole of **4**) and **PϕE10** (10% mole of **4**) were then subjected to thermal curing.

Scheme 8.3

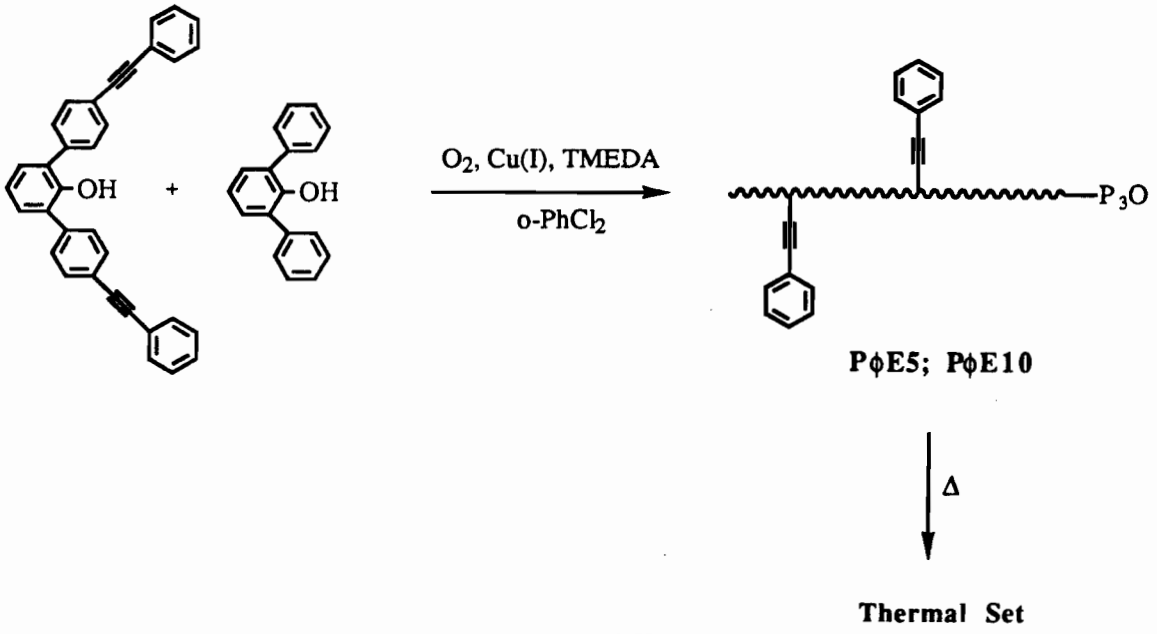

8.3. CROSS-LINKING IN P3O POLYMERS

A DSC trace of monomer **3** (fig. 8.1, curve a) displays a sharp melting endotherm at 179 °C and a broad exotherm due to reaction of the ethynyl group which commences in the melt region and peaks at 227 °C. A DSC trace of monomer **4** (fig.8.1, curve b) shows a melting endotherm at 154 °C and a reaction exotherm onset near 345 °C peaking at 392 °C. From this data, it is indicated that the polymer bearing phenylethynyl groups could survive a much higher temperatures than the ethynyl substituted analog. The actual onset temperature of cross-linking reaction for the corresponding polymers would be expected to be further increased due to the restricted mobility and much lowered density of cure sites in the polymer systems.

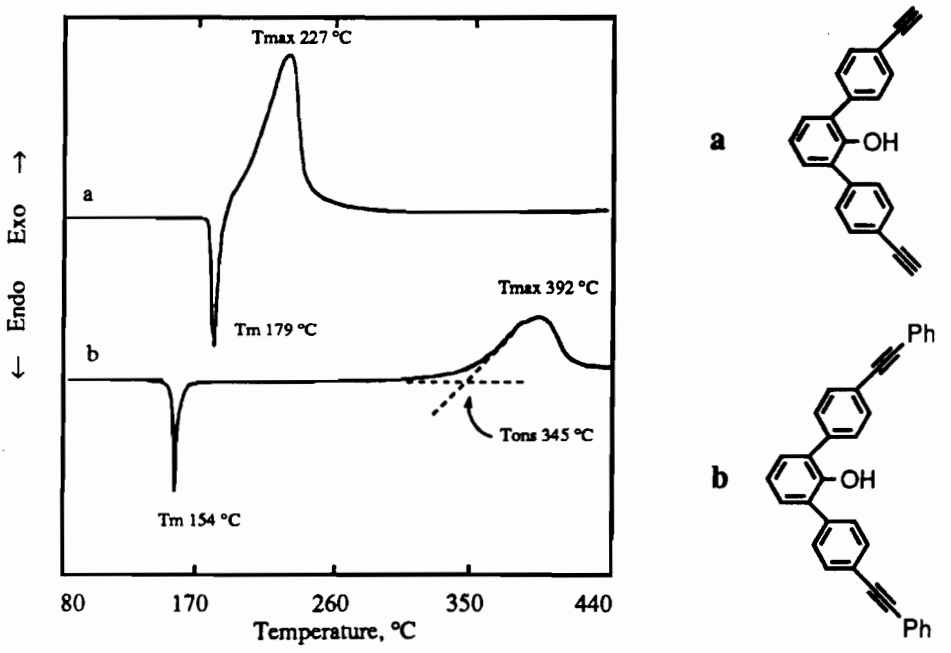

Fig 8.1. DSC traces of monomer containing acetylene
Heating rate: 20 °C/min.

A. Copolymer Bearing Ethynyl Group

Table 8.2 lists the transition temperatures and reaction exotherms from DSC scans of as-made samples **PE5** and **PE10**. The onset temperature of the cross-linking reaction was found in the same region as Tg and reached a maximum near 280 °C. The exothermic maximum for both **PE5** and **PE10** are about 50 °C higher than the corresponding monomers. The much broader thermal reaction temperature range of **PE5** (fig.8.2, curve a) and **PE10** (fig.8.3, curve a) arises from much more restricted mobility in the polymer system than in the small molecules. We found that 5% of comonomer **3** in the P3O backbone (**PE5**, fig.8.2, curve a) does not suppress crystallinity efficiently and a melting endotherm was detected at 401 °C.

Table 8.2. Thermal Behavor of P3O Bearing Ethynyl Group[a]

Copolymer	Tg,°C,	Tc,°C	Tonset,°C	Tmax,°C	Tm,°C
PE5	229	-	230	287(227[b])	401
PE10	230	-	230	276(227[b])	-

a: Heating rate: 20 °C/min. b: Tmax of ethynyl substituted monomer **3**.

The cure experiments for sample **PE5** are shown in figure 8.2. Both curing at 290 °C for 2 h (curve b) and 350 °C for 1 h (curve c) cause the glass transition temperature to shift up to 255 °C and 266 °C, respectively, and significant decreases in intensity. In addition, the increases in melting endotherms indicates that crystallization also occurs upon thermal treatment. This suggests a competitive process between cross-linking and crystallization upon thermal treatment. So the increase in Tg might be attributed to both increased crystallinity and cross-linking formation in the system.

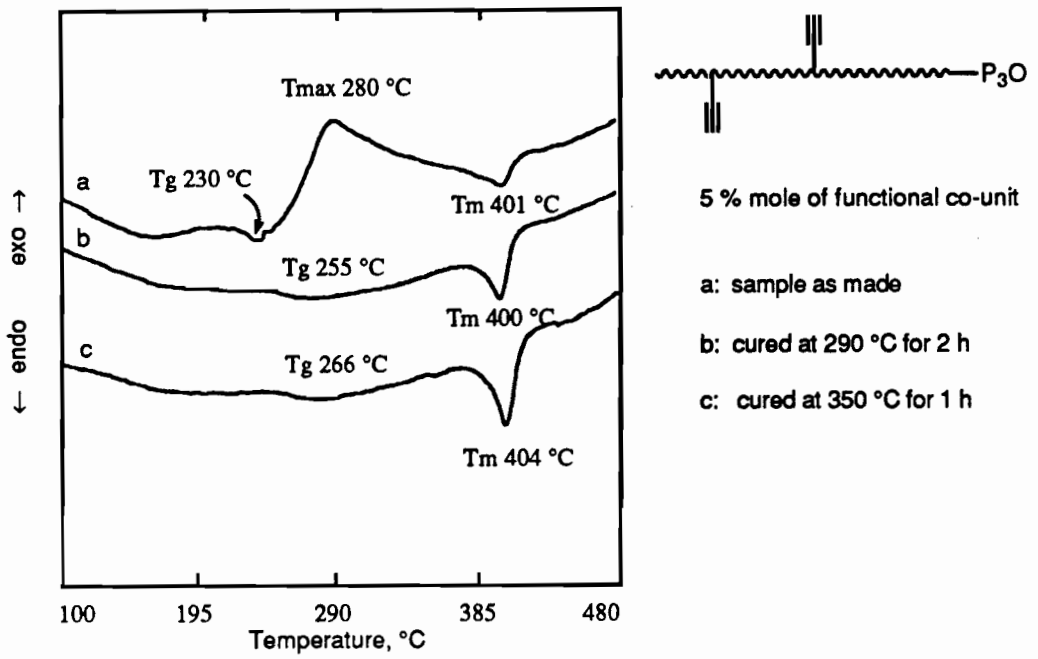

Fig 8.2. DSC traces of cured **PE5** samples (heating rate: 20 °C/min):

The cure experiments on **PE10** studied by DSC are shown in figure 8.3. The amorphous nature of as-made sample **PE10** was confirmed by the absence of a melting endotherm (curve a). Curing at 260 °C (T_{ons}) resulted in a glass transition temperature shift from 230 °C to 274 °C (curve b). Curing at 350 °C gave no evident glass transition (curve c) which indicated intensive cross-linking in the sample.

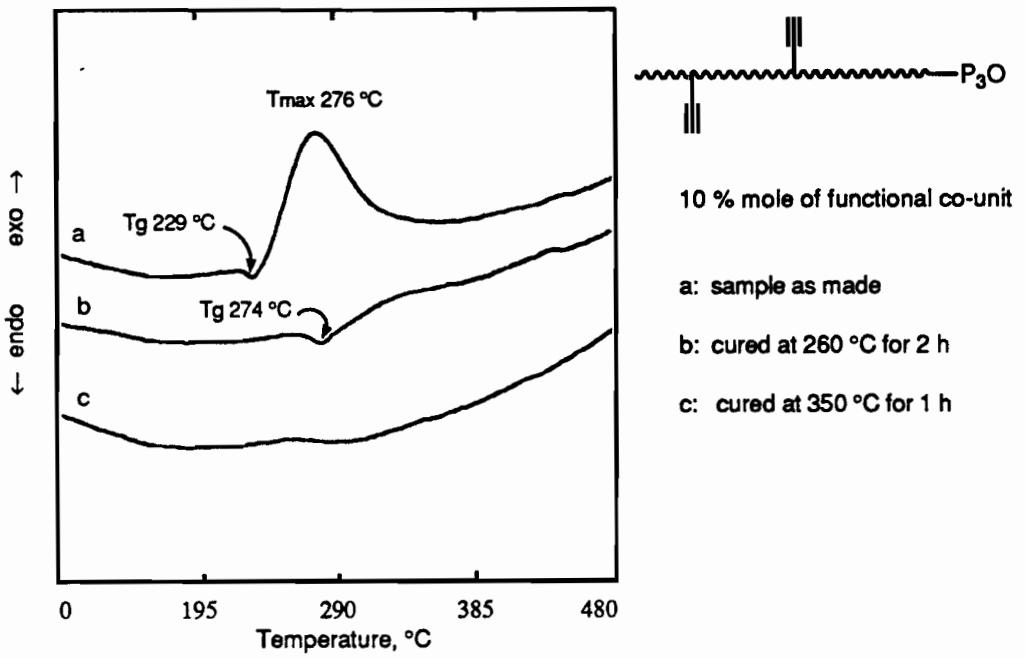

Fig. 8.3. DSC traces of cured PE10 samples (heating rate: 20 °C/min):

B. Copolymer Bearing Phenylethnyl Groups:

Table 8.3 lists the transition temperatures and reaction exotherms from DSC scans for as-made samples **PϕE5** and **PϕE10**. The inherently restricted mobility in the polymer systems caused an approximately 30 °C up-shift of Tmax compared to the corresponding phenylethynyl-substituted monomers.

Table 8.3. Thermal Behavior of Copolymer Bearing Phenylethynyl Group[a]

Copolymer	Tg,°C,	Tc,°C	Tonset,°C	Tmax,°C	Tm,°C
PϕE5	203	284	400	420(392[b])	420
Pϕ10	215	-	379	418(392[b])	-

a: Heating rate: 20 °C/min. b: Tmax of phenylethynyl substituted monomer.

The DSC scan of as made sample **PϕE5** shows that this sample readily crystallizes at 284 °C with a crystallization exotherm and melts at 420 °C (fig. 8.4, curve a). In this

case, the crystallization in **PEϕ5** proceeded without competition from cross-linking due to the much higher onset temperature of cross-linking (400 °C) and the cross-linking reaction commences in the melting region where the mobility restriction is removed.

The scan for **PϕE5**, cured at 380 °C for 2 hours (20 °C below the onset of Tm), showed a melting endotherm peaking at 435 °C and the cross-linking reaction commencing in the melting region (curve b) with intensity similar to its precursor (curve a). The insufficient cross-linking by this curing is believed to result from the restricted mobility due to the crystallization in the system. By raising the curing temperature to the onset of melting (400 °C, 2 h) with the expected removal of the mobility restriction, the resulting sample gave a melting endotherm at 420 °C without further cross-linking reaction which was indicated by the symmetrical melting peak (curve c). Again, the disappearance of glass transition from the curing treatments might be attributed to both crystallinity and cross-link formation in the systems.

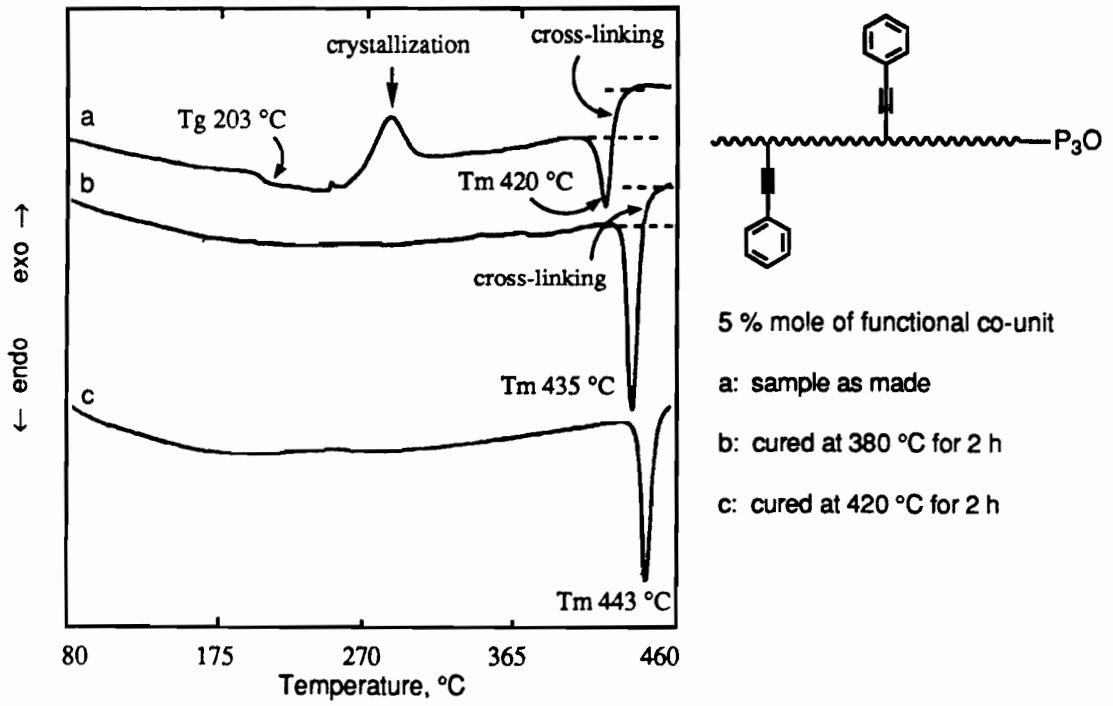

Fig. 8.4. DSC traces of cured **PEϕ5** samples (heating rate: 20 °C/min):

By incorporating 10 mole% of phenylethynyl substituted monomer into P3O, the resultant polymer, **PϕE10**, is largely amorphous. This is indicated by the DSC scan which shows a small and wide bump for a very limited crystallization exotherm (fig. 8.5, curve a). The cross-linking reaction commences at 380 °C (Tons) and reaches a maxima at 420 °C. Both curing at Tons 380 °C for 2 hours (curve b) and Tmax 420 °C for 1 hour (curve c) gave similar DSC curves with no evident glass transition but ill defined transitions over a wide temperature range at higher temperature. We believe in our case that the higher curing temperature resulted in a relatively high cross-link density in the system which led to no evident glass transition in the DSC scan.

Since no crystallization is involved in this system, the cross-linking reaction appears to be the only process upon thermal treatment under the above curing conditions.

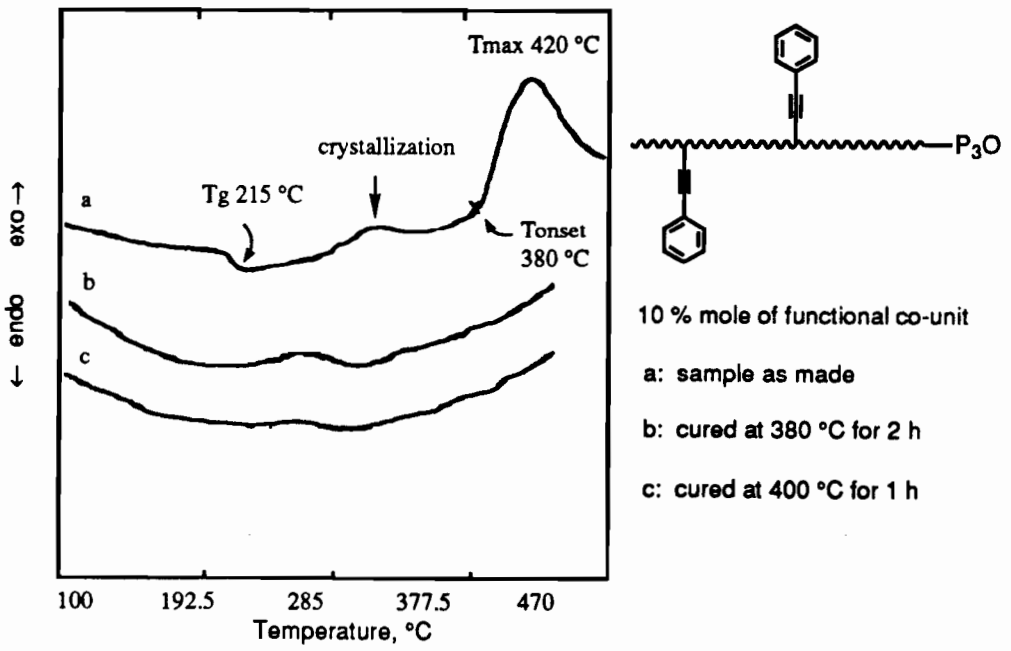

Fig. 8.5. DSC traces of cured **PEϕ10** samples (heating rate: 20 °C/min)

8.4. CONCLUSION

We have designed a system which is capable of cross-linking under curing. By incorporating different types of functional monomers into the P3O polymer, systems are formed which are capable of undergoing thermal curing in either low or high temperature ranges. This provides the possibility that the modified P3O could be processed from both solution and melt. By starting with preformed high molecular weight precursors for curing and a relatively low density of reactive sites on the polymer, the intensive cross-linking associated brittleness is avoided.

Experimental:

The copolymers **PE5**, **PE10**, **PEϕ5** and **PϕE10** were prepared on a 1.5 g scale according to the previously described procedure in chapter 3. The general procedure for the deprotection of the ethynyl group for samples **PE5** and **PE10** is described in the following:

To a solution of copolymer PE10 (1.0 g) in tetrahydrofuran (30 mL), was added 3 equivalents of tetrabutylamonium fluoride monohydrate (per ethynyl function), and the resultant solution was stirred at room temperature for 8 h. The solution was concentrated under reduced pressure to 2/3 volume and added dropwise into methanol (150 mL). The fibrous polymer was dissolved in chloroform (100 mL), washed with water (2 x 100 mL) and dried ($MgSO_4$). The solution was concentrated to approximately 20 mL and precipitated into methanol (100 mL). The polymer was collected as white fiber and dried in a vacuum oven at 80 °C for 24 h, 0.8 g product was obtained.

Reference:

1. Hay, A. S., *Macromolecules*, **1969**, 2, 107; Hay, A.S., **U.S. 1969**, 3,432,466.

   Wrasidlo, W., *Macromolecules*, **1971**, 4, 642.

   Vermeer, J., Boone, W., Bussink, J., and Breakel, H., ***1970 Annual Report, Conference on Electrical Insulation and Dielectric Phenomena***, NAS Publ. p52. **CA**. 153114p, **1971**, 75.

   Technical Bulletin No. 24., Applied Science Laboratories, Inc. State College, Pennsylvania, 16801.

2. Hay, A. S., and Dana, D. E., *J. Polym. Sci. Polym. Chem. Ed.*, **1989**, 27, 873.

3. Hergenrother, P. M., *Chemistry and Properties of Cross-linked Polymers*, Edited by Labana, S. S. Acad. Press., New York, **1977**, 107.

4 Temin, S. C., J. Macromol. Sci-Rev., *Macromol. Chem. Phys.*, **1982-1983**, C22(1), 143.5.

5. Harris, F. W., and Spinelli, H. J., *Reactive Oligomers*, Washington D.C., **1985**.

6. Hergenrother, P. M., *Encyclopedia of Polymer Science and Technology*, Wiley, New York, **1985**, 1, 61.

7. Harris, F. W., Podaki, S. M., and Varaprath, S., *Polym. Prepr.*, **1980**, 21(1), 3.

8. Lucotte, G., Cormier, L., and Delfort, B., *J. Polym. Sci. Chem. Part A: Polym. Chem.*, **1991**, 29, 897.

9. Huang, F., and Marvel, C. S., *J. Polym. Sci. Polym. Chem. Ed.*, **1976**, 14, 2787.

10. Havens, S. J., Moore, Hergenrother, P. M., ACS. *Polym. Prepr.*, **1983**, 24(2), 16.

11. Hedberg, F. L., Lindley, P. M., Lee, C. Y-C., and Golafarb, I. J. *J. Polym. Sci. Polym. Chem. Ed.*, **1982**, 20, 3069.

12. Swanson, S. A., Fleming, W. W., and Hofer, D. C., *Macromolecules*, **1992**, 25, 582.

13. Hergenrother, P. M., J. Macromol. Sci.-Rev. *Macromol. Chem.*, **1980**, C19(1), 1.

Contribution to Knowledge

Modifications of poly(2,6-diphenylphenylene ether) (P3O), to attain reduced melting temperatures and therefore, melt processability, are described.

In first part of the thesis, the synthesis of a series of symmetrically substituted 2,6-diphenylphenol monomers with substituents on the pendant phenyl rings have been investigated. Three different synthetic approaches toward the target monomers have been examined depending on the the nature of the substituents to be introduced. They included center phenolic moiety formation by the condensation between substituted dibenzyl ketones and 1,3-dibromopropane and the subsequent aromatization of the obtained cyclohexanone to the target phenols; direct introduction of substituents as electrophiles by electrophilic substitution at the para position of pendant phenyl rings of protected 2,6-diphenylphenol which is subsequently deprotected to furnish the target phenols; or direct aromatic framework formation by a cross-coupling reaction of bromophenols with substituted arylboric acids.

In the second part, a series of substituted homopolymers and random copolymers have been prepared by oxidative polymerization from the above monomers. Some of the homopolymers are low molecular weight because the intermediates are insoluble due to the high crystallinity. High molecular weight has been achieved for the corresponding copolymers where the crystallinity was decreased by increasing the content of the comonomers.

The third part describes a study of the thermal properties, transition temperatures and crystallizability of the resulting homopolymers and random copolymers.

In homopolymers, the variations in Tg and Tm are influenced by the polarity and the dimensional factors induced by the substituents. A significant reduction in Tm in the range from 80 °C to 150 °C has been obtained in the polymers containing polar substituents, such as bromo, chloro and fluoro groups. The symmetrical arrangement of the substitu-

ents along the length of the polymer chains is the overriding factor determining the crystallnity of the resulting polymers. Under the condition of symmetrical substitution, the crystallizability of the polymers is significantly affected by the nature of the substituents and substitution with polar groups generally results in high crystallinity. Fluoro substitution however behaves very differently and tends to significantly suppress both the Tm and the crystallizability of the resulting polymers.

Fluoro substitution effects have been further investigated by synthesizing a series of fluoro substituted polymers with systematically varied structures. The Tm and the tendency to crystallize of the resulting polymers have been found to correlate with the variation in fluoro substitution. The combination of significant reductions of the Tm which makes the polymers suitable for melt processing and retention of sufficient crystallinity for maintaining favorable properties, has been obtained in this series of polymers. A discussion of the role of the fluoro substitution on the polymer properties is given. The presence of fluorine on the pendant phenyl rings of P3O is believed to cause a decrease in chain cohesion which results in the decreased Tm and crystallizability of the polymers.

The fluoro substitution effects are even more pronounced in the poly(ether ether ketone)s with pendant phenyl rings attached to the backbone, where the parent polymer is a highly rigid, highly crystalline and insoluble material. The introduction of fluorine onto the pendant phenyl rings of this polymer completely eliminated crystallinity and totally amorphous, soluble materials were obtained. The significance of the fluoro substitution effects in terms of improving solubility and the inherently stable C-F bond implies an alternative way to modify or design thermally stable polymers where insolubility is often encountered.

In the random copolymers, composed of 2,6-diphenylphenol DPP, and substituted DPP, with substituents ranging from the small fluorine atom to the large t-butyl group, the variation in Tm and crystallinity are found to vary dramatically when the comonomers are significantly different or vary smoothly when the comonomers are sufficiently alike. In copolymers of 2,6-diphenylphenol with comonomers contain large substituents, such as

the t-butyl group, the Tm and crystallinity tend to drop sharply at low concentration of comonomer and the copolymer tends to become amorphous at higher content of either co-monomer. When the comonomers are sufficiently alike, such as in copolymer 2,6-diphenylphenol/2-phenyl-6-(m-fluorophenyl)phenol, the Tm tends to vary gradually and the crystallinity remains at high level over the entire composition range.

An alternative approach to attain melt processibility for P3O has been investigated by incorporating a small amount of monomer bearing thermally reactive acetylene groups into a P3O polymer. The resulting polymers are inherently amorphous or contain a small amount of crystallinity, and, therefore, are melt processable. The curing of the resulting polymers at a temperature above the processing temperature window yields cross-links in the polymers which provide high temperature stability and solvent resistance.